FUNCTIONAL INTERACTION BETWEEN MAREK'S DISEASE VIRUS U_S3 AND MEQ WITH CHICKEN CREB AND HISTONE DEACETYLASES

A Dissertation

by

YIFEI LIAO

Submitted to the Office of Graduate and Professional Studies of
Texas A&M University
in partial fulfillment of the requirements for the degree of

DOCTOR OF PHILOSOPHY

Chair of Committee,	Blanca Lupiani
Co-Chair of Committee,	Sanjay M. Reddy
Committee Members,	Alistair McGregor
	Waithaka Mwangi
Head of Department,	Ramesh Vemulapalli

May 2021

Major Subject: Biomedical Sciences

ABSTRACT

Marek's disease (MD) is a neoplastic disease of chickens caused by Marek's disease virus (MDV), a member of the *Alphaherpesviridae* subfamily. Three MDV serotypes, including MDV-1, MDV-2 and HVT, have been identified and all encode a U_S3 serine/threonine protein kinase. Functions of U_S3 have been extensively studied in other alphaherpesviruses; however, the functions and substrates of MDV U_S3 have not been studied in detail. MDV-1 also encodes a Meq oncoprotein that is critical for MDV-1 induced T cell transformation. In the first part, we explored the cellular signaling pathways regulated by MDV-1 U_S3 using luciferase reporter systems and identified CREB signaling pathway was highly activated by MDV-1 U_S3. Our results further demonstrated that MDV-1 U_S3 phosphorylates chicken CREB (chCREB) and increases the binding of phospho-CREB (pCREB) at the promoter of CREB responsive cellular and viral genes to activate their transcription. Additionally, we demonstrated that MDV-1 U_S3 interacts with and phosphorylates Meq. In the second part, we identified more cellular substrates of MDV U_S3 and characterized the role of MDV U_S3 in MDV replication and pathogenesis. Our results showed that MDV U_S3 phosphorylates and interacts with chicken histone deacetylase 1 (chHDAC1) and chHDAC2, and we determined the effect of MDV U_S3 mediated phosphorylation in regulating protein stability, transcriptional regulation, and protein interactions of chHDAC1 and 2. In addition, we demonstrated that MDV-2 and HVT U_S3 could partially restore the growth deficiency of MDV-1 U_S3 null virus, and compensate the role of MDV-1 U_S3 in MDV

pathogenesis. In the third part, we examined the interactions between Meq and chHDAC1 and 2. Our immunofluorescence assay and immunoprecipitation assay showed that Meq co-localizes and interacts with chHDAC1 and 2, and Meq is a component of chHDAC1 and 2 associated CoREST, NuRD and Sin3 repressor complexes. In addition, our results showed that Meq induces the degradation of chHDAC1, chHDAC2, and global ubiquitinated proteins via a proteasome dependent pathway. In conclusion, this study identified novel MDV U_S3 substrates, characterized the functions of MDV U_S3 in viral replication and pathogenesis, and investigated the interplay between MDV Meq with host repressors and proteasome degradation pathway.

DEDICATION

To my wife, Xin Fang, and my family for their great support and love

ACKNOWLEDGEMENTS

I would like to thank my committee chair Dr. Lupiani, co-chair Dr. Reddy, and committee members Dr. McGregor and Dr. Mwangi for their continued support throughout the course of my doctoral research work. Their guidance and suggestions helped me to accomplish this work successfully.

I would like to thank Dr. Izumiya (University of California, Davis) for his counsel and suggestions. The critical techniques I learnt from Dr. Izumiya's laboratory helped me in completing this research. I would also like to thank Dr. Osterrieder for providing reagents, Dr. Porter for providing equipment, and Dr. Mouneimne for using of confocal microscope.

Thanks also go to my labmates, Kanika and Mohammad, and other friends for their generous help and encouragement.

Finally, I would like to thank my parents, sister, and parents-in-law for their invaluable support. Their encouragement motivated me to the present position. I sincerely express my love and appreciation to my wife, Xin Fang, for her continuous support. It is my great pleasure to have her on my side throughout this time. Her love brings me out from the stress and difficulty during the research progress. Also, thanks to my adorable cat, Archie, for relieving my pressure with his companion.

CONTRIBUTORS AND FUNDING SOURCES

Contributors

This work was supervised by a dissertation committee consisting of Dr. Lupiani (advisor), Dr. Reddy (co-advisor), and Dr. Mwangi of the Department of Veterinary Pathobiology and Dr. McGregor of Department of Microbial Pathogenesis and Immunology.

The chromatin immunoprecipitation sequencing data analysis for Chapter 2 was provided by Dr. Izumiya (University of California, Davis). The animal experiments in Chapter 3 were processed with help from Kanika and Mohammad of the Department of Veterinary Pathobiology. The confocal immunofluorescence images were taken with the help from Dr. Mouneimne of the Department of Veterinary Integrative Biosciences.

All other experiments performed for this dissertation were completed by the student independently.

Funding Sources

This graduate study was supported by an assistantship from College of Veterinary Medicine & Biomedical Science, Texas A&M University.

This work was also made possible in part by USDA/NIFA/AFRI grant 2014-67015-21787 and 2015-67015-23268, as well as TAMU CVM trainee grant 02-248020-18004 and 02-246799-19003.

NOMENCLATURE

MD	Marek's disease
MDV	Marek's disease virus
Meq	Marek's EcoRI Q fragment
CREB	cAMP response element-binding protein
HDAC	Histone deacetylase
UL	Unique long
US	Unique short
TRL	Terminal repeat long
IRL	Internal repeat long
IRS	Internal repeat short
TRS	Terminal repeat short
FFE	Feather follicular epithelial
EBNA3C	Epstein-Barr virus nuclear antigen 3C
LANA	Latent associated nuclear antigen
CtBP	C terminal binding protein
PTM	Post-translational modifications
BAC	Bacterial artificial chromosomes
RB	Retinoblastoma protein
PML-NBs	Promyelocytic leukemia protein nuclear bodies
USP	Ubiquitin specific protease

DUB	Deubiquitinase
UPP	Ubiquitin-proteasome pathway
SUMO	Small ubiquitin-like modifier
STUbL	SUMO-targeting ubiquitin ligase
CBP	CREB-binding protein
ChIP	Chromatin immunoprecipitation
LAT	Latency associate transcript
ICP4	Infected cell protein 4
CEF	Chicken embryonic fibroblasts
MERE	Meq-responsive element
CRE	cAMP response element
pCREB	phospho-CREB
qRT-PCR	Quantitative reverse transcriptase polymerase chain reaction
IP	Immunoprecipitation
WB	Western blot
IFA	Immunofluorescence assay
HATs	Histone acetyltransferases
HDACi	Histone deacetylase inhibitor
NaB	Sodium butyrate
UIPD	Ubiquitin independent proteasome degradation
CHX	Cycloheximide

TABLE OF CONTENTS

Page

LIST OF FIGURES

Page

LIST OF TABLES

Page

1. INTRODUCTION

1.1. Marek's disease

Marek's disease (MD), which was first described by Dr. Jozsef Marek in 1907, is a highly lymphoproliferative disease of chicken caused by an avian alphaherpesvirus, Marek's disease virus (MDV). MDV infection causes T-cell lymphoma, paralysis of legs and wings, immunosuppression, depression, and finally death of infected chickens (1). Currently, three MDV serotypes have been identified and fully sequenced (Table 1-1). Marek's disease virus serotype 1 (MDV-1) or Gallid alphaherpesvirus 2 (GaHV-2) includes all oncogenic viruses, which is further divided into four sub-groups from least to most virulent: mild (m), virulent (v), very virulent (vv), and very virulent plus (vv+); Marek's disease virus serotype 2 (MDV-2) or Gallid alphaherpesvirus 3 (GaHV-3) includes non-oncogenic viruses; and Meleagrid alphaherpesvirus 1 (MeHV-1, or Turkey herpesvirus, HVT) includes non-oncogenic viruses of turkey (2). Similar to other herpesviruses, the virion structure of MDV consists of four layers, including a double stranded DNA genome, an icosahedral capsid, a tegument layer, and the outside lipid bilayer envelope (3). Based on genome structure, MDV is classified a member of *Mardivirus* genus in *Herpesviridae* family. The genome of MDV is around 160 to 180 kb that consists of a unique long (UL) and a unique short (US) region, each flanked by terminal and internal repeat regions (TRL, IRL, IRS, and TRS). MDV encodes more than one hundred genes that are important for viral DNA replication, virion structure, pathogenesis and oncogenesis (4).

Table 1-1 Classification and representative strain of MDV.

Serotypes	Virulence	Representative strains		
		Strains	GenBank accession number	Total length (bp)
MDV-1	Mild (m)	CVI988	DQ530348.1	178,311
	Virulent (v)	GA	AF147806.2	174,077
	Very virulent (v)	Md5	AF243438.1	177,874
	Very virulent plus (vv+)	686	-	-
MDV-2	Avirulent	SB-1	HQ840738.1	165,994
HVT	Avirulent	FC-126	AF291866.1	159,160

MDV infection exhibits distinct lytic and latent stage in infected chickens. Initial infection of susceptible chickens occurs by inhaling dander shed by infected chickens. The lung is presumed to be first site of MDV infection and the lung phagocytes transmit the virus to lymphocytes in lymphoid organs, where the early cytolytic infection established from 2 to7 days post infection with peaking at day 4 (1). It was generally accepted that the early cytolytic infection of MDV occurs in B lymphocytes, which further activates and infects CD4+ and CD8+ T lymphocytes. However, a recent study from Bertzbach *et al*. challenged the model and their results suggested that B cells are

not required for MDV replication, spread and oncogenicity (5). This study pointed out the possibility that MDV could efficiently infect and replicate in CD4+ and CD8+ T lymphocytes without B lymphocytes and could further transforming the CD4+ T lymphocytes to proliferative tumor cells (5). Approximately 7-8 days post infection, the early cytolytic infection switches to latent infection, where no infectious viral particle is produced and only limited viral proteins or RNAs are expressed (6). Within 2 weeks post infection, some of the latently infected CD4+ T cells will be transformed to tumor cells, resulting to a lymphoproliferative disease in various organs of infected chickens. Around 10-14 days post infection, latently infected or transformed T lymphocytes carried the virus to skin, where the virus reactivates to infect feather follicular epithelial (FFE) cells to produce fully infectious viral particles (1).

The manifestations of MD in infected chickens are depend on the organs being affected, including but not limiting to paralysis when peripheral nerves are damaged, immunosuppression when lymphoid organs are involved, and death when lymphoproliferative lesions appear in visceral organs (1). Currently, vaccination using live vaccines is the primary method for control of MD. Vaccination could successfully protect susceptible chickens from MD associated tumors and mortality; however, it could not block the replication and shedding of virulent viruses (7). In addition, it has been speculated that the widespread use of vaccines contributed to the evolution of virulence of filed viruses (8-10). With the superior protection against vv and vv+ MDV, CVI988 is widely used as vaccine and considered as the “gold standard”.

Due to the cost of vaccination and occasional outbreaks, MD continues to have significant economic impacts on the poultry industry. With well-established gene editing system to manipulate viral genomes and animal model to evaluate viral pathogenicity in the natural host, the MDV infection model represents a unique system to study viral oncogenesis and herpesvirus-host interactions. Several MDV genes and micro-RNAs (miRNAs) have been proven to contribute to the MDV oncogenicity, in which *meq* is the most studied one. MDV encoded Meq is a 339 amino acid long basic leucine zipper (bZIP) protein, which consists of N terminal basic region and leucine zipper region, as well as C terminal transcriptional regulation region. MDV with both copies of *meq* deleted in TRL and IRL regions could not induce tumor in chickens, indicating that Meq is required for MDV mediated transformation of T lymphocytes (11). Meq shares some similar functions of cellular bZIP proteins such as Jun/Fos family transcription factors, and other oncogenic herpesviruses oncoproteins such as Epstein-Barr virus (EBV) encoded EBV nuclear antigen 3C (EBNA3C) and Kaposi's sarcoma-associated herpesvirus (KSHV) encoded latent associated nuclear antigen (LANA). Both Meq and EBNA3C have been shown to interact with C terminal binding protein (CtBP), a well characterized cellular transcriptional repressor (12, 13). The association between Meq and CtBP has been demonstrated to be essential for Meq oncogenecity (12). Both Meq and LANA have been shown to interact with c-Jun to activate AP-1 promoter, and interact with p53 to regulate transcription and cell cycle (14-17).

1.2. Herpesvirus and host interaction

To establish optimal infection, herpesviruses reached a balance with their host in the history of coevolution. In the lytic stage, herpesviruses actively manipulate host factors to produce viral proteins and infectious virions; while in the latent stage, only limited viral proteins and RNAs are expressed to evade host immunity and maintain viral genome. The switch between lytic and latent stage is a complicate and mysterious process where virus, host and environment factors are involved. Thus, the herpesviruses and host interactions, such as post-translational modifications and protein interactions, are important research areas. Investigating these interactions will facilitate the understanding of virus and cell biology, as well as promote the development of novel strategies to control herepsvirus infection.

1.2.1. Post-translational modifications (PTM)

Herpesvirus consists of a broad family of members that cause a wide spectrum of diseases in humans and animals. Based on the biological properties and genome structure, the *Herpesviridae* family is divided to three subfamilies including *alphaherpesvirinae*, *betaherpesvirinae* and *gammaherpesvirinae*. All herpesviruses share similar life cycle that consists of lytic and latent stage. The switch between lytic and latent stage is a complicate and sequential processes, where numerous viral and cellular proteins involved. It is no surprising that herpesviruses have evolved abilities to evade or mimic cellular pathways to benefit their survival and propagation. PTM, such as phosphorylation, ubiquitination, sumoylation and acetylation, are the most common

machineries that utilized by herpesviruses. Apart from hijacking host regulators, herpesviruses also encode their own protein kinases to regulate phosphorylation, as well as other enzymes that involved in ubiquitination and sumoylation.

1.2.1.1. Phosphorylation

Herpesvirus encode two serine/threonine protein kinases, including UL13 ortholog that is conserved among the entire *Herpesviridae* and U_S3 ortholog that is only encoded by *Alphaherpesvirinae*. Even though not essential for virus growth in cell culture, various functions and substrates have been attributed to both UL13 and U_S3.

1.2.1.1.1. UL13

UL13 ortholog is conserved within *Herpesviridae* even they are named differently, such as herpes simplex virus type 1 (HSV-1) UL13, varicella zoster virus (VZV) ORF47, MDV-1 UL13, human cytomegalovirus (HCMV) UL97, human herpesvirus 6 (HHV-6) U69, EBV BGLF4, and KSHV ORF36 (18). With the conserved amino acid sequence, UL13 ortholog shares some common features, such as subcellular localization, packaging in virions as a component of teguments, and autophosphorylation (18). Using human protein microarray, Li *et al*. explored the common substrates for UL13 protein kinase from 4191 candidate human proteins, and found 110 proteins are shared by at least three kinases among HSV-1 UL13, HCMV UL97, EBV BGLF4, and KSHV ORF36 (19). In these 110 proteins, DNA damage response (DDR) proteins were significantly enriched, and they demonstrated that TIP60, an upstream regulator of the

DDR pathway, was required for efficient virus replication (19). Important functions of individual UL13 ortholog from HSV-1, MDV-1, HCMV, EBV and KSHV are briefly described here.

HSV-1 UL13. HSV-1 UL13 is a component of viral tegument and plays a role in virus replication possibly via regulating tegument assembly (20) and transcriptional regulation of viral genes such as ICP0 and U_S11 (21). As a viral protein kinase, HSV-1 UL13 functions by phosphorylating numerous viral and cellular proteins. Currently, viral proteins, including ICP0, ICP22, UL41, UL49, and U_S3, have been identified as substrates of HSV-1 UL13; HSV-1 UL13 also phosphorylates cellular proteins such as EF-1δ and RNA polymerase II (22). It has been shown that HSV-1 UL13 mediated phosphorylation of ICP22 is important for its transcriptional regulation activity (21) and both HSV-1 UL13 and ICP22 have been shown to regulate the phosphorylation of RNA polymerase II to promote viral gene expression (23).

MDV-1 UL13. Some studies have been performed to characterize the function of MDV-1 UL13. An early study with a bacterial artificial chromosomes (BAC) carrying genome of MDV-1 RB-1B strain that harbors frameshift mutations in UL13, UL44, and U_S6 genes suggested that UL13 is required for horizontal transmission of MDV-1 (24). Recently, Krieter *et al*. confirmed that MDV-1 UL13 is required for interindividual spread of virus and demonstrated that it is not essential for cell-to-cell spread, disease induction, and oncogenicity of MDV-1 (25).

HCMV UL97. HCMV UL97 was originally discovered by its unique activity in phosphorylating nucleoside analog ganciclovir (26, 27). Later studies showed that

HCMV UL97 is constituent of tegument and plays important role in virus replication. It has been shown that HCMV UL97 phosphorylates the viral nuclear egress complex (NEC) to modulate nuclear egress of viral particle (28). Thus, HCMV UL97 also known as the target of the antiviral drug maribavir, which specifically inhibit the activity of HCMV UL97 to impair viral replication (29). Cellular proteins such as HDAC1, lamin A/C, RNA polymerase II, and retinoblastoma protein (RB) have also been identified as substrates of HCMV UL97 (28, 30-32).

EBV BGLF4 and KSHV ORF36. In addition to the conserved functions as stated above, EBV BGLF4 and KSHV ORF36 show significant similarities in their substrates. First, both EBV BGLF4 and KSHV ORF36 suppress the interferon regulatory factor 3 (IRF-3) pathway in a kinase activity independent manner (33, 34). Second, both EBV BGLF4 and KSHV ORF36 phosphorylate their own bZIP domain containing protein, EBV BZLF1 and KSHV K-bZIP, respectively (35, 36). EBV BGLF4 has been proven to interact and phosphorylate BZLF1 at serine 209 site, and this interaction is required for BZLF1 to repress BZLF1 transactivation activity on its own promoter (36). KSHV ORF36 has been determined to phosphorylate K-bZIP at threonine 111 which is the same site targeted by cyclin-dependent kinase CDK2, and phosphorylation of K-bZIP by ORF36 inhibit the transcription repression activity of K-bZIP (35, 37). Other unique functions and substrates have also been attributed to KSHV ORF36 and EBV BGLF4. KSHV ORF36 could activate the c-Jun N-terminal kinase pathway and mimic cellular S6 kinase (S6KB1) to phosphorylate ribosomal S6 protein to enhance global

protein synthesis (38, 39). EBV BGLF4 has been shown to down-regulate NF-kB transactivation activity by phosphorylating UXT protein (40).

1.2.1.1.2. U_S3

The U_S3 protein kinase is encoded by members of alphaherpesvirus subfamily, and contains conserved kinase domain including ATP-binding region and catalytic active site (41). The U_S3 orthologs include HSV-1 U_S3, VZV ORF66, MDV U_S3, pseudorabies virus (PRV) U_S3, bovine herpesvirus type 1 (BHV-1) U_S3, and equine herpesvirus type 1 (EHV-1) U_S3. Compared to other alphaherpesviruses, PRV and HSV-1 U_S3 genes contain two transcriptional start sites (TSS) and thus encode two isoforms, U_S3 and $U_S3.5$ (42-44). U_S3 plays important role in virus growth *in vitro* and *in vivo*, as deletion of U_S3 resulted in growth deficiency of alphaherpesviruses in cell culture and animals (41). Additionally, U_S3 is involved in gene expression regulation, apoptosis inhibition, virion morphogenesis, cellular actin cytoskeleton remodeling, and inhibition of host antiviral responses (41). Despite relatively low protein sequence similarity, the functions of U_S3 orthologs are highly conserved in different alphaherpesviruses. Thus, important functions of HSV-1 and MDV-1 U_S3 are briefly described here.

HSV-1 U_S3. Functions of U_S3 protein were extensively investigated in HSV-1. HSV-1 U_S3 protein shuttles between nucleus and cytoplasm, and the kinase activity is important for its subcellular localization (41, 45). To date, multiple functions have been attributed to HSV-1 Us3, including apoptosis inhibition (46, 47), evasion of host immune system (48, 49), mRNA translation stimulation (50), regulation of viral and

cellular gene expression (51), and promoting nucleocapsids transportation across nuclear membrane (52). The consensus target sequence of HSV-1 U_S3 have been identified as RnX(S/T)YY, where R is Arg; n$\geqslant$2; X is one of Arg, Ala, Val, Pro, or Ser; and Y can be any amino acid expect acidic residue (41). HSV-1 U_S3 autophosphorylates at serine 147 (S147) site to promotes its kinase activity and ensure its proper subcellular localization (53). In addition, viral proteins, including UL31, UL34, UL47, glycoprotein B (gB), dUTPase, U_S8A, U_S9, and ICP22, are also substrates of HSV-1 U_S3 (22, 54, 55). HSV-1 U_S3 mediated phosphorylation direct linked to its function; such as HSV-1 U_S3 mediated UL31 phosphorylation translocates both UL31 and UL34 to the nuclear rim (56, 57), and phosphorylation of gB by HSV-1 U_S3 is important for viral replication and nuclear egress of nucleocapsids (54). Cellular proteins, such as, p65, BAD, HDAC-1 and HDAC-2, programmed cell death protein 4 (PDCD4), lamin A/C, interferon regulatory factor 3 (IRF-3), cellular motor protein KIF3A, and protein kinase A (PKA) (45, 46, 58-60), are also phosphorylated by HSV-1 U_S3. It has been shown that HSV-1 U_S3 mediates the phosphorylation of BAD protein to protect transfected cells from apoptosis (46), and HSV-1 U_S3 induced phosphorylation of lamin A/C contributes to the transport of nucleocapsids to the inner nuclear membrane of infected cells (61). In addition, overexpression of HSV-2 U_S3 is able to disrupt promyelocytic leukemia protein nuclear bodies (PML-NBs) in a kinase activity dependent way (62). PML-NBs formed by several proteins, including PML, Sp100 and Daxx, which plays essential roles in programmed cell death and gene expression regulation (63). The ability of U_S3 to disrupt

PML-NBs was speculated to contribute to anti-apoptotic activity and transcriptional regulation function of U_S3.

MDV-1 U_S3. The known functions of MDV-1 U_S3 are mostly derived from its homolog in HSV-1. It has been determined that MDV-1 U_S3 and its kinase activity are important of efficient growth and plaque size of MDV-1 in cell culture (64). In addition, MDV-1 U_S3 has been shown to involved in actin stress fiber breakdown and is required for de-envelopment of perinuclear virions (65). Similar to HSV-1 U_S3, MDV-1 U_S3 protein is able to mimic the function of PKA to block apoptosis induced by staurosporine is a kinase activity depended way (64). Currently, the only known substrate of MDV-1 U_S3 is MDV-1 pp38, a viral protein that is essential for efficient lytic replication of MDV-1 *in vivo* (64). Schumacher *et al*. demonstrated that MDV-1 U_S3 physically interacts with and phosphorylates pp38 (64); however, the phosphorylation sites and potential functions of MDV-1 U_S3 mediated pp38 phosphorylation remains to be studied. Regarding multiple functions and substrates of HSV-1 U_S3 have been determined, the potential substrates and functions derived from MDV U_S3 induced phosphorylation are our primary research interest. We have identified novel substrates for MDV U_S3 and results are described in detail in following chapters.

1.2.1.2. Ubiquitination and proteasome dependent degradation

Ubiquitination is an enzymatic procedure that a single ubiquitin molecule (monoubiquitination) or a polyubiquitin chain (polyubiquitination) is tagged to the substrate protein via a sequential process catalyzed by three enzymes: E1 activating

enzyme, E2 conjugating enzyme and E3 ligase (66). This process can be reversed by the activity of another enzyme called ubiquitin specific protease (USP) or deubiquitinase (DUB). Ubiquitin protein contains seven internal lysine residues (K6, K11, K27, K29, K33, K48, and K63) and one N-terminal methionine (M1) residue as the modification sites, and the outcomes vary when different lysine sites are modified (67). It has been shown that ubiquitination affects various cellular functions by regulating the degradation of proteins, modulating signaling pathways, translocating the subcellular localization of proteins, and interfering protein-protein interaction network (68-70). In cells, the most abundant polyubiquitinations are K48- and K63-linked chains that exhibit different effects. Covalent attachment of ubiquitin to K48 position of ubiquitin generally target proteins for degradation by proteasome, while K63-linked chains is normally non-degradative and is involved in signal transduction regulation (71). After tagged by K48-linked ubiquitin chain, the ubiquitinated substrates are usually recognized and degraded by 26S proteasome, a protein complex consists of 20S core particle (CP) and 19S regulatory particle (PR) (71). The ubiquitin-proteasome pathway (UPP) is important regulatory machinery in cells, which plays essential role to remove unnecessary or dysfunctional proteins and regulate gene expression (72). Considering the important functions of cellular ubiquitination system and UPP, herpesviruses encode their own viral E3 ligase and viral deubiquitinase to modulate host ubiquitination system.

HSV-1 infected cell protein 0 (ICP0). HSV-1 ICP0 is an immediate early (IE) protein that acts as a transactivator to regulate expression of viral and cellular genes (73). It is required for efficient viral replication in cells infected at low multiplicity, but not at

high multiplicity (74). ICP0 contains two distinct E3 ligase domains, a N-terminal RING finger-E3 ligase domain and C-terminal cdc34-dependent E3 ligase domain (73). It has been shown that these two domains are in conjugating with different E2 enzymes that N-terminal E3 ligase activity is specific for UbcH5a and UbcH6 E2 enzyme, while C-terminal E3 ligase activity is UbcH3 (cdd34) dependent (73). It has been shown that ICP0 induces the co-localization of conjugated ubiquitin with PML-NBs (75) and mediates the degradation of PML and Sp100 via proteasome dependent pathway (76). Apart from internal E3 ligase activity domain, ICP0 also interacts with cellular E3 ligase and ubiquitin specific protease (USP). The ICP0 co-localizes and interacts with RNF8, an E3 ligase involved in DNA damage repair; and the RING finger domain of ICP0 mediates the ubiquitination and degradation of RNF8 (77). In addition, ICP0 interacts with USP7 to inhibit ICP0 autoubiquitination, while promotes USP7 polyubiquitination to degrade USP7 in infected cells (78).

KSHV transcription activator (RTA). The KSHV encoded RTA is the master regulator of viral gene expression and plays essential role in switch between latent and lytic infection of KSHV (79). It has been demonstrated that KSHV RTA contains a non-canonical Cys-plus-His-rich region that exhibits ubiquitin ligase activity, which promotes polyubiquitination and degradation of interferon regulatory factor 7 (IRF7) (80). Additionally, KSHV-RTA binding protein (K-RBP) and Hey1 (a cellular transcriptional repressor) have been shown to be ubiquitinated and degraded by KSHV RTA (81, 82).

Viral USPs. All herpesviruses encode their own USP, such as HSV-1 UL36, MDV-1 UL36, HCMV UL48, and KSHV ORF64. HSV-1 UL36 is a large tegument protein that contains a N-terminal conserved deubiquitinase domain, named as UL36USP (83, 84). Interestingly, the enzymatic activity of deubiquitinase domain can only be detected after cleaved from the full length UL36 during the viral replication (83). Kattenhorn *et al*. further characterized the enzymatic activity of UL36USP and found that the recombinant UL36USP specifically cleave K48-linked poly-ubiquitin chain (83). However, later studies determined that both K48- and K63-linked chains are the targets of UL36USP (85). Recently, HSV-1 UL36USP has been shown to deubiquitinating TNF receptor-associated factor (TRAF3) to inhibit IFN-β production (86) and deubiquitinating IκBα to abrogate NF-κB activation that mediates the evasion of HSV-1 from host antiviral innate immunity (87). Similarly, it has been suggested that HCMV USP targets host antiviral innate immunity to promote oncogenesis (88). Jarosinski *et al*. demonstrated that the USP activity of UL36 is conserved in MDV-1 (89). Importantly, they found that the USP activity of UL36 is essential for MDV-1 induced T cell lymphoma in infected chickens, but dispensable for horizontal transmission of MDV-1 (89). The ORF64 USP of KSHV has been shown to catalyze both K48- and K63-linked ubiquitin chains, and involved in viral lytic replication (90).

1.2.1.3. Sumoylation

Compared to other modifications, sumoylation is a relative new type of modification. A total four small ubiquitin-like modifier (SUMO) isoforms, including

SUMO-1, SUMO-2, SUMO-3, and SUMO-4, have been identified since it was first identified in 1997 (91). Similar to ubiquitination, sumoylation is also a sequential process mediated by three enzyme, E1 activation enzyme, E2 conjugating enzyme, and E3 ligase, which can be reversed by desumoylating enzymes named Sentrin-specific proteases (SENP). Normally, sumoylation alters the subcellular localization and interaction network of substrates; however, sumoylated proteins could also be targeted for degradation via enzymes called sumo-targeting ubiquitin ligase (STUbL) (92).

Recent studies suggested that herpesviruses regulate host sumoylation systems to benefit their replication. HSV-1 ICP0 has been shown to degrade SUMO-2 and SUMO-3 (SUMO-2/3) through proteasome dependent pathway (93). EBV BGLF4 physically associates with SUMO-1 and SUMO-2 through the SUMO interaction motifs (SIM), and the SUMO interaction property of BGLF4 has been suggested to be important for efficient lytic replication of EBV (94). In addition, Bentz *et al*. showed that EBV latent membrane protein 1 (LMP1) interacts with SUMO E2 conjugating enzyme Ubc9 to modulate host sumoylation system (95). Recently, KSHV RTA has been shown to exhibit STUbL like function to degrade sumoylated PML (96).

In addition to manipulate host sumoylation system, viral proteins have been shown to be sumoylated and even mimic SUMO E3 ligase activity. Interestingly, KSHV K-bZIP protein exhibits both of the functions. KSHV *K8* is an early lytic gene that encodes a 237 amino acid long protein K-bZIP that contains a basic leucine zipper domain. Izumiya *et al*. demonstrated that K-bZIP is sumoylated by both SUMO1 and SUMO-2/3 and the sumoylation site has been identified at lysine 158 (K158) (97).

Additionally, they found that K-bZIP interacts with SUMO E2 conjugating enzyme Ubc9 and recruits it to K-bZIP target promoter to repress the transcription (97). Later, K-bZIP has been identified a viral SUMO E3 ligase that catalyzes the sumoylation of itself and its interaction partners, such as p53 and Rb (98).

1.2.1.4. Coordination of PTM

Currently, hundreds of PTM have been identified. A single substrate can be modified by same PTM at different sites or by different PTM at same site. Thus, it is not surprising that PTM competing or coordinating to regulate protein functions. In 2013, Woodsmith *et al*. systematically analyzed dual PTM in human proteins and identified more than 300 combinatorial modified proteins (99). An example for coordinating PTM is p53 protein. P53 is a well-characterized tumor suppressor that involved in numerous cell processes. It has been reported that phosphorylation of p53 at serine 15 (S15) and S46 sites are required for acetylation of p53 (100, 101). Another great example for protein that undergoes same PTM at multiple sites is histone deacetylases (HDAC). HDAC1 and HDAC2 are two highly homologous proteins that play critical roles in regulating protein acetylation and numerous cellular signaling pathways (102). Both HDAC1 and HDAC2 are being widely modified in their C-terminal residues. Casein kinase II (CKII) phosphorylates HDAC1 at S421 and S423 to regulate its enzymatic activity, transcriptional regulation activity, and protein interaction activity (103). The CKII target sites in HDAC2 have been identified as S394, S422, and S424 (104). Additionally, CKII mediated phosphorylation of HDAC2 enhances its enzymatic

activity, but has no effect on its transcriptional repression activity (104). Later, Sun *et al*. showed that CKII mediated phosphorylation of HDAC2 affects to chromatin distribution of HDAC2; specifically, unmodified HDAC2 selectively binds to coding region of genes, while phosphorylated HDAC2 primarily associates with the promoter of genes (105). In Chapter 3, we identified that HDAC1 and HDAC2 as the substrates of MDV U_S3. We further determined the phosphorylation sites in HDAC1 and HDAC2, and characterized the potential impact of MDV U_S3 induced HDAC1 and HDAC2 phosphorylation.

1.2.2. Protein interactions

Apart from PTM, interactions between viral and cellular proteins have also been extensively studied. bZIP proteins are a group of transcription factors that contain basic region and leucine zipper domain, which mediates the DNA binding and protein dimerization, respectively (106). Several host bZIP protein families, including Jun, Fos, ATF, and CREB, have been characterized to be important for transcription regulation and cancer development (107-109). Some herpesviruses also encode their own bZIP protein, such as MDV-1 Meq, EBV BZLF1 and KSHV K-bZIP. The important functions and interactions of these proteins are briefly described here.

MDV-1 Meq. Meq is expressed in both lytic and latent stage of MDV-1 infection. As the major MDV-1 oncoprotein, multiple functions have been attributed to MDV-1 Meq, including transformation, transcription regulation, cell cycle regulation, and anti-apoptosis (11, 14, 110). Especially, the interaction network of Meq has been

shown to be important for its function. Meq forms homodimer with itself and heterodimer with Jun/Fos transcription factors to repress and activate transcription, respectively; and the Meq-CtBP interaction has been proved to be essential for Meq oncogenicity (12, 111). Some other cellular proteins have also been shown to interact with Meq, such as CDK2 interacts with and phosphorylates Meq to facilitate its cytoplasmic localization (110); Meq interacts with heat-shock protein 70 (Hsp70) in MDV-1 transformed tumors (112); Meq associates with tumor suppressor protein p53 to interfere it mediated transcriptional regulation and apoptosis (15); Meq interacts with p85 to activate phosphatidylinositol 3-kinase (PI3K)/Akt signaling pathway to facilitate viral replication (113). In the Chapter 4, we identified the novel interaction between MDV-1 Meq and host repressors HDAC1 and HDAC2.

EBV BZLF1. BZLF1 (also known as Zta), unlike MDV-1 Meq, is an immediate early protein of EBV that acts as master regulator to activate expression of early viral genes and induce the reactivation of latently infected EBV (114). Given the essential role in EBV infection, the interaction network of BZLF1 has been extensively studied. BZLF1 has been shown to interact with and recruit host chromatin-remodeling enzymes SNF2h and INO80 to the promoter of lytic genes to reactivate EBV (115), and associate with another EBV protein BMRF1 to modulate EBV lytic infection (116). In addition, it has been shown that CREB-binding protein (CBP) interacts with BZLF1 to promote its transactivation activity (117), which could be repressed by phospholipid scramblase 1 (PLSCR1), another interaction partner of BZLF1 (118). BZLF1 also undergoes PTM

that the sumoylation of BZLF1 has been shown to repress its transcriptional regulation activity by interacting with HDAC3 (119).

KSHV K-bZIP. K-bZIP, an analog of EBV BZLF1, is an immediate early protein of KSHV. The PTM largely modulate the transcriptional regulation activity of K-bZIP, where sumoylation mediates the transcription repression of K-bZIP that could be reversed by phosphorylation (35, 79, 97). K-bZIP has been shown to interact with p53 to negatively regulate its transcriptional activity (120). It also interacts with and recruits HDAC2 to viral OriLyt and ORF50 promoters to regulate KSHV replication (121). Other cellular proteins, including CBP, PML, CDK2 and IRF-3, are also interaction partners of K-bZIP (122-126).

2. ROLE OF MAREK'S DISEASE VIRUS ENCODED U_S3 SERINE/THREONINE PROTEIN KINASE IN REGULATING MDV MEQ AND CELLULAR CREB PHOSPHORYLATION [*]

2.1. Introduction

Marek's disease (MD) is a highly contagious lymphoproliferative disease of chickens, which was first described by József Marek in 1907 (6). Later, the causative agent of MD was identified as Marek's disease virus (MDV), which was classified as a member of the *Alphaherpesviridae* subfamily based on DNA sequence homology and genome organization (127, 128). Infection of chickens with highly virulent strains of MDV result in the formation of T cell lymphomas as early as two weeks post infection (1). Three MDV serotypes have been identified and their genome sequenced: MDV-1 (*Gallid alphaherpesvirus* type 2, GaHV-2), which include oncogenic MDV and their cell-culture attenuated variants; MDV-2 (GaHV-3), which include the naturally non-oncogenic MDV; and turkey herpesvirus (HVT; *Meleagrid alphaherpesvirus* type 1, MeHV-1) (2, 6). Similar to other alphaherpesviruses, the 160-180 kb, double-stranded DNA genome of MDV, which encodes more than one hundred putative genes, consists of a long and a short unique regions (U_L, U_S), each flanked by inverted repeats (TR_L,

[*]Reprinted with permission from "Role of Marek's Disease Virus (MDV)-Encoded US3 Serine/Threonine Protein Kinase in Regulating MDV Meq and Cellular CREB Phosphorylation" by Yifei Liao, Blanca Lupiani, Kanika Bajwa, Owais A. Khan, Yoshihiro Izumiya, Sanjay M. Reddy, 2020. Journal of Virology, Volume 94, Issue 17, Copyright [2020] by American Society for Microbiology.

IR_L, IR_S, and TR_S), (4, 129). Two genes, *meq* and *vTR* within the TR_L & IR_L regions have been shown to be directly involved in MDV lymphomagenesis (11, 130).

MDV (MDV refers to MDV-1 in the following text unless specified) encoded U_S3 protein is a serine/threonine protein kinase, which is highly conserved among all alphaherpesviruses. U_S3 contains a kinase activity domain, consisting of an ATP-binding domain and a catalytic active site, which is important for its kinase activity (41). The functions of U_S3 have been extensively explored in herpes simplex virus type 1 (HSV-1). Although it is not essential for virus growth *in vitro*, multiple functions have been attributed to U_S3, including transcription regulation, cytoskeletal rearrangements, anti-apoptosis, and interference with the interferon (IFN) system (41). In addition, HSV-1 U_S3 shuttles between the nucleus and the cytoplasm, and the kinase activity is important for its subcellular localization (41, 45). In addition to auto-phosphorylation, several cellular and viral proteins have been identified as U_S3 substrates. HSV-1 U_S3 viral protein substrates include U_L31, U_L34, and glycoprotein B (gB) (22, 51). Cellular proteins such as p65, histone deacetylase-1 (HDAC-1) and HDAC-2, programmed cell death protein 4 (PDCD4), and cAMP response element-binding protein (CREB), are also substrates of HSV-1 U_S3 (45, 58, 59, 131). It has been reported that MDV U_S3 is involved in actin stress fiber breakdown and is important for de-envelopment of perinuclear virions (65). In addition, MDV pp38 protein was identified as a substrate and interaction partner of MDV U_S3, and MDV U_S3 was shown to be important for protecting cells from apoptosis in a kinase activity depended manner (64, 132).

MDV encodes a 339 amino acid long b-ZIP protein, called Meq, which consists of a N-terminal DNA binding domain, a leucine zipper domain, and a C-terminal transactivation/transrepression domain (11). Meq is expressed during both lytic infection phase and in lymphoblastoid tumor cells (133), and deletion of both copies of the *meq* gene from the MDV genome results in absence of tumors in infected chickens, indicating that Meq is essential for transformation of lymphocytes (11). Meq has been identified as a homolog of the Jun-Fos family of transcription factors. Through the leucine zipper region, Meq forms homodimers with itself and heterodimers with cellular c-Jun and c-Fos (111, 134), which binds to specific DNA sequences, called Meq-responsive element I and II (MERE I and MERE II), respectively (135). In addition, a chromatin immunoprecipitation (ChIP) study showed that Meq directly binds to the MDV lytic origin of replication, and Meq and ICP4 promoters (14). Further, application of advanced high-throughput technologies, such as microarray and next-generation sequencing, provided a comprehensive view of Meq binding sites within the chicken genome and its role in regulating cellular pathways including ERK/MAPK, Jak-STAT, and ErbB pathways (136).

CREB is a transcription factor that binds, as a dimer, to the conserved cAMP response element (CRE), TGACGTCA (137, 138). CREB is highly conserved between humans and chickens, and can form heterodimers with MDV Meq (14). Phosphorylation of CREB at Serine 133 (S133) by various cellular protein kinases, such as PKA, calmodulin-dependent kinase (CaMK) IV and MAPK-activated ribosomal S6 kinases (RSKs), activates CREB, resulting in the recruitment of CREB-binding protein

(CBP)/p300 to the promoter of CREB target genes to further affect the chromatin structure, enabling synthesis of RNA by RNA polymerase II (137, 139). HSV-1 U_S3 has been shown to phosphorylate endogenous and co-transfected CREB at S133 (131). Studies from several herpesviruses suggest that activation of CREB plays an important role in herpesvirus infection. Kaposi's sarcoma-associated herpesvirus (KSHV) utilizes multiple cellular signal pathways to activate CREB to regulate expression of Cyclooxygenase 2 (COX-2), a host factor that plays an important role in KSHV latency and pathogenesis (140). Another recent study showed that varicella-zoster virus (VZV) infection up-regulates CREB phosphorylation, which does not require VZV encoded serine/threonine protein kinases, and the interaction between pCREB and CBP/p300 is important for skin infection by VZV (141). In addition, other studies showed that activation of CBP/p300 plays an important role in regulating herpesvirus reactivation from latency (142, 143).

In this study, we aimed to identify MDV U_S3 viral and cellular substrates, and to investigate the role of MDV U_S3 in regulating MDV-host interaction. Our results show that MDV U_S3 interacts with, and phosphorylates MDV Meq and chicken CREB (chCREB). Further, qRT-PCR and ChIP experiments showed that MDV U_S3 enhances enrichment of phospho-CREB (pCREB) to the promoter of CREB target genes to up-regulate their expression, and MDV U_S3 is important for the expression of several MDV genes during infection. Overall, our studies point to the role of MDV U_S3 in transcriptional regulation of both host and viral genes during MDV infection.

2.2. Results

MDV U_S3 and chCREB transactivate CREB response element (CRE) in a luciferase reporter assay. To identify the biological function of MDV U_S3, we first explored possible signaling pathways regulated by U_S3. We utilized signaling reporter systems, which examined specific transcription factor activity as each reporter construct encode tandem specific DNA responsive elements for the transcriptional factor (e.g. STAT3 and CREB) (Figure 2-1A). We tested a total of 29 reporter constructs and found that MDV U_S3 strongly induces luciferase expression from several reporter constructs that include CREB, KLF4, ATF6, HNF4, and PPAR (Figure 2-1A). Among them, the CREB pathway showed the highest activation after transfecting with MDV U_S3 expression plasmid. More importantly, the activation was found to be kinase dependent, as transient expression of an MDV U_S3 kinase dead mutant (U_S3-K220A) did not activate the CREB reporter construct (Figure 2-1B). We also found that phosphorylation of Serine 119 (S119) of chicken CREB (chCREB) (corresponding to S133 of hCREB) is important for this transactivation activity (Figure 2-1C). Furthermore, transfection of cells with chCREB_S119D (phosphorylation mimic form) resulted in higher levels of CRE responsive elements transactivation, while chCREB_S119A (non-phosphorylated form) showed lower levels of transactivation.

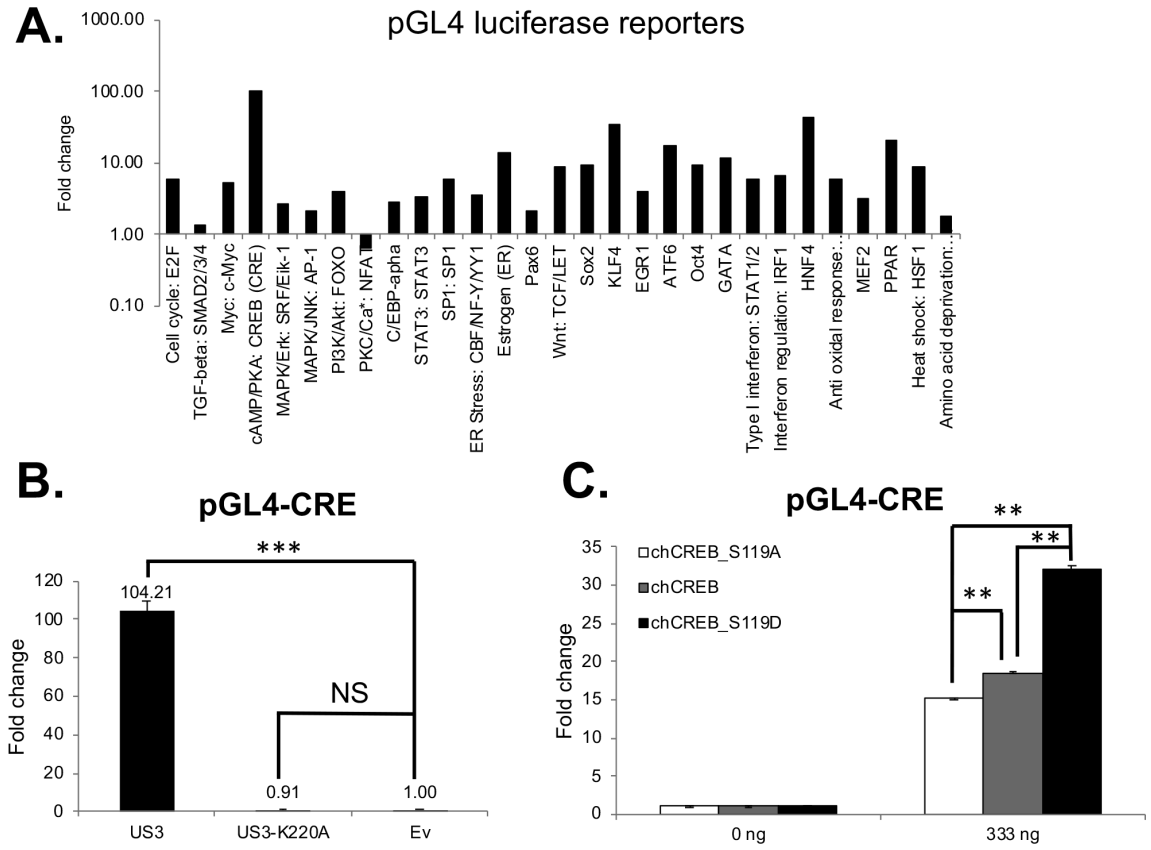

Figure 2-1 MDV U_S3 and chCREB transactivate CREB response element (CRE) in a luciferase reporter assay.
(A) pcDNA-U_S3 or pcDNA empty vector (Ev) were co-transfected with the indicated luciferase reporter plasmids. *Firefly* luciferase was measured 48 hours post transfection. Values were presented as fold change relative to Ev. (B) pcDNA-U_S3, pcDNA-U_S3-K220A, or pcDNA Ev were co-transfected with pGL4-CRE reporter vector and *Renilla* luciferase vector into 293T cells. Forty-eight hours after transfection, *firefly* luciferase and *Renillla* luciferase activity were measured using Dual-Glo® Luciferase Assay System as per manufacturer's protocol. Numbers above the column indicate the fold change relative to Ev. (C) 293T cells were co-transfected with different amounts of pcDNA-chCREB_S119A, pcDNA-chCREB, pcDNA-chCREB_S119D with pGL4-CRE reporter vector and *Renilla* luciferase vector. Dual luciferase assay was performed as stated above. The experiment was repeated three times in triplicate. Error bars indicate standard error of the mean (SEM). NS: not significant, **: $p<0.01$, ***: $p<0.001$.

MDV U_S3 increases phosphorylation of CREB. To explore the role of MDV U_S3 in regulating CREB phosphorylation, levels of phospho-CREB (pCREB) were

examined in pcDNA-FLAG-U_S3 plasmid (wild type, FLAG-U_S3), pcDNA-FLAG-U_S3-K220A plasmid (kinase dead, FLAG-U_S3-K220A), or pcDNA empty vector plasmid (Ev) transfected 293T cells. Forty-eight hours after transfection, total cell lysates were subjected to SDS-PAGE and Western blot analysis (WB) with pCREB antibody that specifically recognizes hCREB Serine133 phosphorylation (corresponding to chCREB Serine 119, Figure 2-2E). As shown in Figure 2-2A left panel, expression of FLAG-U_S3, but not FLAG-U_S3-K220A, increased the levels of pCREB. Quantification of the WB results showed that the pCREB/total CREB (tCREB) ratio in pcDNA-FLAG-U_S3 transfected cells was about 1.7 fold higher than pcDNA-FLAG-U_S3-K220A and about 1.3 fold higher than pcDNA Ev transfected cells (Figure 2-2A right panel). In addition, the pCREB/tCREB ratio in pcDNA-FLAG-U_S3-K220A transfected cells was slightly lower than pcDNA Ev transfected cells, which may be due to competition between kinase dead U_S3 and other cellular protein kinases (144, 145). These results were confirmed by co-transfecting pcDNA-hCREB or pcDNA-chCREB with pcDNA-FLAG-U_S3, pcDNA-FLAG-U_S3-K220A, or pcDNA Ev into 293T (Figure 2-2B) and DF-1 (Figure 2-2C) cells, respectively. WB analysis and quantification confirmed that overexpression of MDV U_S3 clearly increased the pCREB/tCREB ratio (3-4 fold) compared to U_S3-K220A or Ev in co-transfected cells. To further examine the role of U_S3 in regulating CREB phosphorylation during natural infection, we analyzed pCREB levels in MDV infected chicken embryonic fibroblasts (CEF). As shown in Figure 2-2D, pCREB levels were higher in 686-BAC parental virus infected CEF than non-infected CEF, while pCREB levels in 686-BACΔU_S3 (U_S3 null virus) infected CEF was slightly

lower than non-infected CEF, in agreement with transfection experiments (Figure 2-2A). MDV pp38 phosphorylation was used as a control to demonstrate the effects of U_S3 deletion in 686-BACΔU_S3 virus (Figure 2-2D). Because U_S3 of all three MDV serotypes present a conserved catalytic active site (APPENDAIX A, Figure S1A), we examined if the ability to phosphorylate CREB was conserved in all three serotypes. Similar to MDV, MDV-2 and HVT U_S3 also increased the levels of pCREB/tCREB in transfection studies (APPENDAIX A, Figure S1B, C).

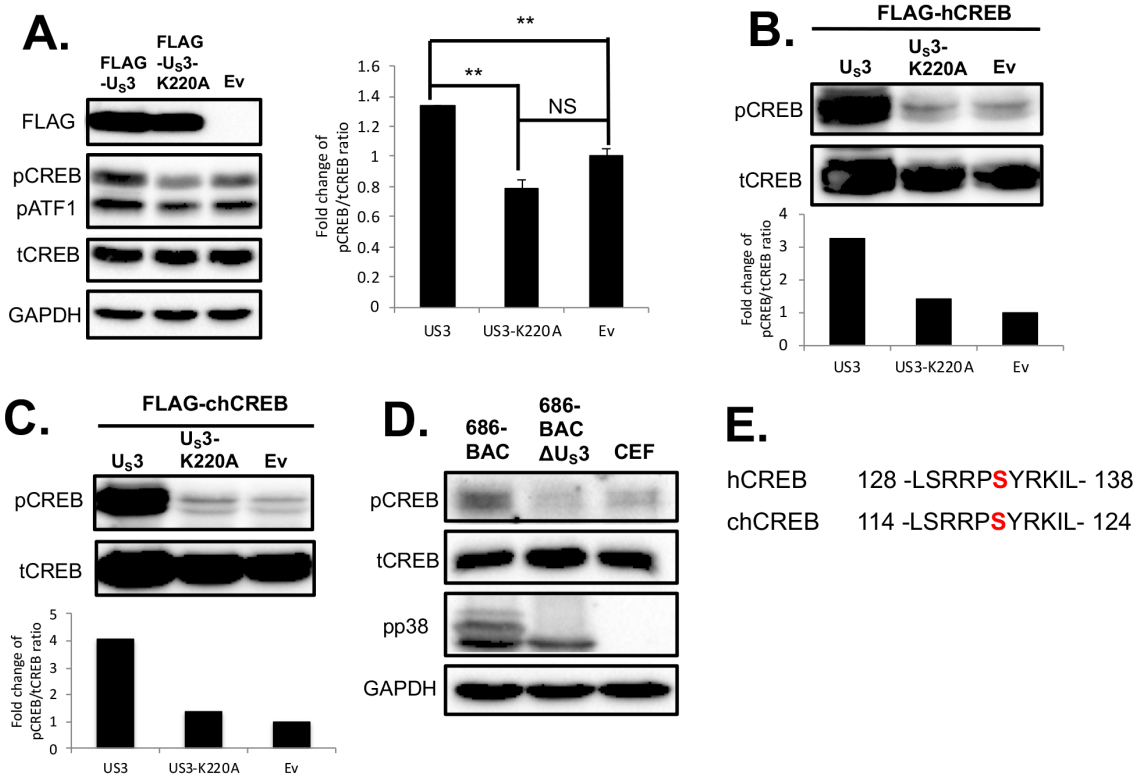

Figure 2-2 MDV U_S3 increases phosphorylation of CREB.
(A) pcDNA-FLAG-U_S3, pcDNA-FLAG-U_S3-K220A, or pcDNA-empty vector (Ev) were transfected into 293T cells. Cells were lysed 48 hours post transfection followed by Western blot (WB) analysis with the indicated antibodies (left). Representative data of three independent cell culture experiments are presented. pCREB/tCREB ratio was quantified with Image J software (right), and presented as fold change compared to Ev. T-test was performed between groups. **: $p<0.01$, NS: not significant. 293T cells (B)

and DF-1 cells (C) were co-transfected with the indicated plasmids. Forty-eight hours after transfection, cells were lysed and subjected to SDS-PAGE and WB with the indicated antibodies. Upper panels show WB results, bottom panels show fold change of pCREB/tCREB ratio. (D) CEF were infected with 686-BAC or 686-BACΔU_S3 viruses. Seven days after infection, cells were lysed and subjected to SDS-PAGE and WB with the indicated antibodies. (E) Amino acid sequence alignment of a major phosphorylation subdomain of human CREB (hCREB) and chicken CREB (chCREB) protein. Serine residue detected by pCREB antibody is shown in bold red. Numbers indicate amino acid location, and dashes represent amino acids not shown in this alignment.

Overexpression of MDV U_S3 enhances enrichment of pCREB to the promoter of *c-Fos* to up-regulate its expression. To examine the role of U_S3 mediated CREB phosphorylation in gene regulation, we performed qRT-PCR of *c-Fos*, a CREB target gene, which also forms heterodimers with MDV Meq (14, 146). Because of high reproducibility and high efficiency of transient transfection, we carried out these experiments in 293T cells. Transient expression of MDV U_S3 in 293T cells increased the expression of *c-Fos* when compared to U_S3-K220A and Ev (Figure 2-3A). Interestingly, compared to Ev, expression of U_S3-K220A inhibited expression of *c-Fos* (Figure 2-3A). Similar results were observed when pcDNA-U_S3 of MDV-2 and HVT were transfected (APPENDAIX A, Figure S1D). To further confirm our results in chicken cells, we repeated the same experiment in chicken DF-1 cells. Our results show that transfection of pcDNA-U_S3 increased mRNA level of *c-Fos* in DF-1 cells, but transfection of pcDNA-U_S3-K220A had no effect in *c-Fos* expression when compared to pcDNA Ev (Figure 2-3B). These results suggest that MDV U_S3 could activate CREB target gene expression, presumably through induction of CREB phosphorylation.

As shown above, our results show that MDV U_S3 increases phosphorylation of CREB and up-regulates expression of a CREB target gene. In order to prove if U_S3 is

responsible for activation of pCREB and *c-Fos* expression, we examined MDV U_S3 dependent pCREB recruitment to the *c-Fos* promoter. To study this, 293T cells (Figure 2-3C) or DF-1 cells (Figure 2-3D) were co-transfected with pcDNA-U_S3, pcDNA-U_S3-K220A, or pcDNA-Ev with pcDNA-hCREB or pcDNA-chCREB, respectively. Forty-eight hours post transfection, cells were fixed and subjected to chromatin immunoprecipitation (ChIP) assay with pCREB antibody and normal IgG, followed by qPCR analysis of *c-Fos* promoter as previously reported (147, 148). As shown in Figure 2-3C, compared to U_S3-K220A (gray bar) or Ev (black bar), overexpression of wild type U_S3 (white bar) consistently increased the enrichment of pCREB to the *c-Fos* promoter but not to the *c-Fos* coding region used as negative control (c-Fos_Ng). In addition, the enrichment of pCREB to human *c-Fos* promoter was significantly lower in pcDNA-U_S3-K220A transfected cells when compared with pcDNA-Ev; these results are consistent with above qRT-PCR results, in which overexpression of U_S3-K220A significantly decreased mRNA levels of human *c-Fos* gene (Figure 2-3A). Similar experiments were also performed in DF-1 cells. As shown in Figure 2-3D, the promoter of chicken *c-Fos* was highly occupied by pCREB in pcDNA-U_S3 and pcDNA-chCREB co-transfected cells. Consistent with DF-1 qRT-PCR results (Figure 2-3B), expression of U_S3-K220A did not affect the occupation of pCREB to chicken *c-Fos* promoter. These data suggest that MDV U_S3 up-regulates the expression of CREB target genes by enhancing pCREB levels and further increasing the recruitment of pCREB to target promoters.

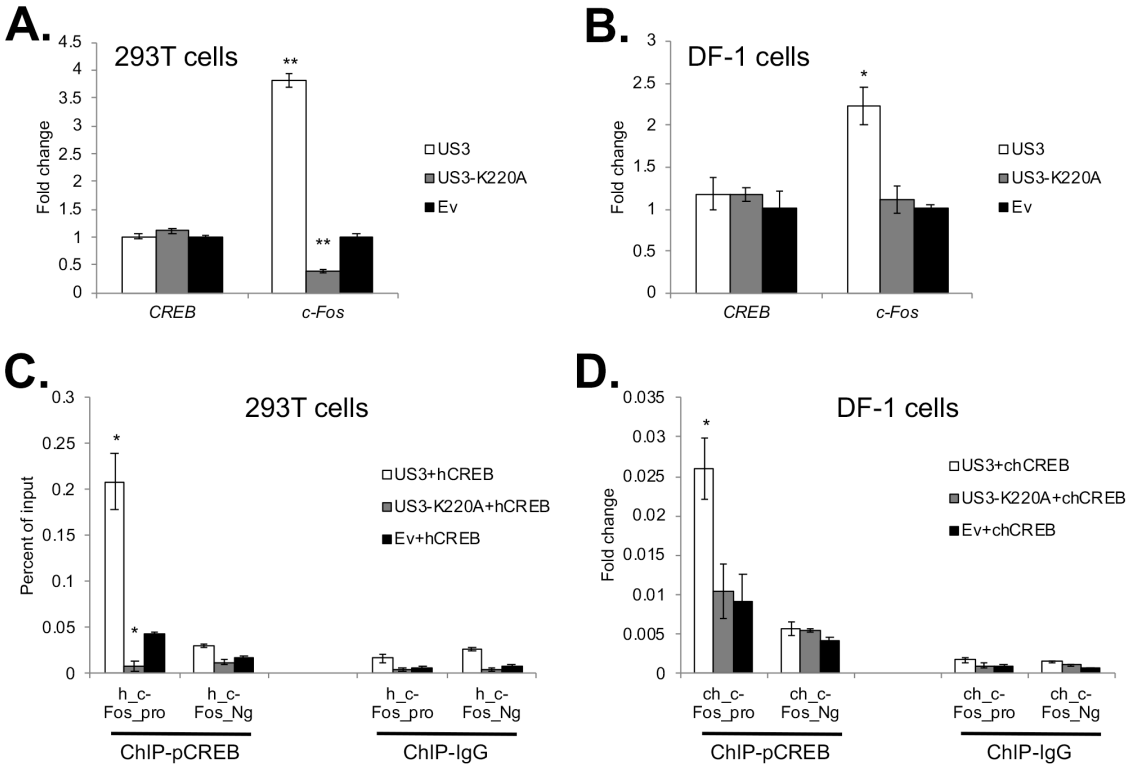

Figure 2-3 Overexpression of MDV U_S3 enhances enrichment of pCREB to the *c-Fos* promoter to up-regulate its expression.
293T cells (A) or DF-1 cells (B) were transfected with pcDNA-U_S3, pcDNA-U_S3-K220A, or pcDNA-empty vector (Ev). Forty-eight hours after transfection, cells were harvested for RNA isolation followed by cDNA synthesis and qRT-PCR analysis for *c-Fos*. qRT-PCR data were analyzed using the $2^{-\Delta\Delta CT}$ method. Human GAPDH or chicken GAPDH were used as an internal control. Data represent average ± standard deviation (SD) of three independent experiments. Values are presented as fold change relative to Ev. 293T cells were co-transfected with pcDNA-U_S3, pcDNA-U_S3-K220A, or pcDNA Ev and pcDNA-hCREB (C) or pcDNA-chCREB (D). Forty-eight hours after transfection, cells were fixed with formaldehyde solution, subjected to chromatin immunoprecipitation (ChIP) assay with rabbit anti-pCREB antibody (left panel) and normal rabbit IgG antibody (right panel) followed by qPCR analysis with the indicated primers. ChIP enrichment signals were normalized to those derived from input DNA control. pro=promoter, Ng=negative control. *: $p<0.05$, **: $p<0.01$.

MDV U_S3 is important for the expression of several MDV genes. In addition to cellular genes, we next performed qRT-PCR with primers specific for 91 MDV encoded genes to determine if MDV U_S3 plays a role in viral gene expression during

infection. To examine the role of U_S3 expression and its kinase activity in regulating viral genes expression in naturally infected cells, CEF were infected with same number of plaque-forming units (PFU) of 686-BAC (parental), 686-BACΔU_S3 (U_S3 null), or 686-BAC_U_S3-K220A (U_S3 kinase dead) viruses. The growth kinetics of these viruses was first determined by viral genome copy number. As reported earlier (64), deletion of U_S3 or U_S3 kinase dead mutant reduced the replication of MDV when compared to parental virus (Figure 2-4B). Seven days after infection with 686-BAC, 686-BACΔU_S3, or 686-BAC_U_S3-K220A viruses, cells were harvested for RNA isolation and cDNA synthesis. MDV gene expression analysis was performed by qRT-PCR and results are shown as heat map in Figure 2-4A, where red color indicates up-regulation and green color indicates down-regulation. Deletion of U_S3 significantly up-regulates 15 MDV genes and down-regulates 19 MDV genes, while inactivation of U_S3 kinase activity significantly up-regulates 14 MDV genes and down-regulates 10 MDV genes. In total 16 MDV genes were regulated differently upon infection with 686-BACΔU_S3 and 686-BAC_U_S3-K220A viruses; we speculate that these differences might be due to a kinase independent function of U_S3. Promoters of highly down-regulated genes (*MDV009* and *MDV058*) that responded to both 686-BACΔU_S3 and 686-BAC_U_S3-K220A viruses were cloned into pGL3, a luciferase reporter vector. Dual luciferase assay was performed to investigate the role of U_S3 and chCREB in regulating the transcription activity of these promoters. Transcriptional activity of *MDV009* promoter (MDV009p) and *MDV058* promoter (MDV058p) were up-regulated in pcDNA-U_S3 transfected cells (purple bar), as well as pcDNA-U_S3 and pcDNA-chCREB co-transfected cells (blue bar)

(APPENDAIX A, Figure S2A). Further, ChIP assay with pCREB antibody was performed with 686-BAC, 686-BACΔU$_S$3, and 686-BAC_U$_S$3-K220A viruses infected cells. Our qPCR results showed that the enrichment of pCREB to the *MDV009* and *MDV058* promoters was significantly higher in 686-BAC than 686-BACΔU$_S$3 and 686-BAC_U$_S$3-K220A viral genomes (Figure 2-4C), indicating that U$_S$3 phosphorylates and activates chCREB to up-regulate expression of both *MDV009* and *MDV058* genes.

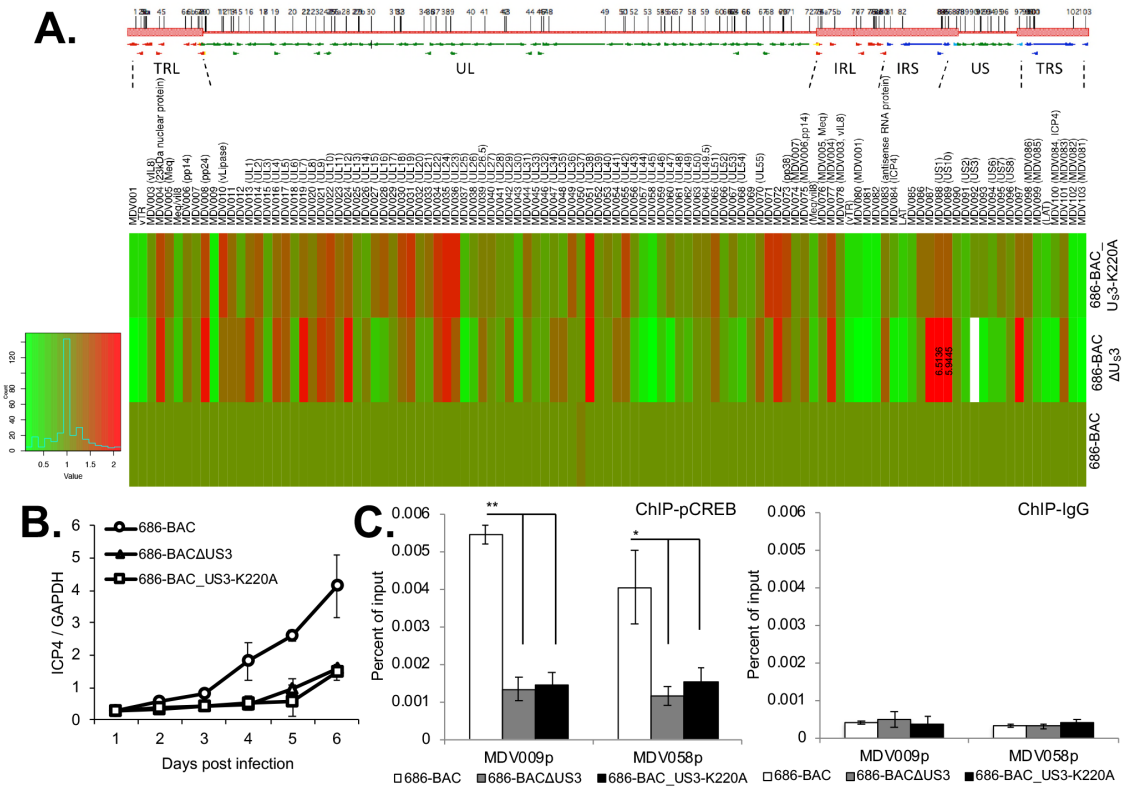

Figure 2-4 MDV U$_S$3 is important for viral gene expression.
CEF were infected with 686-BAC, 686-BACΔU$_S$3, or 686-BAC-U$_S$3-K220A viruses. (A) Seven days after infection, cells were harvested for RNA isolation. RNA was used for cDNA synthesis followed by qRT-PCR analysis with indicated gene primers. qRT-PCR data were analyzed using the $2^{-\Delta\Delta CT}$ method. Chicken GAPDH was used as an internal control. Heat map presents qRT-PCR analysis data as fold change value of each studied gene, in which red color indicates up-regulation and green color indicates down-regulation. To better present the data, *MDV088* and *MDV089* are marked as outliers and labeled with fold change in the heat map. The open reading frame (ORF) map indicating

the location of MDV genes within the MDV genome is shown above the heat map. (B) Cells were harvested for DNA isolation daily after infection. Genome copy number of 686-BAC, 686-BACΔU_S3, and 686-BAC-U_S3-K220A viruses were measured by qPCR. (C) Seven days after infection, cells were fixed with formaldehyde solution and were subjected to ChIP with rabbit anti-pCREB antibody (left panel) and normal rabbit IgG antibody (right panel) followed by qPCR analysis with the indicated primers. ChIP enrichment values were normalized to those derived from input DNA control. NS: not significant,*: $p<0.05$, **: $p<0.01$.

Co-recruitment of MDV Meq and chCREB protein to viral promoters. A previous study by Levy et al (14) showed that Meq forms dimers with CREB. In addition, they showed that CREB target genes closely align with Meq recruitment sites on the MDV genome (14). To confirm a potential association among Meq, U_S3 and CREB, we first determined Meq recruitment sites on the MDV genome using ChIP sequencing (ChIP-seq) analysis. Our results clearly demonstrate that Meq recruitment sites are largely enriched at both repeat regions of the genome, more specifically *meq* and *ICP4/LAT* (Figure 2-5A) regions. As expected from reported studies, Meq indeed formed protein complex with CREB, as well as its coactivators, CBP/p300 in transfected cells (Figure 2-5B). In addition, ChIP-PCR analysis demonstrated that Meq and chCREB are co-recruited to the *LAT* (LATp) and *meq* (MEQp) promoters independent of U_S3 induced phosphorylation, while for MDV009p and MDV058p, recruitment of pCREB is enhanced in the presence of U_S3 (Figure 2-5C & APPENDAIX A, Figure S2B). Further, luciferase assays studies indicated that Meq cooperates with chCREB to activate viral promoters (APPENDAIX A, Figure S2C) and CRE (APPENDAIX A, Figure S2D).

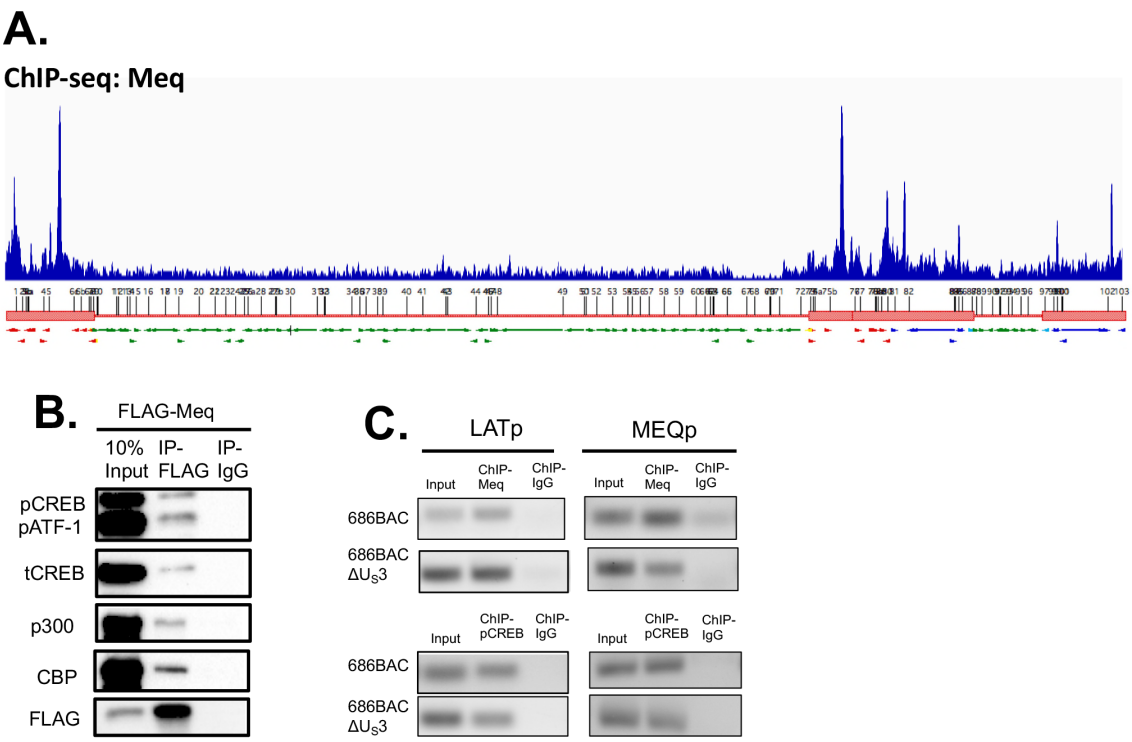

Figure 2-5 Co-recruitment of MDV Meq and chCREB to viral promoters.
(A) Chromatin immunoprecipitation sequencing (ChIP-Seq) analysis of Meq binding to the MDV genome. ChIP enrichment signals were normalized to those derived from input DNA control. (B) 293T cells were transfected with pcDNA-FLAG-Meq. Forty-eight hours after transfection, 500 µg total cell lysates were used for IP with mouse anti-FLAG antibody or normal mouse IgG. WB was performed with the indicated antibodies. (C) CEF were infected with 686-BAC or 686-BACΔUS3 viruses. Seven days after infection, cells were fixed and subjected to ChIP with rabbit anti-Meq antibody, rabbit anti-pCREB antibody or normal rabbit IgG antibody. ChIP-PCRs were performed with the indicated primers.

MDV US3 interacts with and phosphorylates Meq. Next, we examined the physical association between MDV US3 and Meq proteins. Interestingly, our results show that Meq was efficiently coprecipitated by FLAG-US3, while only weakly associated with FLAG-US3-K220A; these results suggest that the kinase activity of US3 is important for its interaction with Meq (Figure 2-6A). In addition, our IFA results show that Meq co-localizes with both wild type US3 and US3-K220A in the cell nuclei

(APPENDAIX A, Figure S3). The interaction between U_S3 and Meq was also examined in CEF cells infected with a recombinant 686-BAC virus containing a C-terminal FLAG tagged U_S3 (686-BAC-U_S3FLAG). Seven days after infection with 686-BAC-U_S3FLAG, CEF were lysed in lysis buffer followed by IP with FLAG antibody, or with normal IgG as a negative control. A previous study showed that MDV U_S3 interacts with MDV pp38 protein (64), we used this interaction as a control. As shown in Figure 2-6B, both Meq and pp38 were coprecipitated by U_S3 protein in IP with FLAG antibody but not with normal IgG.

Finally, *in vitro* kinase assay showed that, similar to other U_S3 protein kinase encoded by other alphaherpesviruses (149, 150), MDV U_S3 exhibits auto-phosphorylation activity (Figure 2-6C(b), lane 1, 3, and 5). In addition, in the presence of U_S3, both pp38 (Figure 2-6C(b), lane 3) and Meq (Figure 2-6C(b), lane 5) are phosphorylated compared to the reactions without U_S3 (Figure 2-6C(b), lane 2 and 4). Total proteins were stained with Coomassie brilliant blue (CBB) (Figure 2-6C (a)). Taken together, these results suggest that MDV U_S3 protein associates with, and phosphorylates Meq. A proposed model of the roles of U_S3, Meq, and CREB in regulating gene expression is illustrated in Figure 2-6D.

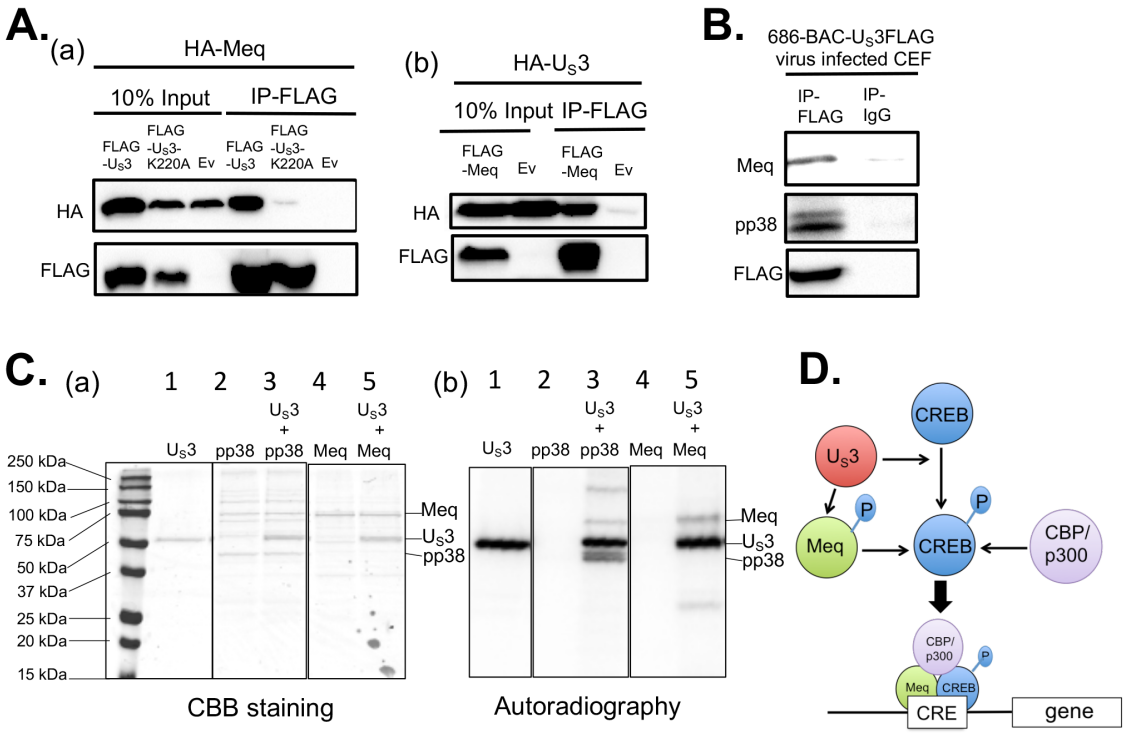

Figure 2-6 MDV U_S3 interacts with and phosphorylates Meq.
(A) 293T cells were transfected with the indicated plasmids. Forty-eight hours after transfection, cells were lysed and subjected to IP with anti-FLAG agarose beads followed by WB with rabbit anti-HA antibody and rabbit anti-FLAG antibody. (B) CEF infected with 686-BAC-U_S3FLAG virus were lysed 7 days later and subjected to IP with mouse anti-FLAG antibody or normal mouse IgG, WB was performed with rabbit anti-Meq antibody, mouse anti-pp38 antibody, and rabbit anti-FLAG antibody. (C) Purified U_S3, Meq and pp38 proteins were subjected to *in vitro* kinase assay followed by Coomassie brilliant blue (CBB) staining (a) and autoradiography (b). (D) Schematic representation of the roles of U_S3, Meq, CREB, and CBP/p300 in regulating gene expression. MDV Meq cooperates with pCREB-CBP/p300 complexes to activate gene expression.

2.3. Discussion

Post-translational modifications, such as methylation, phosphorylation, ubiquitylation and SUMOylation, play an important role in regulating target protein functions including gene regulation, protein stability, and protein-protein interactions

(151). Among such modifications, phosphorylation is one of the most common and extensively studied, which affects a variety of viral and cellular processes.

Previous reports indicated that alphaherpesviruses encoded U_S3 serine/threonine protein kinase is a multifunctional protein, which is involved in virus replication, virion morphogenesis, viral and cellular gene expression regulation, actin cytoskeleton remodeling, and anti-apoptosis (41). U_S3 of all alphaherpesviruses contains a highly conserved ATP-binding domain and a catalytic active site, even though overall U_S3 amino acid sequence similarity varies among different alphaherpesviruses. Among them, the substrates and functions of HSV-1 U_S3 have been widely explored. HSV-1 U_S3 phosphorylates viral proteins, including UL31, UL34, glycoprotein B (gB), dUTPase (22, 51, 152); cellular proteins such as p65, HDAC-1, HDAC-2, PDCD4, CREB, interferon regulatory factor 3 (IRF3), and cellular motor protein KIF3A (45, 49, 58-60). Initial characterization of MDV encoded U_S3, showed that MDV U_S3 is not essential for virus growth in cell culture, although U_S3 null virus and U_S3 kinase dead virus induced smaller plaques and exhibited reduced growth rate in infected CEF compared to parental virus (64, 65).

To study the role of MDV U_S3, we first performed a series of luciferase assays to explore the cellular signaling pathways in which U_S3 is involved. The reporter vector pGL4-CRE was highly responsive to expression of MDV U_S3. A few other signaling pathways, including KLF4, ATF6, HNF4 and PPAR, were also responsive to U_S3 overexpression (Figure 2-1). Cellular kinases target multiple other cellular kinases for cross talk, thus U_S3 may activate one or more cellular kinases which may be responsible

for multiple downstream signal activation detected in our screening. Future proteomics studies may comprehensively reveal U_S3 direct and indirect substrates. Nonetheless, we were able to demonstrate that overexpression of MDV U_S3 enhanced phosphorylation of CREB (Figure 2-2), although we currently do not know if U_S3 directly or indirectly phosphorylates CREB. CREB responds to multiple stimuli such as growth factors, peptide hormones and Ca2+ influx, and CREB activates diverse array of target genes that are important for cell proliferation, differentiation, and neuronal development (137, 153). Since CREB is phosphorylated by various cellular kinases, the exact mechanisms utilized by MDV U_S3 to increase CREB phosphorylation remain to be elucidated. Importantly, the ability of MDV U_S3 to induce CREB phosphorylation is conserved among all three MDV serotypes (APPENDAIX A, Figure S1), despite of relatively low sequence identity between MDV U_S3 and MDV-2 (59%) or HVT U_S3 (60%). Induction of MDV U_S3-mediated CREB phosphorylation increases the recruitment of pCREB to the *c-Fos* promoter, resulting in activation of *c-Fos* expression (Figure 2-3), and indicating that MDV U_S3 alone can modulate cellular signaling pathways through activation of CREB.

Taking advantages of a well-established two-step red-mediated recombination system, we generated MDV U_S3 deletion (686-BACΔU_S3) and U_S3-K220A kinase dead mutant (686-BAC_U_S3-K220A) viruses. Infection of cells with 686-BACΔU_S3 and 686-BAC_U_S3-K220A mutant viruses in combination with a newly established MDV qPCR array revealed that MDV U_S3 is involved in the regulation of 34 MDV genes and kinase activity of U_S3 is important for the expression of 24 MDV genes (Figure 2-4). The

existence of genes differentially regulated upon infection with 686-BACΔUS3 and 686-BAC_US3-K220A viruses suggests that US3 may have kinase-independent activities that are involved in regulating viral gene expression. Among these MDV US3 activated genes, the *MDV009* (uncharacterized gene 9 protein) and *MDV058* (UL45) promoters of MDV 686-BAC have significantly higher occupancy of pCREB compared to MDV 686-BACΔUS3 and 686-BAC_US3-K220A viruses (Figure 2-4). Using the online promoter analysis tool, PROMO (http://alggen.lsi.upc.es/cgi-bin/promo_v3/promo/promoinit.cgi?dirDB=TF_8.3) we could not find the full length CRE motif (TGACGTCA) in these promoters. Instead, we found some predicted c-Jun and c-Fos binding sites, which are also the MDV Meq binding motif. In addition, previous work showed that only 26% of CREB binding sites contain full length CRE (154). We speculate that pCREB might be recruited though the non-consensus motif by Meq or other bZIP factors to these promoters. In addition, it is interesting to note that most of the ORFs located in the IRS/TRS were dramatically down-regulated by deletion of US3. This is supported by RNA-seq studies with chicken T-cell lymphomas which showed that these regions are transcriptionally highly active (manuscript under preparation), and also have multiple Meq binding sites (14).

We speculate that Meq and CREB co-regulate these genomic regions as our ChIP-seq and ChIP-PCRs demonstrated that Meq and CREB are co-recruited to the *LAT* and *meq* promoters (Figure 2-5). Based on these results we propose that one of the biological functions of MDV US3 is to ensure that those genomic regions are activated in the event that active cellular kinase signaling pathways are unavailable in the infected

cells. Another interesting observation is that the interaction between Meq and U_S3 is phosphorylation dependent; indicating that additional proteins may be recruited to Meq by U_S3 mediated phosphorylation, facilitating the formation of protein complex. This raises an interesting possibility that MDV U_S3 could trigger protein complex assembly, similar to what cellular ATR/ATM does (155). Although a previous study showed that CDK2 phosphorylation of Meq at Serine 42 translocates Meq to the cytoplasm and decreases the DNA binding activity of Meq (110), we did not find that co-transfection of MDV U_S3 altered the subcellular localization of Meq (APPENDAIX A, Figure S3), indicating that MDV U_S3 might target a serine/threonine residue different from CDK2. Further studies are needed to map the U_S3 phosphorylation site of Meq and subsequent generation of Meq phosphorylation mutant viruses to explore the role of Meq phosphorylation in MDV pathogenesis and tumorigenesis. We suggest that viral kinases could play important roles in overriding key cellular signaling pathway to aid MDV replication. Taken together, our studies clearly demonstrated one of the functions of MDV U_S3 is regulation of viral and cellular transcriptions through CREB activation.

2.4. Materials and methods

Cell culture. Primary chicken embryonic fibroblasts (CEF), prepared from 10-11 day old chicken embryos, were grown in Leibowitz–McCoy (LM, 1:1) medium supplemented with 5% newborn calf serum at 37°C in the presence of 5% CO_2. DF-1, a chicken fibroblast cell line, and 293T, a human embryonic kidney epithelial cell line,

were grown in Dulbecco's modified Eagle medium (DMEM) supplemented with 10% fetal bovine serum, in the presence of 5% CO_2.

Mutagenesis of MDV 686-BAC. Deletion of U_S3 gene from MDV 686-BAC was performed by two-step red-mediated recombination as described previously (156). All primers used for MDV 686-BAC mutagenesis are listed in Table 2-1. Briefly, the entire U_S3 open reading frame (ORF) was first replaced with kanamycin resistance (*Kan*^{R}) gene amplified from plasmid pEPKan-S using primers U_S3-Kan-F and U_S3-Kan-R. Next, *Kan*^{R} gene was deleted by inducing the expression of I-*Sce*I with addition of 1% arabinose to the bacteria growth media to generate 686-BACΔU_S3.

To generate 686-BAC-U_S3FLAG, U_S3 ORF with C-terminal FLAG tag was cloned into pUC19 plasmid to generate pUC19-U_S3FLAG. To generate 686-BAC_U_S3-K220A, lysine (K) 220 of U_S3 was mutated to alanine (A) using primers U_S3-K220A-F and U_S3-K220A-R to generate pUC19-U_S3-K220A. Then, *Kan*^{R} gene was amplified with primers U_S3EcoRVKan-F and U_S3EcoRVKan-R with pEPKan-S plasmid as the template. The amplified product was digested and cloned into the EcoRV site of pUC19-U_S3FLAG or pUC19-U_S3-K220A to generate pUC19-U_S3FLAG-Kan or pUC19-U_S3-K220A-Kan. Next, the Us3-FLAG or U_S3-K220A with *Kan*^{R} insertion was amplified with primers U_S3-F and U_S3FLAG-R to generate Us3FLAG-Kan or U_S3-K220A-Kan transfer cassette, which was transfected by electroporation into competent cells carrying 686-BACΔU_S3 DNA to generate 686-BAC-U_S3FLAG or 686-BAC_U_S3-K220A. BAC DNA of 686-BACΔU_S3, 686-BAC-U_S3FLAG, and 686-BAC_U_S3-K220A were transfected

into CEF by the calcium phosphate precipitation method to produce recombinant viruses.

Table 2-1 List of primers used in mutagenesis of MDV 686-BAC.

Primer	Sequence (5' to 3')
U_S3-Kan-F	TTATACTCTGGTAGAATATGAAACAGGGTTAAAACTAGGTAA TAGACTGGAGGATGACGACGATAAGTAGGG
U_S3-Kan-R	TAGTATATATTATAAAATGAATCATTGAAGTTATTTTTGACGG GTGTTTACCAGTCTATTACCTAGTTTTAACCCTGTTTCATATT CTACCAGAGTATAACAACCAATTAACCAATTCTGATTAG
U_S3-K220A-F	TGATGTAGCAACTGAAAATA
U_S3-K220A-R	TATTTTCAGTTGCTACATCA
U_S3EcoRVKan-F	GATC**GATATC**ATGGGACCATTGCCACTAAATCAAATAATTAC GATAGAACGGGGTTTGCTAGGATGACGACGATAAGTAGGG
U_S3EcoRVKan-R	GATC**GATATC**CAACCAATTAACCAATTCTGATTAG
U_S3-F	TTATACTCTGGTAGAATATGAAACAGGGTTAAAACTAGGTAA TAGACTGGATGTCTTCGAGTCCGGAGGC
U_S3FLAG-R	GCGTAGTATATATTATAAAATGAATCATTGAAGTTATTTTTGA CGGGTGTTTACTTGTCGTCATCGTCTTTGTAGTCCATATGAG CGGCAGTTATCG

* The sequences underlined are homologous of pEPKan-S plasmid and were used to amplify the *Kan*^{R} gene cassette. The sequences in bold are restriction enzyme sites.

Immunofluorescence assay (IFA). One day before transfection, 293T cells were seeded on coverslips placed in 6-well plates. Next day, pcDNA-HA-U_S3 or pcDNA-HA-U_S3-K220A plasmid were co-transfected, using polyethylenimine (PEI, 1 mg/ml), with pcDNA-FLAG-Meq expression plasmid into 293T cells. Forty-eight hours after transfection, cells were fixed with 3.7% formaldehyde-PBS for 5 min at room temperature followed by three washes with PBS. Then, cells were permeabilized with 1.0% Triton X-100 and 1.0% NP-40 in PBS for 10 min respectively, followed by three washes with PBS. After blocking with 5% nonfat milk for 1 hour at room temperature,

cells were incubated with mouse anti-HA antibody and rabbit anti-FLAG antibody for 1 hour followed by another hour incubation with goat anti-mouse-Texas Red and goat anti-rabbit-Alex Flour 488 antibodies at room temperature. After three washes with PBS, cells were stained with 4', 6-diamidino-2-phenylindole (DAPI) for 5 min at room temperature. Cells on coverslips were mounted on glass slides with ProLong™ Diamond Antifade Mountant and visualized with a Zeiss LSM 780 NLO Multiphoton Microscope.

Immunoprecipitation (IP) and Western blot (WB) assay.

IP with cell lysates isolated from 293T and DF-1 cells. 293T and DF-1 cells were seeded onto 60 mm plates one day before transfection with the indicated plasmids and PEI reagent. Forty-eight hours after transfection, cells were lysed using EBC lysis buffer (50 mM Tris-HCl, 120 mM NaCl, 0.5% NP-40, 50 mM NaF, 200 μM Na_2VO_4, 1 mM phenylmethylsulfonyl fluoride) supplemented with protease inhibitors as described previously (35). 500 μg cell lysates were incubated with 25 μl of anti-FLAG agarose beads (Sigma) overnight at 4°C with gentle rotation. Next day, agarose beads were washed five times with EBC lysis buffer and boiled for 5 min in 2x sodium dodecyl sulfate (SDS) loading buffer. 10% input control (50 μg cell lysates) together with immunoprecipitated samples were applied for SDS-polyacrylamide gel electrophoresis (PAGE) and transferred to polyvinylidene difluoride (PVDF) membrane (Millipore). PVDF membranes were blocked with 5% nonfat milk in PBS containing 0.1% Tween 20 (PBST) for 1 hour at room temperature, followed by incubation with primary antibody overnight at 4°C and horseradish peroxidase (HRP) conjugated secondary antibodies for 1 hour at room temperature. After three washes with PBST, membranes were visualized

with Super Signal West Pico PLUS Chemiluminescent Substrate (Thermo Fisher Scientific) using ChemiDoc™ MP Imaging System (Bio-Rad).

IP with cell lysates from recombinant 686-BAC-U$_S$3FLAG virus infected CEF. Seven days after infection with recombinant virus, CEF were harvested for protein extraction with EBC lysis buffer supplemented with protease inhibitors. 500 µg cell lysates were incubated with 2 µg mouse anti-FLAG antibody (Sigma) or normal mouse IgG (Cell Signaling Technology) overnight at 4°C with gentle rotation. Next day, 25 µl of protein A and protein G Sepharose beads (Invitrogen) mixture were added to the immune complex and rotated for 2-3 hours at 4°C, followed by five washes with EBC lysis buffer and then subjected to SDS-PAGE and WB analysis as described above. Quantification of WB bands intensity was performed with Image J software.

Generation of recombinant baculoviruses and protein purification.

Spodoptera frugiperda Sf9 cells were maintained in EX-CELL 420 medium (Simga). Recombinant baculoviruses expressing N-terminal FLAG tagged U$_S$3, Meq and pp38 were generated using Bac-to-Bac® Baculovirus Expression System (Invitrogen) according to the manufacturer's instruction. Briefly, entire ORF of U$_S$3, Meq and pp38 were cloned into pFastBac1-FLAG vector followed by transformation of DH10Bac *E. coli* to generate the recombinant bacmid. Recombinant bacmid DNA was transfected into Sf9 cells with PEI reagent to generate recombinant viruses. Protein expression was confirmed by WB with anti-FLAG antibody (Thermo Fisher Scientific). To produce and purify large amounts of proteins, 100 ml Sf9 cells were infected with recombinant baculovirus, which were harvested and lysed two days post infection. Then, FLAG

tagged proteins were captured with anti-FLAG agarose beads (Sigma) and eluted with 3x FLAG peptide (Sigma) as described previously (35). Concentration of purified proteins was measured with SDS-PAGE using bovine serum albumin (BSA) as a standard.

***In vitro* kinase assay.** *In vitro* kinase assay was performed as described previously (35). Briefly, purified protein kinase (MDV U_S3) was incubated with purified substrates (MDV Meq or pp38) in kinase buffer supplemented with 10 μCi [γ-^{32}P] ATP at 37°C for 30 min. The reaction was stopped by adding 2x SDS loading buffer, and samples were then subjected to electrophoresis followed by Commassie brilliant blue (CBB) staining. The gel was then dried and subjected to autoradiography.

RNA isolation and quantitative reverse transcriptase polymerase chain reaction (qRT-PCR). Transfected 293T or DF-1 cells, and infected CEF were harvested for RNA isolation using TRIzol reagent (Invitrogen) as per manufacturer's protocol. Dnase I (Ambion) treatment was carried out after total RNA isolation following manufacturer's instructions. 1-5 μg of total RNA from each sample was used for cDNA synthesis with Oligo(dT)$_{12-18}$ primer (Invitrogen) using M-MLV Reverse Transcriptase (M-MLV RT, Invitrogen). qRT-PCR reaction was performed with iCycler iQ™ Real-Time PCR Detection System (Bio-Rad) using iTaq™ Universal SYBR® Green Supermix (Bio-Rad). A melt curve analysis was performed to confirm the amplification of a single product. Experiments were repeated three times in triplicate. Gene expression was normalized to GAPDH signal, and the qRT-PCR data was analyzed using the $2^{-\Delta\Delta CT}$ method (157).

Genomic DNA isolation and MDV genome copy number. The extraction of genomic DNA from infected CEF was performed using a standard phenol-chloroform protocol, as previously described (158). MDV genome copy number was determined by qPCR assay with specific primers to MDV *ICP4* and chicken *GAPDH* modified from previously described protocol (159).

Dual luciferase reporter (DLR) assays. 293T cells were seeded on 12-well plates one day before transfection. The indicated plasmids were transfected together with reporter and *Renilla* luciferase vectors. Two days after transfection, firefly and *Renillla* luciferase activity were measured for each sample using Dual-Glo® Luciferase Assay System (Promega) according to manufacturer's instruction. For data analysis, firefly luciferase data was normalized to *Renillla* luciferase activity, and fold changes were calculated by comparing the values generated with empty vector transfected cells. Experiments were repeated three times in triplicate, and fold changes were shown as average ± standard error of the mean (SEM).

Chromatin immunoprecipitation (ChIP) and ChIP-seq analysis. ChIP assays were performed as described previously with minor modifications (14). Briefly, transfected 293T and DF-1 cells or infected CEF were fixed with 1% formaldehyde solution for 10 min at room temperature with gentle shaking and quenched with glycine. Chromatin was sheared using a Diagenode Bioruptor to an average size of about 300 bp, and diluted 1:10 followed by incubation with antibody at 4°C overnight with gentle rotation. 1% of diluted chromatin was collected to serve as input control and stored at -20°C until used. Next day, chromatin immunocomplexes were incubated with BSA-

blocked magnetic protein A/G Dynabeads for 2-3 hours at 4°C with gentle rotation. Chromatin immunocomplexes were then collected and washed four times. Immunoprecipitated chromatin was eluted in elution buffer by heating at 65°C for 30 min. Eluted chromatin and 1% input control were reverse crosslinked by incubating at 65°C overnight in the presence of 0.2 M sodium chloride (NaCl) followed by purification with PCR purification kit (Qiagen) according to manufacturer's instruction. PCR or qPCR analyses were performed in triplicate with input DNA (1:50 dilution) and ChIP DNA (1:5 dilution). ChIP enrichment signals were normalized to those derived from the input DNA control. Data represent average ± standard deviation of triplicate.

ChIP-seq analysis was performed as described previously (160). Briefly, Chromatin DNA from 1 x 10^8 chicken T-cell lymphoma cell line (SR8136) were used to precipitate Meq bound chromatin with 10 μg of rabbit anti-Meq antibody. ChIP enriched or input DNA was used to generate Illumina-compatible libraries with KAPA LTO Library preparation Kit (Kapa Biosystems) according to manufacturer's recommendations. Libraries were submitted for sequencing on an Illumina HiSeq 2500 sequencing system. The ChIP-Seq data was aligned to the Gullus_gullus-5.0; GCA_000002315.3 of the chicken genome by using the Bowtie 2 algorithm, and all the redundant tags were removed by trimmomatic algorithm. Peak calling was performed using MACS2 program with combined input as a reference set. The peaks and reads alignments were visualized using the Integrative Genomics Viewer (IGV) from Broad Institute.

3. MAREK'S DISEASE VIRUS U_S3 PROTEIN KINASE PHOSPHORYLATES CHICKEN HDAC 1 AND 2 AND REGULATES VIRAL REPLICATION AND PATHOGENESIS [*]

3.1. Introduction

Marek's disease virus (MDV), an avian alphaherpesvirus, is the etiological agent of Marek's disease (MD) which is associated with rapid induction of T-cell lymphomas in chickens. Currently, three antigenically related MDVs have been identified and sequenced, including MDV-1 (also known as *Gallid alphaherpesvirus* 2 [GaHV-2]), MDV-2 (also known as *Gallid alphaherpesvirus* 3 [GaHV-3]), and turkey herpesvirus (HVT; also known as *Meleagrid alphaherpesvirus* type 1 [MeHV-1] or MDV-3) (2). Only MDV-1 can cause tumors in infected chickens, while MDV-2 and HVT are naturally non-oncogenic viruses from chickens and turkeys, respectively. Attenuated MDV-1 along with MDV-2 and HVT have been used, alone or in combination, as vaccines to protect susceptible chickens from MD. MDV is classified as a member of the *Alphaherpesvirinae* subfamily, which also includes animal herpesviruses such as pseudorabies virus (PRV) and bovine herpesvirus type 1 (BHV-1), as well as human herpesviruses such as herpes simplex virus type 1 and 2 (HSV-1 and -2) and varicella zoster virus (VZV). The genome of MDV-1 is approximately 177 kb in length and

---

[*]Reprinted with permission from "Marek's disease virus U_S3 protein kinase phosphorylates chicken HDAC 1 and 2 and regulates viral replication and pathogenesis" by Yifei Liao, Blanca Lupiani, Mohammad AI-Mahmood, Sanjay M. Reddy, 2021. *PLOS Pathogens*, Volume 17, Issue 2, Copyright [2021] by Liao et al.

encodes more than 100 genes (4). Most MDV-1 genes have homologues in other alphaherpesviruses and share similar functions, except some unique MDV genes such as *meq* and *vTR* which are directly involved in MDV oncogenicity (11, 130).

Like other alphaherpesviruses, MDV encodes a U_S3 serine/threonine protein kinase which has been shown to be involved in apoptosis resistance, actin stress fiber breakdown and cell-to-cell spread (64, 65). The U_S3 orthologs contain a conserved ATP-binding domain and a catalytic active domain, although the complete U_S3 protein sequence similarity is variable (41). Compared to other alphaherpesviruses, HSV-1 and PRV U_S3 genes contain two characterized transcriptional start sites and encode two overlapping isoforms named U_S3 and $U_S3.5$ (42, 44). It has been reported that U_S3 is important for virus growth *in vitro*, as deletion of U_S3 results in growth deficiency of HSV-1, PRV, VZV, and MDV (41). In addition, various functions have been attributed to U_S3, such as apoptosis resistance, virion morphogenesis, transcriptional regulation, and cytoskeletal re-arrangements (41). As a viral protein kinase, the substrates of HSV-1 U_S3 have been extensively studied. Viral proteins such as ICP22, glycoprotein B, UL31 and UL34 have been identified as substrates of HSV-1 U_S3 (161). It also phosphorylates cellular proteins such as lamin A/C, Bad, and programmed cell death protein 4 (PDCD4) (161). In addition, Walters *et al.* have identified histone deacetylase 1 (HDAC1) and HDAC2 (HDAC1 and 2) as conserved targets of VZV, HSV-1, and PRV U_S3 orthologs (58, 162). Schumacher *et al.* demonstrated that MDV-1 U_S3 interacts with and phosphorylates viral protein pp38, an MDV protein involved in early lytic infection in lymphocytes (64). We have recently identified MDV-1 Meq and cellular cAMP response

element-binding protein (CREB) as targets of MDV-1 U_S3 (163). In addition, we have shown that MDV-1 U_S3 induced CREB phosphorylation up-regulates the transcription of *c-Fos* and several viral genes (163).

Histone deacetylases (HDACs) are a class of enzyme that can reverse the acetylation of histone lysine residues (164). Currently, eighteen HDACs have been identified in mammals and are grouped into four classes: class I consists of HDAC1, 2, 3, and 8; class II consists of HDAC4, 5, 6, 7, 9, and 10; class III consists of seven NAD^+-dependent Sirtuin 1-7; and class IV has only one member, HDAC11 (102). Class I HDACs are expressed in all tissues and play crucial roles in tissue development, cell differentiation and proliferation, and cancer formation (102, 165). More specifically, HDAC1 and 2 are highly homologous proteins and show conserved or specific functions depending on the stimuli (102). HDAC1 and 2 not only act as protein modifiers, but are in turn modified by other cellular regulators mainly through three mechanisms: post-translational modifications, protein interaction network, and subcellular localization (102). Casein kinase II (CKII), the main upstream protein kinase of HDAC1 and 2, phosphorylates HDAC1 at serine 393 (S393), S421 and S423, and HDAC2 at S394, S422 and S424. CKII mediated phosphorylation of HDAC1 and 2 has been shown to regulate their catalytic activity and protein interactions (103, 104, 166). As stated above, HDAC1 and 2 are also phosphorylated by alphaherpesviruses U_S3 serine/threonine protein kinase (162). In addition, it has been reported that overexpression of HSV-1 U_S3 affects the amount and distribution of HDAC1 (167). The phosphorylation sites of HDAC1 and HDAC2 targeted by HSV-1 U_S3 and VZV ORF66 (the U_S3 ortholog in

VZV) have been identified as S406 and S407, respectively (58, 162). It has been shown that inhibition of HDAC activity increases the plaque size and plaquing efficiency of U_S3 null VZV and PRV, suggesting that U_S3 targets HDACs to reduce viral genome silencing and allow for efficient viral replication (58).

In this study, we investigated the role of MDV U_S3 in the phosphorylation of chicken HDAC1 and 2 (chHDAC1 and 2). Our results show that U_S3 of all three MDV serotypes can phosphorylate chHDAC1: MDV-1 and HVT U_S3 target chHDAC1 at S406, while MDV-2 U_S3 has two more target sites, S410 and S415. On the other hand, we found that MDV-1 U_S3 phosphorylates chHDAC2 at S407 and MDV-2 U_S3 phosphorylates chHDAC2 at S407 and S411; however, chHDAC2 is not a substrate of HVT U_S3. We further characterized the impact of MDV U_S3 induced phosphorylation in regulating chHDAC1 and 2 functions. Our results show that MDV U_S3 induced phosphorylation regulates protein stability, transcriptional regulation activity, and protein interactions of chHDAC1 and 2. We also found that U_S3 from all three MDV serotypes physically interacts with chHDAC1 and 2. In addition, using a natural virus-host model, we demonstrated that MDV-2 and HVT U_S3 partially compensate the function of MDV-1 U_S3 associated with MDV-1 replication and pathogenesis. Overall, our results reveal the role of U_S3 from all three MDV serotypes in regulating phosphorylation of chHDAC1 and 2, as well as in viral replication and pathogenesis.

3.2. Results

MDV U_S3 phosphorylates chHDAC1 and 2. To study if U_S3 of all three MDV serotypes phosphorylates chHDAC1 and 2, we examined the electrophoretic mobilities of chHDAC1 and 2 upon transfection of MDV U_S3. As shown in Figure 3-1A, transfection of 293T cells with pcDNA expressing wild type U_S3 from MDV-1, MDV-2, and HVT resulted in an additional slow migrating protein species of FLAG-chHDAC1 when compared to kinase dead U_S3 (K220A for MDV-1 U_S3, K211A for MDV-2 U_S3, and K212A for HVT U_S3) and empty vector (Ev) transfected cells. Interestingly, the amount of the higher molecular weight FLAG-chHDAC1 protein in wild type MDV-2 U_S3 transfected cells was higher than in MDV-1 U_S3 and HVT U_S3 transfected cells (Figure 3-1A). Similar results were observed for chHDAC2, except that we could not detect larger species of chHDAC2 in wild type HVT U_S3 transfected cells (Figure 3-1B). Next, the electrophoretic mobilities of endogenous chHDAC1 and 2 were examined in chicken DF-1 cells. After transfecting with pcDNA expressing wild type U_S3, kinase dead U_S3 or Ev, whole cell lysates were subjected to Western blot (WB) analysis with HDAC1 and 2 antibodies to specifically detect endogenous chHDAC1 and 2. Our results show that transfection of wild type MDV-1 and MDV-2 U_S3, but not HVT U_S3, led to two closely migrating chHDAC1 protein species. In addition, similar to Ev, transfection of kinase dead U_S3 of all three MDV serotypes did not result in modification of chHDAC1 as indicated by a single lower chHDAC1 protein band (Figure 3-1C, first panel). On the other hand, although transfection of wild type U_S3, kinase dead U_S3 or Ev resulted in two closely migrating chHDAC2 protein species, the amount of the larger

molecular weight endogenous chHDAC2 was higher in wild type MDV-1 and MDV-2 U_S3 transfected cells (Figure 3-1C, second panel). To determine if the higher molecular weight species of chHDAC1 and 2 were the result of phosphorylation, we performed dephosphorylation assay using Lambda protein phosphatase (Lambda PP). Whole cell lysates extracted from HA tagged MDV-1 U_S3 or Ev and FLAG-chHDAC1 or FLAG-chHDAC2 cotransfected 293T cells were either mock treated or treated with Lambda PP, followed by WB to examine the protein mobility. In mock treated samples, transfection with wild type MDV-1 U_S3 resulted in additional slow migrating protein species of chHDAC1 and 2, which were completely eliminated by Lambda PP treatment (Figure 3-1D), indicating MDV-1 U_S3 induced modification of chHDAC1 and 2 is due to phosphorylation.

Considering that U_S3 from all three MDV serotypes showed distinct ability to phosphorylate chHDAC1 and 2, we investigated whether the same applies to other substrates. It has been shown previously that HSV-1 U_S3 mimics the function of cellular protein kinase A (PKA) (132). Here, we determined the ability of U_S3 from all three MDV serotypes to phosphorylate substrates of cellular protein kinases, including PKA, protein kinase C (PKC), and AMP-activated protein kinase (AMPK). Our results show that wild type MDV-1 and MDV-2 U_S3 strongly increased the phosphorylation of PKA, PKC, and AMPK, while HVT U_S3 only slightly increased their phosphorylation (APPENDIX A, Figure S4).

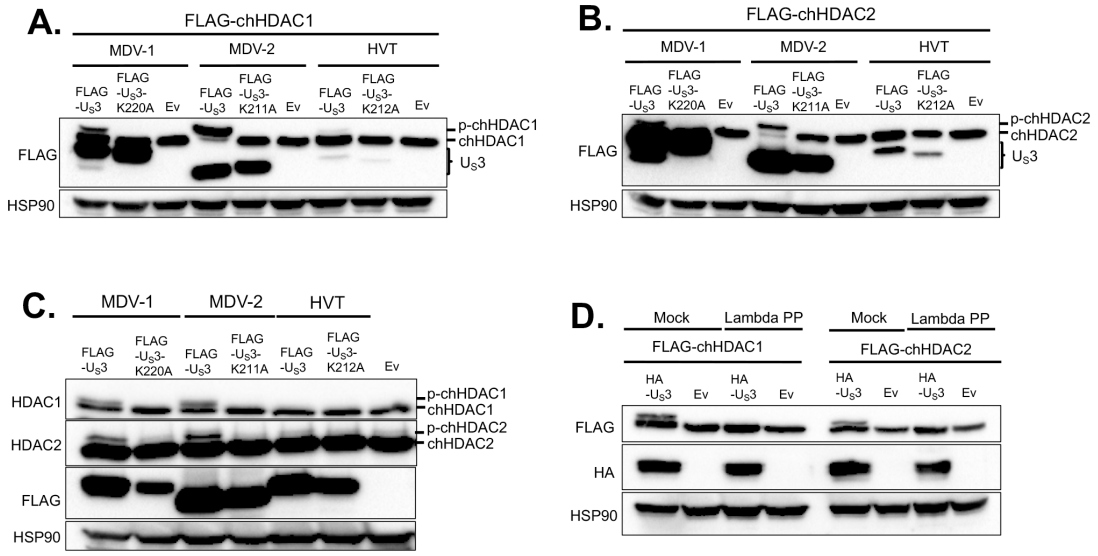

Figure 3-1 MDV U_S3 mediates the phosphorylation of chHDAC1 and 2. pcDNA-FLAG-chHDAC1 (A) or pcDNA-FLAG-chHDAC2 (B) were cotransfected with pcDNA FLAG tagged wild type MDV-1, MDV-2, or HVT U_S3, kinase dead U_S3 (pcDNA-FLAG-U_S3-K220A for MDV-1, pcDNA-FLAG-U_S3-K211A for MDV-2, and pcDNA-FLAG-U_S3-K212A for HVT), or pcDNA empty vector (Ev) to 293T cells. Forty-eight hours later, cells were lysed and subjected to Western blot (WB) analysis with FLAG antibody. HSP90 was stained as loading control. (C) DF-1 cells were transfected with the indicated plasmids for 48 hours, followed by WB with HDAC1, HDAC2, FLAG, and HSP90 antibodies. (D) pcDNA-FLAG-chHDAC1 (left) or pcDNA-FLAG-chHDAC2 (right) were cotransfected with pcDNA-HA-MDV-1-U_S3 or pcDNA Ev into 293T cells for 48 hours. Whole cell lysates were either mock treated or treated with Lambda protein phosphatase (Lambda PP) prior to SDS-PAGE. WB was carried out with FLAG, HA, and HSP90 antibodies.

Identification of the chHDAC1 and 2 phosphorylation sites targeted by MDV U_S3. It has been reported that HSV-1 U_S3, VZV ORF66, and PRV U_S3 phosphorylate HDAC1 at S406 and HDAC2 at S407 (58, 162). We were interested in identifying chHDAC1 and 2 phosphorylation sites targeted by MDV U_S3. Because most post-translational modifications of HDAC1 and 2 happen at their C-terminal end, we first compared the C-terminal amino acid sequences of human HDAC1 and 2 with

chicken HDAC1 and 2. Amino acid sequence alignments show that there are conserved serine (S) and threonine (T) sites (bold underlined) between human and chicken HDAC1 and 2, while there are also some unique S and T sites (bold italics) in chicken HDAC1 protein (Figure 3-2A).

Based on previous reports (162), we first mutated five conserved S sites (Figure 3-2A, marked with asterisk) in chHDAC1 and 2 to alanine (A). pcDNA expressing FLAG-chHDAC1 mutants were cotransfected with wild type MDV-1, MDV-2, HVT U_S3, or Ev. After 48 hours, cells were lysed and subjected to WB to examine the electrophoretic mobilities of chHDAC1 mutants. As shown in Figure 3-2B, mutation of S406A completely blocked chHDAC1 phosphorylation mediated by MDV-1 and HVT U_S3 as the larger protein species was eliminated, while other mutations, including S393A, S401A, S421A, and S423A, had no effect in MDV-1 and HVT U_S3 induced chHDAC1 phosphorylation. Interestingly, we could still detect the chHDAC1 slow migrating protein species in the S406A mutant and MDV-2 U_S3 cotransfected cells suggesting that MDV-2 U_S3 has additional target sites (Figure 3-2B). For chHDAC2, we could not detect larger protein species in the S407A mutant and MDV-1 U_S3 cotransfected cells, indicating that S407 of chHDAC2 is the only target site for MDV-1 U_S3 (Figure 3-2C). Similarly, MDV-2 U_S3 has more targets in chHDAC2 as S407A mutation could not completely inhibit chHDAC2 phosphorylation (Figure 3-2C). Consistent with above result (Figure 3-1B), HVT U_S3 did not induce phosphorylation of chHDAC2 (Figure 3-2C).

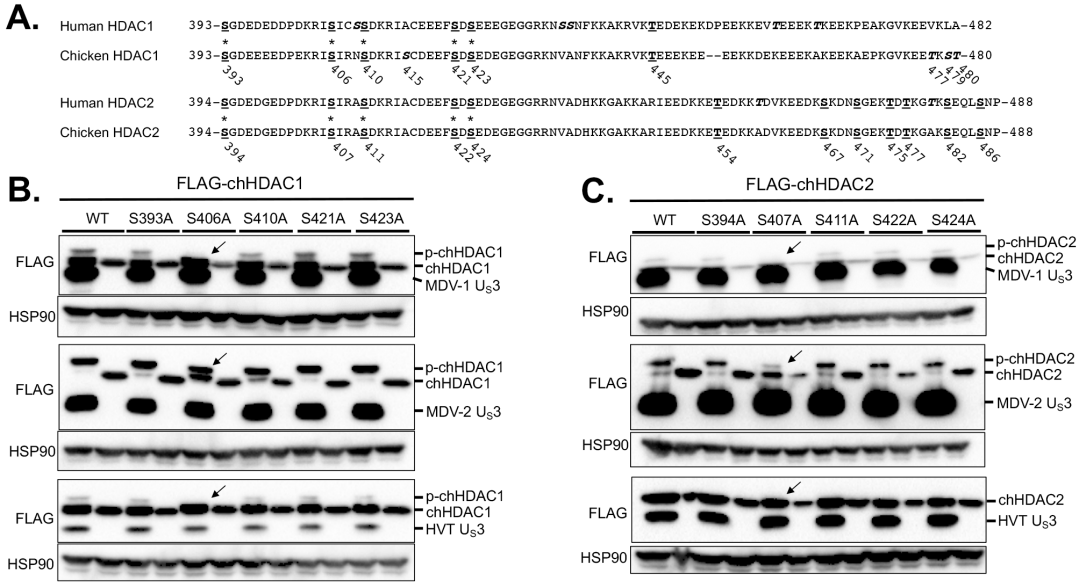

Figure 3-2 Identification of the phosphorylation sites in chHDAC1 and 2.
(A) Amino acid sequence alignments of human HDAC1 and chicken HDAC1, and human HDAC2 and chicken HDAC2. Conserved serine (S) and threonine (T) sites are presented as bold underlined, and unique S and T sites are presented as bold italics (those marked with an * were mutated to alanine, A). The position of S and T in chicken HDAC1 and 2 are labeled below the amino acid sequences. pcDNA FLAG tagged MDV-1, MDV-2, or HVT U_S3, or pcDNA empty vector were cotransfected with pcDNA-FLAG-chHDAC1 (B) or pcDNA-FLAG-chHDAC2 mutants (C) into 293T cells. Forty-eight hours later, cells were lysed and subjected to Western blot with FLAG and HSP90 antibodies. Protein bands of expected phosphorylated chHDAC1 (p-chHDAC1) and p-chHDAC2 are marked by black arrow.

Next, we mutated all other S and T sites in the C-terminus of chHDAC1, and examined the electrophoretic mobility of chHDAC1 mutants in MDV-2 U_S3 cotransfected cells. Our results show that S406A, S410A, and S415A mutations resulted in higher amount of unmodified chHDAC1 (the smaller protein species) compared to wild type chHDAC1 (Figure 3-3A), indicating that MDV-2 U_S3 may phosphorylate chHDAC1 at these three sites. These results were confirmed by the generation of double and triple chHDAC1 mutations where the triple mutant S406/410/415A completely

eliminated MDV-2 U_S3 mediated phosphorylation of chHDAC1 (Figure 3-3B). We further confirmed our results by examining the protein mobility of S to aspartic acid (D) mutant chHDAC1 (phosphorylation mimic form). As shown in Figure 3-3B, S406/410/415A triple mutation resulted in a single smallest protein species, while S406/410/415D triple mutation resulted in a single largest protein species. Using similar strategy, we showed that MDV-2 U_S3 phosphorylates chHDAC2 at S407 and S411 residues (Figure 3-3C).

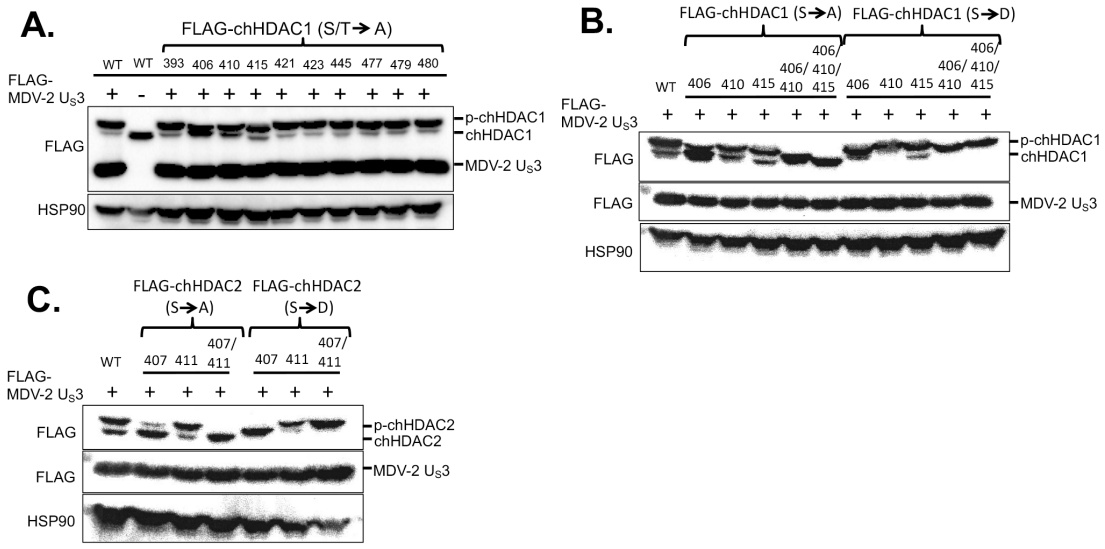

Figure 3-3 Mapping the MDV-2 U_S3 target sites in chHDAC1 and 2.
(A) pcDNA-FLAG-chHDAC1 single amino acid mutant plasmids was transfected with or without pcDNA-FLAG-MDV-2-U_S3 into 293T cells for 48 hours, followed by Western blot (WB) with FLAG and HSP90 antibodies. FLAG tagged single or multiple serine sites mutant chHDAC1 (B) or chHDAC2 (C) were cotransfected with pcDNA-FLAG-MDV-2-U_S3 into 293T cells. Forty-eight hours later, WB was processed with FLAG antibody to examine the mobility of chHDAC1 or chHDAC2. HSP90 antibody was used as indicators of protein loading control.

Phosphorylation enhances the stability of chHDAC1, but not chHDAC2. To dissect the effect of MDV U_S3 induced phosphorylation on chHDAC1 and 2, we first

examined the stability of phosphorylated and unmodified chHDAC1 and 2 in the presence of cycloheximide (CHX), a protein synthesis inhibitor. Our results show that chHDAC1-S406/410/415D mutant degrades slower than wild type chHDAC1 after CHX treatment, while chHDAC1-S406/410/415A mutant degrades faster, indicating that MDV U_S3 induced phosphorylation stabilizes chHDAC1 protein (Figure 3-4A). On the other hand, degradation of chHDAC2-S407/411A and chHDAC2-S407/411D mutants were similar to wild type chHDAC2, suggesting that MDV U_S3 induced phosphorylation does not affect the stability of chHDAC2 (Figure 3-4B).

MDV U_S3 induced phosphorylation regulates the transcriptional regulation activity of chHDAC1 and 2. To study the effect of phosphorylation in regulating chHDAC1 and 2 transcriptional regulation activity, we first examined the transcription of HDAC1 and 2 target genes, *p21* and *p27* (168, 169), in MDV U_S3 transfected cells. DF-1 cells were transfected with pCDNA expressing wild type or kinase dead MDV-1, MDV-2, and HVT U_S3, or Ev. Our qRT-PCR results show that wild type, but not kinase dead, U_S3, from MDV-1, MDV-2 and HVT, significantly up-regulate the expression of chicken *p21* (*chp21*) and *chp27* (Figure 3-4C).

In addition, we found that treatment with sodium butyrate (NaB), a HDAC inhibitor, up-regulated the transcriptional activity of the well characterized MDV bidirectional *pp14* and *pp38* promoters (14), in a dose dependent manner (Figure 3-4D), suggesting that HDACs repress the transcriptional activity of *pp14* and *pp38* promoters. Next, we specifically examined the role of chHDAC1 and 2 in regulating the transcriptional activity of *pp14* and *pp38* promoters. Our results show that chHDAC1

significantly represses the transcriptional activity of *pp14* promoter, but not *pp38* promoter, while chHDCA2 suppresses the activity of both promoters (Figure 3-4E). In addition, compared to wild type chHDAC1, chHDAC1-S406/410/415A mutant represses the transcriptional activity of *pp14* promoter, while chHDAC1-S406/410/415D mutant activates the transcriptional activity of *pp14* promoter, indicating that MDV induced phosphorylation inhibit the repressive effect of chHDAC1 on the *pp14* promoter (Figure 3-4F). As expected, wild type chHDAC1, chHDAC1-S406/410/415A and chHDAC1-S406/410/415D had no effect on the transcriptional activity of *pp38* promoter (Figure 3-4F). Our results also show that MDV U_S3 induced phosphorylation of chHDAC2 did not affect its role in regulating *pp14* and *pp38* promoter activity as chHDAC2-S407/411A and chHDAC2-S407/411D performed similar to wild type chHDAC2 in the dual luciferase assay (Figure 3-4G).

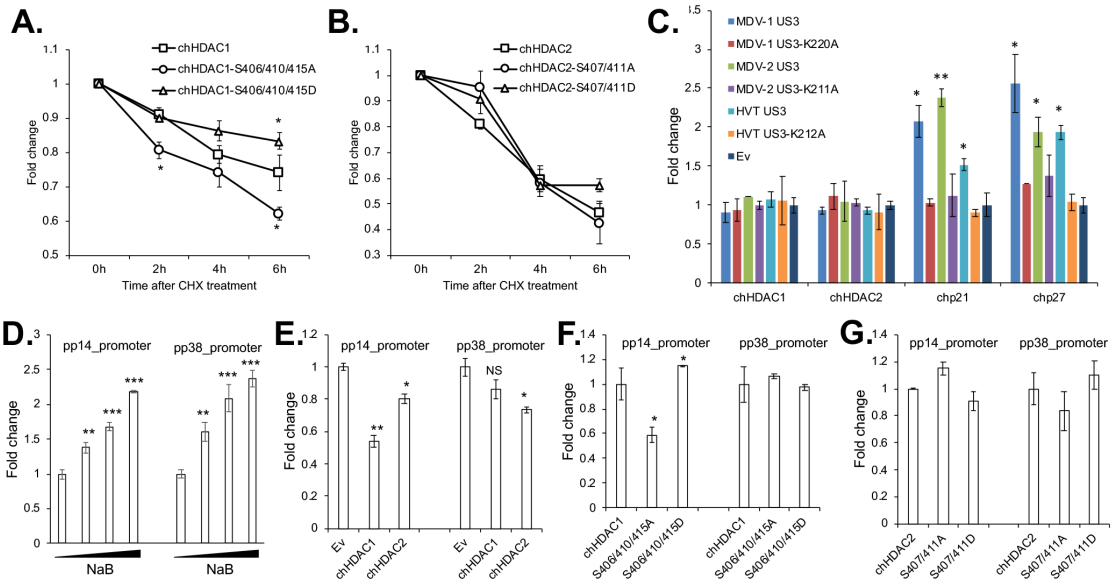

Figure 3-4 MDV U_S3 induced phosphorylation regulates the stability and transcriptional regulation activity of chHDAC1 and 2.

pcDNA FLAG tagged wild type chHDAC1, chHDAC1-S406/410/415A mutant, or chHDAC1-S406/410/415D mutant (A); pcDNA FLAG tagged wild type chHDAC2, chHDAC2-S407/411A, or chHDAC2-S407/411D (B) were transfected into 293T cells. Twenty-four hours later, cells were treated with CHX (1 mg/ml) for 0-, 2-, 4-, or 6-hours. Then, cells were lysed and subjected to Western blot (WB) with FLAG and HSP90 antibodies. chHDAC1 or chHDAC2 protein levels were quantified with Image J, normalized to HSP90 protein level, and presented as fold change relative to non-treated cells. (C) DF-1 cells were transfected with wild type or kinase dead MDV-1, MDV-2, or HVT U_S3, or empty vector (Ev). Forty-eight hours later, cells were harvest for RNA isolation followed by cDNA synthesis. qRT-PCR was carried out with the indicated primers. qRT-PCR data were analyzed by the $2^{-\Delta\Delta CT}$ method using chicken *GAPDH* as internal control. Values were presented as fold change relative to Ev transfected cells. (D) 293T cells were transfected with pGL3-pp14_promoter or pGL3-pp38_promoter with *Renilla* luciferase vector. Twenty-four hours after transfection, cells were treated with different amount of sodium butyrate (NaB) overnight, followed by *Firefly* luciferase and *Renillla* luciferase activity measurement. Experiments were repeated two times in triplicate. Values were presented as fold change relative to non-treated cells. (E, F, G) The indicated plasmids were cotransfected with pGL3-pp14_promoter or pGL3-pp38_promoter and *Renilla* luciferase vector. Forty-eight hours later, cells were lysed with passive lysis buffer and processed as stated above. Values were presented as fold change relative to Ev (E), chHDAC1 (F) or chHDAC2 (G) transfected cells. NS: not significant, *: $p<0.05$, **: $p<0.01$, ***: $p<0.001$.

MDV U_S3 induced chHDAC1 and 2 phosphorylation regulates their interactions. HDAC1 and 2 form homodimers and heterodimers through their N terminal dimerization domain, and are components of repressor protein complexes, including CoREST, Sin3, and NuRD (102). Here, we determined the effect of MDV U_S3 induced phosphorylation in regulating chHDAC1 and 2 homodimerization, heterodimerization, and interaction with other proteins. As shown in Figure 3-5A, pcDNA expressing FLAG-chHDCA1 phosphorylation site mutants were cotransfected with HA-chHDAC1 (Figure 3-5A(a)) or HA-chHDAC2 (Figure 3-5A(b)) into 293T cells followed by immunoprecipitation (IP) and WB. Our results show that mutation of chHDCA1 phosphorylation sites did not affect their interaction with HA-chHDAC1

(Figure 3-5A (a)), indicating that MDV U_S3 induced chHDAC1 phosphorylation has no effect on chHDAC1 homodimerization. On the other hand, compared to wild type chHDAC1, chHDAC1-S406/410/415A interacted weakly with HA-chHDAC2 while chHDAC1-S410D and chHDAC1-S406/410/415D showed strong interaction with HA-chHDAC2, indicating that MDV U_S3 induced phosphorylation enhances the affinity between chHDAC1 and chHDCA2 (Figure 3-5A (b)). We also studied the interactions between chHDAC1 mutants and NuRD protein complex. Our results show that chHDAC1-S406A, chHDAC1-S406/410/415A, and all chHDAC1 S to D mutants exhibit lower affinity for MTA1 and MBD3 when compared to wild type chHDAC1 (Figure 3-5A (b)).

Next, similar experiments were performed to determine whether MDV U_S3 induced chHDAC2 phosphorylation would affect the chHDAC2 interaction network. Our results show that chHDAC2 S to A mutations did not affect its homodimerization ability while chHDAC2 S to D mutants exhibit stronger interaction with wild type chHDAC2 (Figure 3-5B (a)). However, none of the chHDAC2 mutants showed any difference in their interactions with chHDAC1 (Figure 3-5B (b)), suggesting that MDV U_S3 induced chHDAC2 phosphorylation enhances its homodimerization but does not affect its heterodimerization. The interaction between chHDAC2 mutants and cellular interaction partners were also examined. Compared to wild type chHDAC2, chHDAC2 S411A and S407D mutants showed similar levels of association with MTA1 and MBD3, while S407A, S407/411A, S411D, and S407/411D clearly showed less interaction with MTA1 and MBD3 (Figure 3-5B (b)).

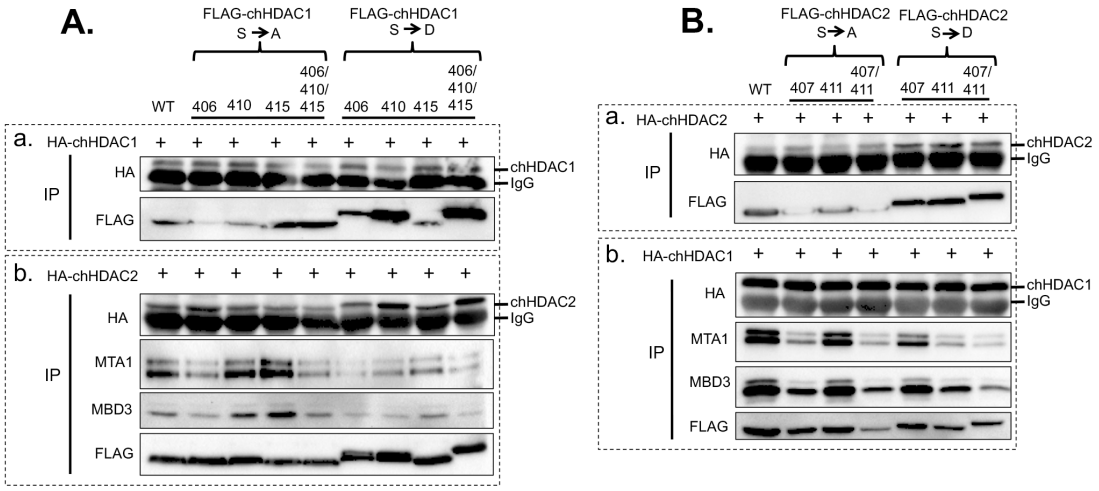

Figure 3-5 MDV U_S3 induced chHDAC1 and 2 phosphorylation regulates their interactions.
(A) pcDNA FLAG tagged wild type chHDAC1 or mutant chHDAC1 were cotransfected with pcDNA-HA-chHDAC1 (a) or pcDNA-HA-chHDAC2 (b) into 293T cells. Forty-eight hours later, cells were lysed and subjected to immunoprecipitation (IP) followed by Western blot (WB) analysis with the indicated antibodies. (B) pcDNA FLAG tagged wild type chHDAC2 or mutant chHDAC2 were transfected with pcDNA-HA-chHDAC2 (a) or pcDNA-HA-chHDAC1 (b). IP and WB were processed as stated above.

MDV U_S3 interacts with chHDAC1 and 2. Apart from phosphorylation, we found that MDV-1 U_S3 physically interacts with chHDAC1 and 2. Plasmids expressing FLAG tagged wild type MDV-1 U_S3, kinase dead (MDV-1 U_S3-K220A) U_S3, or Ev were cotransfected with plasmids expressing HA-chHDAC1 or HA-chHDAC2, into 293T cells. Forty-eight hours later, whole cell lysates were subjected to IP with mouse anti-FLAG agarose beads followed by WB analysis. As shown in Figure 3-6A, wild type MDV-1 U_S3 efficiently co-precipitated unmodified chHDAC1 and phosphorylated chHDAC1, while MDV-1 U_S3-K220A only weakly co-precipitated unmodified chHDAC1, indicating that MDV-1 U_S3 interacts with chHDAC1 via a kinase activity dependent manner. Similar interaction pattern was observed between MDV-U_S3 and

chHDAC2 (Figure 3-6D). We also examined the interaction between U_S3 of MDV-2 and HVT, and chHDAC1 and 2. Our results show that wild type MDV-2 U_S3 associates with unmodified and phosphorylated chHDAC1 and 2, while MDV-2 U_S3-K211A (kinase dead) only weakly interacts with unmodified chHDAC1 and 2 (Figure 3-6B and 6E). Similar results were found for HVT U_S3 (Figure 3-6C and 6F), with the exception that HVT U_S3 failed to phosphorylate chHDAC2, as stated above. Same results were observed in reverse experiments where IP were performed to pull-down FLAG tagged chHDAC1 or chHDAC2 and WB were performed to detect HA tagged wild type U_S3 or kinase dead U_S3 (APPENDIX A, Figure S5).

We also examined the subcellular co-localization of MDV-1 U_S3 and endogenous chHDAC1 and 2. Our results show that MDV-1 U_S3 co-localizes with chHDAC1 (Figure 3-6G, upper panel) and chHDAC2 (Figure 3-6H, upper panel) in the nucleus of MDV-1 U_S3 transfected DF-1 cells. In addition, unlike HSV-1 U_S3 (167), transfection of MDV-1 U_S3 did not affect the subcellular localization and distribution of chHDAC1 (Figure 3-6G) and chHDAC2 (Figure 3-6H) when compared to Ev transfected cells.

We have recently demonstrated that MDV-1 U_S3 interacts with MDV Meq oncoprotein (163). Here we also examined whether the presence of Meq affects the interaction between MDV-1 U_S3 and chHDAC1 and 2. Our IP results show that FLAG tagged MDV-1 U_S3 could coprecipitate Meq as well as unmodified and phosphorylated chHDAC1 (Figure 3-6I) or chHDAC2 (Figure 3-6J). We also observed that level of chHDAC1 and 2 proteins were lower in the presence of Meq in both input and IP

samples, which is most likely due to Meq mediated degradation of chHDAC1 and 2. These results suggest that Meq has no effect on the association between MDV-1 U_S3 and chHDAC1 and 2.

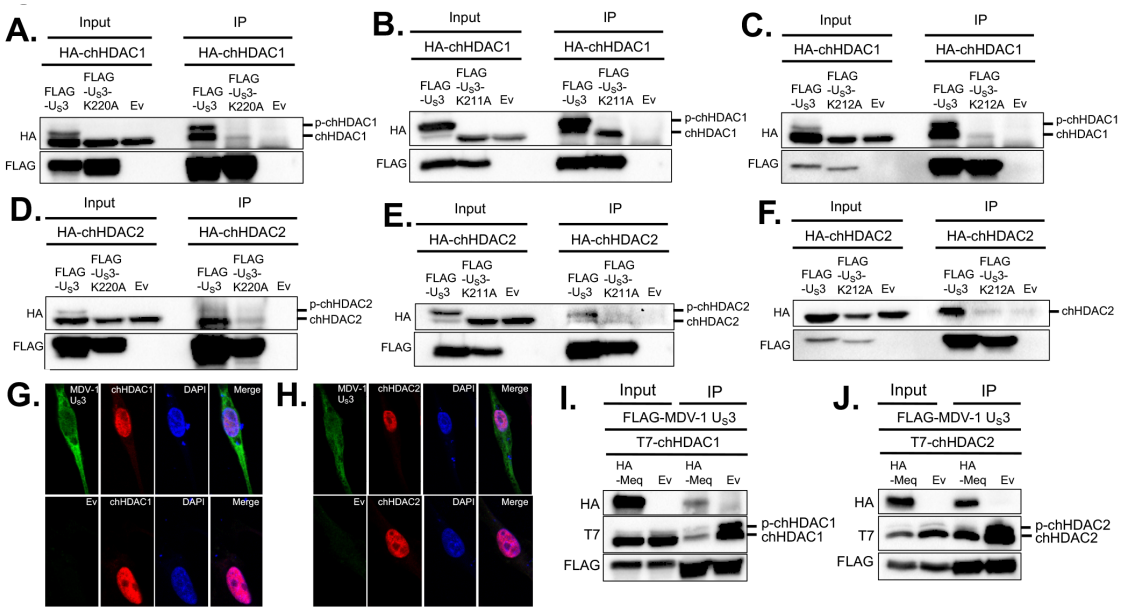

Figure 3-6 MDV U_S3 interacts with chHDAC1 and 2. pcDNA-FLAG-MDV-1-U_S3, pcDNA-FLAG-MDV-1-U_S3-K220A, or pcDNA empty vector (Ev) were cotransfected with pcDNA-HA-chHDAC1 (A) or pcDNA-HA-chHDAC2 (D) into 293T cells. After 48 hours, cells were lysed and subjected to immunoprecipitation (IP). Western blot (WB) analysis was performed with HA and FLAG antibodies. The interactions between MDV-2 U_S3 and chHDAC1 (B) or chHDAC2 (E), as well as HVT U_S3 and chHDAC1 (C) or chHDAC2 (F) were determined by a similar method. DF-1 cells were transfected with pcDNA-FLAG-MDV-1-U_S3 or Ev. Forty-eight hours later, cells were fixed for immunofluorescence assay with FLAG and HDAC1 (G) or HDAC2 (H) antibodies. DAPI was used to stain cell nuclei. All images were recorded using a confocal microscope. pcDNA-FLAG-MDV-1-U_S3 was cotransfected with pcDNA-HA-Meq or pcDNA Ev, as well as pcDNA-T7-chHDAC1 (I) or pcDNA-T7-chHDAC2 (J) into 293T cells. Forty-eight hours later, IP was performed with mouse anti-FLAG agarose beads, followed by WB with HA, T7 and FLAG antibodies.

HDAC activity affects replication, but not plaque size of MDV-1. It has been reported that inhibition of HDAC activity by sodium butyrate (NaB) treatment enhances

growth, plaquing efficiency, and plaque size of VZV ORF66 null virus but not parental virus (162). In addition, NaB treatment enhanced plaquing efficiency of PRV U_S3 null virus but not HSV-1 U_S3 null virus (58). To explore the role of chHDAC1 and 2 in regulating MDV replication, we examined the replication and plaque size of parental MDV-1, U_S3 deletion MDV-1 (MDV-1-ΔU_S3), and U_S3 deletion revertant MDV-1 (MDV-1-ΔU_S3_Rev) in NaB treated chicken embryonic fibroblasts (CEF). Our results show that treatment with NaB did not affect the plaque size of parental MDV-1, MDV-1-ΔU_S3, and MDV-1-ΔU_S3_Rev (Figure 3-7A). Surprisingly, the replication of MDV-1, MDV-1-ΔU_S3, and MDV-1-ΔU_S3_Rev in CEF, as measured by MDV-1 genome copy number, was suppressed by treatment with NaB (Figure 3-7B). These results suggest that HDACs enzymatic activity is required for efficient replication, but not plaque size, of MDV in CEF.

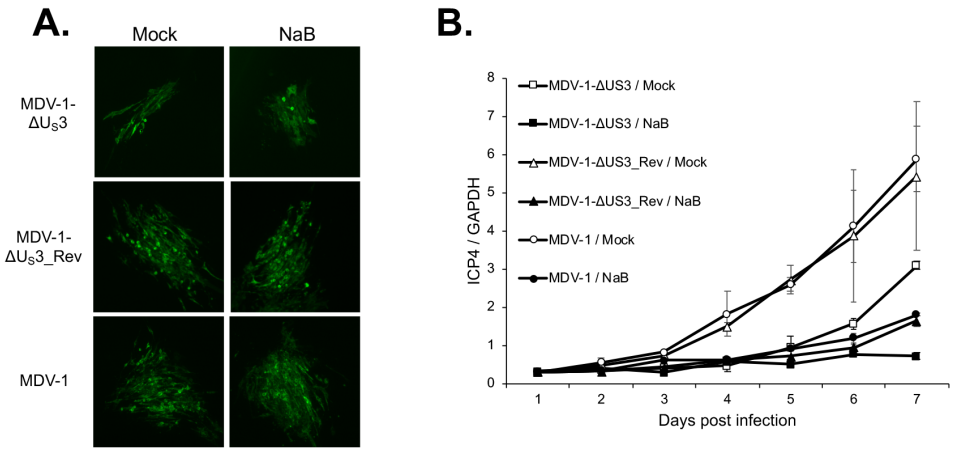

Figure 3-7 Sodium butyrate (NaB) treatment does not rescue growth deficiency of MDV-1 U_S3 null virus.
(A) Mock treated or NaB (1 mg/ml) treated chicken embryonic fibroblasts (CEF) were infected with MDV-1-ΔU_S3, MDV-1-ΔU_S3_Rev, or parental MDV-1 viruses, respectively. Seven days later, cells were fixed and subjected to immunofluorescence assay with MDV pp38 mouse monoclonal antibody and goat anti-mouse Alexa Fluor

488. All images were taken with a 10x objective. (B) Mock treated or NaB (1 mg/ml) treated CEF was infected with MDV-1-ΔUS3, MDV-1-ΔUS3_Rev, or parental MDV-1 viruses, respectively. Cells were harvested daily until 7 days post infection, followed by genomic DNA isolation. Viral genome copy number was determined by qPCR using MDV *ICP4* and chicken *GAPDH* primers, and presented as the ratio of *ICP4* to *GAPDH* copy number with error bar representing the standard deviation.

MDV-2 US3 and HVT US3 can partially rescue virus replication of MDV-1 US3 null virus *in vitro*. It has been reported that HSV-2 US3 could compensate some functions of HSV-1 US3, such as apoptosis inhibition and cell morphology modulation, while also resulted in aberrant localization of UL34, a substrate of HSV-1 US3 (170). Here, we studied whether MDV-2 or HVT US3 could rescue functions of MDV-1 US3. We first generated chimeric viruses MDV-1-MDV-2/US3 and MDV-1-HVT/US3 by replacing MDV-1 US3 with MDV-2 US3 and HVT US3, respectively. As previously reported (64), we observed that deletion of US3 significantly reduced the plaque size of MDV-1 (Figure 3-8A). In addition, as expected, we found that MDV-2 US3 and HVT US3 could partially restore the plaque size of MDV-1-ΔUS3 virus, and the plaque size of MDV-1-MDV-2/US3 and MDV-1-HVT/US3 was not different (Figure 3-8A). *In vitro* growth kinetics of parental, US3 deletion, chimeric and revertant viruses, show that US3 deletion reduced the growth of MDV, as indicated by fewer plaque numbers, and that MDV-2 US3 and HVT US3 partially rescue the growth deficiency of US3 deletion virus (Figure 3-8B). We speculate that reduced plaque numbers caused by US3 deletion might due to lower plaque forming efficiency or/and less viral genome copy numbers. To further distinguish these two possibilities, we analyzed the viral genome copy number after infecting with chimeric and revertant viruses. Our results show that deletion of US3

resulted in lower viral genome copy number, a phenotype which was partially restored by MDV-2 U_S3 and HVT U_S3 (Figure 3-8C). We conclude that MDV-1 U_S3 is involved in the replication of viral genome and MDV plaque forming efficiency.

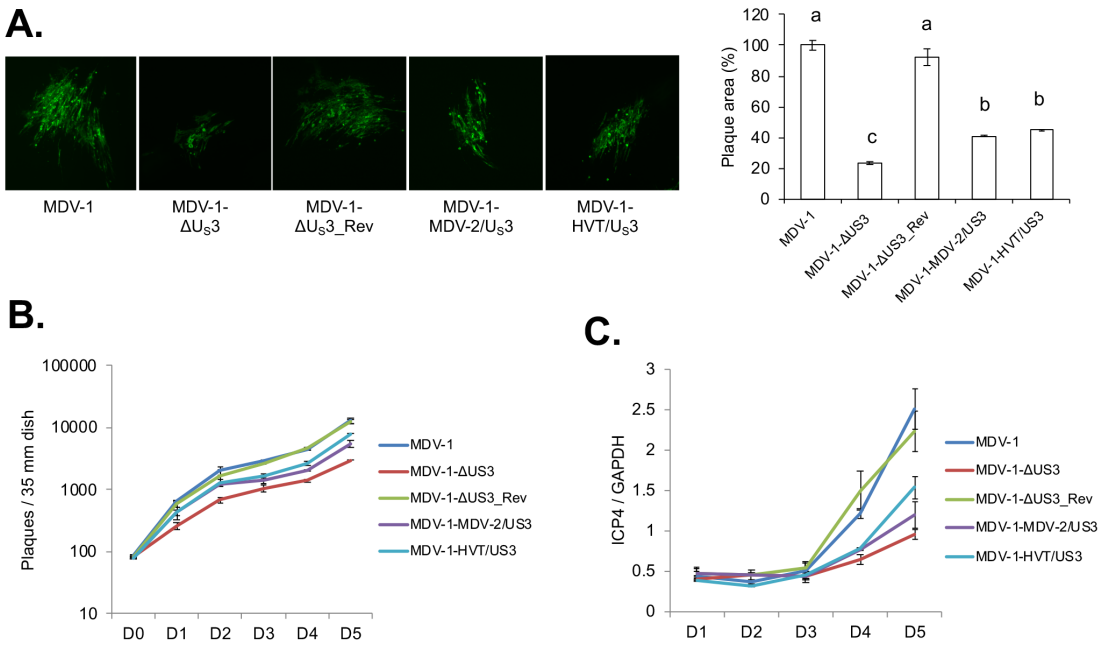

Figure 3-8 *In vitro* characterization of chimeric and revertant MDVs.
(A) Chicken embryonic fibroblasts (CEF) were infected with parental MDV-1, MDV-1-ΔU_S3, MDV-1-ΔU_S3_Rev, MDV-1-MDV-2/U_S3, or MDV-1-HVT/U_S3 viruses and fixed at 7 days post infection. Immunofluorescence assay (IFA) was performed using MDV pp38 mouse monoclonal antibody and goat anti-mouse-Alexa Fluor 488 antibody. Plaques were visualized with a fluorescence microscope (left). For each virus, plaque sizes (50-100 plaques) were measured, and presented as mean plaque sizes relative to parental MDV-1 virus (right). The mean plaque size of parental MDV-1 virus was set to 100%. The error bar represents the standard deviation of two independent experiments. (B) CEF were infected with 100 plaque-forming units (PFU) of the indicated viruses. At the given days post infection, cells were trypsinized, serial diluted, and co-seeded with fresh CEF. Numbers of plaques for each virus were counted, after IFA with pp38 antibody, and presented as mean virus titer. The error bar shows standard deviation of two independent experiments. (C) CEF were infected with 100 PFU of the indicated viruses. Cells were harvested daily until 5 days post infection and subjected to genomic DNA isolation. The genome copy number of each virus was determined by qPCR, using MDV *ICP4* and chicken *GAPDH* primers, and presented as the ratio of *ICP4* to *GAPDH* copy number with error bar representing the standard deviation.

MDV-2 U_S3 and HVT U_S3 can partially rescue the replication and pathogenesis of MDV-1 U_S3 null virus in chickens. To further characterizing the chimeric viruses *in vivo*, we examined the replication and pathogenesis of chimeric viruses in chickens a natural virus-host model. MDV establishes an early cytolytic infection 2-7 days post infection and switches to latent infection beginning 7-8 days post infection in lymphoid organs (1, 171). Within 2 weeks post infection, latently infected T lymphocytes become transformed and migrate to the skin where they reactivate to produce fully infectious MDV in feather follicular epithelial cells (1). The reactivated viruses then undergo late cytolytic infection beginning approximately 3 to 4 weeks post infection (1, 171).

In vivo replication. To examine whether MDV-2 U_S3 and HVT U_S3 can rescue the replication of MDV-1 U_S3 null virus *in vivo*, we examined the viral load in spleen of infected chickens during early cytolytic infection, latent infection, and late cytolytic infection stages. One-day-old chickens were inoculated subcutaneously with the different viruses. One group of chickens remained as uninoculated control. Five chickens from each group were randomly selected at 6, 14, and 28 days post inoculation, and spleens were collected for DNA isolation followed by qPCR to determine MDV genome copy number. Our results show that deletion of MDV-1 U_S3 significantly reduces MDV replication in spleen at 6, 14, and 28 days post inoculation, which can be fully resorted in the revertant virus (MDV-1-ΔU_S3_Rev) (Figure 3-9A). In addition, similar to *in vitro* results (Figure 3-8C), genome copy number of MDV-1-MDV-2/U_S3 and MDV-1-HVT/U_S3 was higher than MDV-1-ΔU_S3 and lower than parental (MDV-1) and

revertant (MDV-1-ΔU$_S$3_Rev) viruses at 6, 14, and 28 days post inoculation (Figure 3-9A), indicating that MDV-2 U$_S$3 and HVT U$_S$3 can partially compensate the function of MDV-1 U$_S$3 in MDV replication *in vivo*.

Lymphoid organ atrophy. Early cytolytic infection by MDV-1 causes lymphoid organ atrophy in chickens. Five chickens from each group were randomly selected at 14 days post inoculation, and lymphoid organs (bursa and thymus) to body weight ratios were calculated. Our results show that bursa/body weight ratio was significantly lower in parental MDV-1, MDV-1-ΔU$_S$3_Rev, and MDV-1-MDV-2/U$_S$3 infected chickens when compare to uninoculated chickens, while MDV-1-ΔU$_S$3 and MDV-1-HVT/U$_S$3 infection did not affect the bursa/body weight ratio (Figure 3-9B, left). Parental MDV-1 and MDV-1-ΔU$_S$3_Rev infection also significantly reduced the thymus/body weight ratio (Figure 3-9B, right). In addition, the thymus/body weight ratio of MDV-1-ΔU$_S$3, MDV-1-MDV-2/U$_S$3, and MDV-1-HVT/U$_S$3 infected chickens was significantly lower than uninoculated chickens but significantly higher than parental MDV-1 and MDV-1-ΔU$_S$3_Rev infected chickens (Figure 3-9B, right). These results suggest that MDV-2 U$_S$3 affects MDV-1 replication in both B- and T- cells, while HVT U$_S$3 only affects MDV-1 replication in T-cells.

Survival rate and oncogenicity. To evaluate the pathogenicity of chimeric viruses, one-day-old chickens were inoculated subcutaneously and monitored for 10 weeks to evaluate MDV associated mortality and tumors. We observed MDV associated mortality in parental MDV-1 and MDV-1-ΔU$_S$3_Rev infected chickens beginning 21-22 days post inoculation, all chickens died by day 34-35 post inoculation, and all chickens had gross

MDV specific tumors; MDV-1-MDV-2/U_S3 and MDV-1-HVT/U_S3 infected chickens started showing MDV associated mortality at 24-25 days post inoculation, all died by day 40 post inoculation, and 11 out of 12 chickens had gross MDV specific tumors; mortality in the MDV-1-ΔU_S3 infected group started 28 days post inoculation, 9 out of 12 chickens died by the end of experiment, and only 7 out of 12 chickens had gross MDV specific tumors (Figure 3-9C and 9D). Uninoculated control group showed no MDV associated mortality or tumors. These results suggest that deletion of MDV-1 U_S3 attenuate the virulence of MDV-1, which can be partially restored MDV-2 and HVT U_S3.

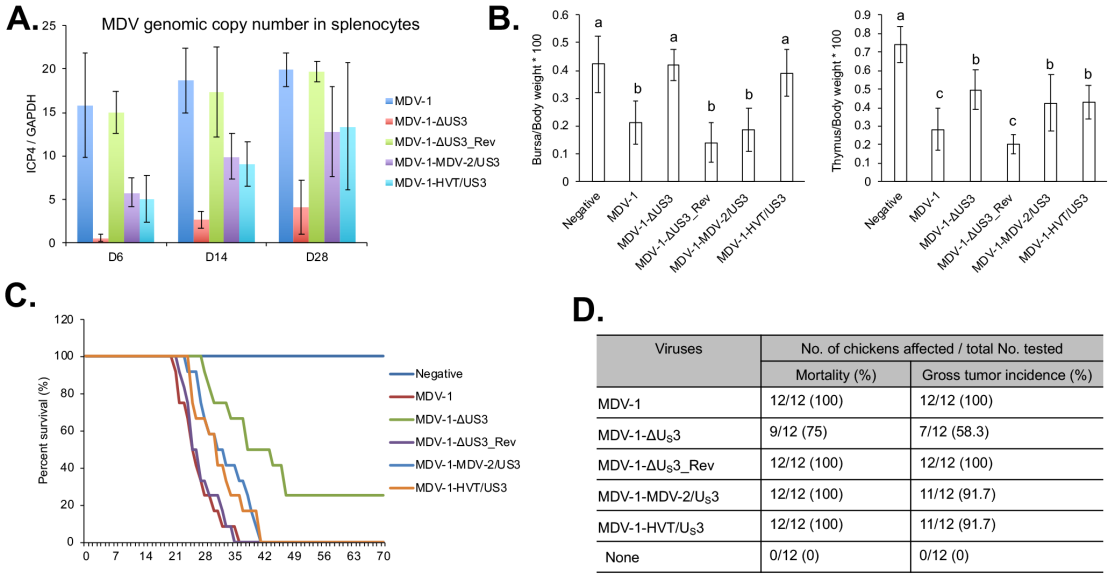

Viruses	No. of chickens affected / total No. tested	
	Mortality (%)	Gross tumor incidence (%)
MDV-1	12/12 (100)	12/12 (100)
MDV-1-ΔUS3	9/12 (75)	7/12 (58.3)
MDV-1-ΔUS3_Rev	12/12 (100)	12/12 (100)
MDV-1-MDV-2/US3	12/12 (100)	11/12 (91.7)
MDV-1-HVT/US3	12/12 (100)	11/12 (91.7)
None	0/12 (0)	0/12 (0)

Figure 3-9 *In vivo* characterization of chimeric and revertant MDVs.
(A) On 6, 14, and 28 days post inoculation, splenocytes isolated from 5 chickens infected with the indicated viruses were used for genomic DNA extraction. MDV genomic copy number was determined by qPCR. The relative MDV genomic copy number was presented as the average ratio of *ICP4* to *GAPDH* copy number with error bar representing the standard deviation. (B) On day 14 post inoculation, bursa, thymus, and body weights of 5 chickens infected with the indicated viruses were measured, and presented as ratio of bursa to body weight (left) and ratio of thymus to body weight (right). The graph represents the average ratio of 5 chickens with error bars showing the standard deviation. Significant difference between groups are marked as letters where different letter represent significant different at $p<0.05$. (C, D) After inoculating with the indicated viruses, chickens were maintained in isolation. The mortality of each group was recorded daily for 10 weeks and percent survival of chickens over time presented in the graph (C). Chickens that died during the experiment were examined for gross MDV specific tumors. The mortality rate and tumor incidence of each group are summarized (D).

3.3. Discussion

Herpesvirus life cycle consists of distinct lytic and latent phases. Upon infection with a herpesvirus, host factors rapidly respond to silence viral gene expression to further limit viral replication. A well-known group of host repressor is the HDAC enzyme family which mediate the removal of acetyl molecules from modified lysine residues and subsequently repress gene expression. HDACs regulate herpesviruses infection and in turn herpesviruses have evolved mechanisms to modulate HDACs repressor complexes. One of the strategies utilized by herpesviruses is through virus-host protein interactions. HSV-1 ICP0 has been shown to associate with HDAC1 to interrupt CoREST complex and Kaposi's sarcoma-associated herpesvirus (KSHV) K-bZIP has been reported to interact with HDAC2 to recruit it to viral promoters (121, 167). A second strategy is through post-translational modification. HSV-1 U_S3 protein kinase phosphorylates HDAC1 and 2 to promote efficient viral gene expression and genome replication (167). Other studies further demonstrated that VZV ORF66 and PRV U_S3 exhibit similar function by phosphorylating HDAC1 and 2 (58, 162). Until this study, the role of MDV U_S3 in regulating HDAC1 and 2 phosphorylation and function was not known.

The aim of our study was to investigate if MDV U_S3 phosphorylate HDAC1 and 2, and the potential effect of MDV U_S3 induced phosphorylation. Since all three serotypes MDV encode a U_S3 protein kinase which share a conserved kinase activity domain (163), we first analyzed the role U_S3 from all three MDV serotypes in chHDAC1 and 2 phosphorylation. Our findings show that U_S3 from MDV-1 and MDV-

2 phosphorylate both chHDAC1 and 2, while HVT U_S3 only phosphorylates chHDAC1 (Figure 3-1). Interestingly, we observed that MDV-2 U_S3 exhibits stronger capacity to phosphorylate chHDAC1 and 2 when compared to MDV-1 and HVT U_S3 (Figure 3-1). These findings demonstrate that MDV U_S3 shares the ability of HSV-1 U_S3, VZV ORF66, and PRV U_S3 to phosphorylate chHDAC1 and 2. We further investigated the MDV U_S3 target sites in chHDAC1 and 2 and identified novel phosphorylation sites in both proteins. Specifically, our results show that MDV-1 and HVT U_S3 phosphorylate chHDAC1 at S406 and MDV-2 phosphorylates chHDAC1 at S406, S410, and S415; MDV-1 phosphorylates chHDAC2 at S407 and MDV-2 phosphorylates chHDAC1 at S407 and S411 (Figure 3-2 and Figure 3-3). We speculate that this phosphorylation is through indirect pathway as previous studies showed that HDAC2 is an indirect substrate of VZV ORF66 (162). CKII has been identified as the main upstream kinase of HDAC1 and 2, and HDAC1, but not HDAC2, was shown to be a substrate of protein kinase A (PKA) (102). Although our results show that MDV U_S3 mimics the function of cellular PKA, PKC, and AMPK to increase phosphorylation of their substrates (APPENDIX A, Figure S4), further studies will be needed to identify cellular kinases involved in MDV U_S3 mediated phosphorylation of chHDAC1 and 2. In addition, the mechanism behind the differential phosphorylation capacity of U_S3 from all three MDV serotypes needs further studies. The protein sequence alignment and 3D structure prediction show that the catalytic active site containing region of U_S3 from all three MDV serotypes is highly conserved; however, the N terminal 100 amino acids of MDV-1, MDV-2, and HVT U_S3 are highly variable. We hypothesize that MDV-1, MDV-2, and

HVT U_S3 may associate with different host factors or manipulate different cellular signaling pathways through the N-terminal variable region to exhibit distinguishing functions. Next generation sequencing and proteomic methods will help to comprehensively study the interplay between MDV U_S3 and host factors.

Although HDAC1 and 2 have been identified as the substrate of alphaherpesviruses U_S3, the effect of U_S3 mediated phosphorylation on the biochemical properties of HDAC1 and 2 have not yet been studied. Here, we investigated the effect of MDV U_S3 induced phosphorylation on the functions of chHDAC1 and 2. Our results show that MDV-2 induced phosphorylation enhanced the stability of chHDAC1 but does not affect the stability of chHDAC2 (Figure 3-4A and 4B). In addition, expression of chHDAC1 and 2 target genes, *chp21* and *chp27*, are also up-regulated in response to overexpression of MDV-1, MDV-2, and HVT U_S3 (Figure 3-4C), suggesting that MDV U_S3 induced phosphorylation inhibits the transcriptional repressive function of chHDAC1 and 2 to allow for efficient gene expression. p21 and p27 are well characterized CIP/Kip family of cyclin-dependent kinase (CDK) inhibitors which are involved in cell cycle regulation and apoptosis inhibition (172, 173). We speculate that MDV U_S3 induced *chp21* and *chp27* expression contributes to its apoptosis inhibition function as previously reported (47, 64, 174). Furthermore, the up-regulated expression of *chp21* and *chp27,* in response to transfection of MDV U_S3, suggests that MDV U_S3 may function in cell cycle regulation. We also found that S406/410/415 phosphorylation of chHDAC1 weakens its repressive effect on the MDV *pp14* promoter but not on the MDV *pp38* promoter, while S407/411 phosphorylation of chHDAC2 has no effect on its

repressive effect of MDV *pp14* and *pp38* promoters (Figure 3-4D to 4G). These results suggest that chHDAC1 and 2 regulate the transcription of MDV genes in both phosphorylation dependent and independent manner. Besides transcriptional regulation, the interaction networks of chHDAC1 and 2 were also affected by MDV U_S3 mediated phosphorylation (Figure 3-5), similar to CKII induced phosphorylation (166). Further, we found that MDV U_S3 physically associates with chHDAC1 and 2 in a phosphorylation dependent manner (Figure 3-6 and APPENDIX A, Figure S5), suggesting MDV U_S3 may also regulate the function of chHDAC1 and 2 through interactions other than phosphorylation.

In contradiction to previous report by Walters *et al.* (162), who described that sodium butyrate (NaB) treatment increased the plaquing efficiency, plaque size, and growth of VZV ORF66 null virus but not wild type virus in MeWo cells, our results show that NaB treatment did not affect the plaque size of MDV-1 US3 null (MDV-1-ΔU_S3) virus but inhibited the growth of MDV-1-ΔU_S3 and parental MDV-1 viruses (Figure 3-7). These results suggest that HDACs enzymatic activity is required for efficient growth, but not plaque size, of MDV-1; and unlike VZV ORF66 which regulates growth of VZV by inhibiting HDAC enzymatic activity (162), MDV-1 U_S3 may regulate replication of MDV-1 by elevating the enzymatic activity of chHDACs. Since the replication of both MDV-1-ΔU_S3 and parental MDV-1 viruses was inhibited by NaB treatment (Figure 3-7), we hypothesize there are other viral factors, such as MDV-1 UL13 protein kinase, that also target chHDACs to facilitate the replication of MDV-1. It has been reported that mouse gammaherpesvirus 68 (MHV68) ORF36

protein kinase (an HSV-1 UL13 orthologous), interacts with HDAC1 and 2 to promote viral replication (175). Thus, we speculate that MDV-1 UL13 may share this function and, in combination with MDV-1 U_S3, targets chHDACs to regulate the replication of MDV-1. In addition, NaB treatment inhibits class I and class II HDACs (176), which makes it difficult to distinguish the role of individual HDAC in regulating herpesvirus replication. Further studies using knockout methods, such as short hairpin RNA (shRNA) and clustered regularly interspaced short palindromic repeats (CRISPR), that specifically target individual HDAC will help reveal the specific function of each HDAC in regulating herpesvirus gene expression and replication.

To further dissect the role of MDV U_S3 in MDV replication and pathogenesis, we constructed chimeric viruses by replacing U_S3 of MDV-1 with that of MDV-2 and HVT. First, we observed that deletion of MDV-1 U_S3 resulted in smaller plaque size (Figure 3-8A), lower plaquing efficiency (Figure 3-8B), and genome replication (Figure 3-8C), which suggests that MDV-1 U_S3 is involved in the replication of viral genome as well as MDV plaque forming efficiency. In addition, we characterized the chimeric viruses *in vitro* and our results show that MDV-2 and HVT U_S3 could partially rescue the plaque size and growth of MDV-1-ΔU_S3 virus (Figure 3-8). Similarly, we found MDV-1 U_S3 deletion resulted in growth deficiency of MDV-1-ΔU_S3 in splenocytes of infected chickens, which can be partially recovered by MDV-2 and HVT U_S3 (Figure 3-9A). We also analyzed the lymphoid organ atrophy of chimeric viruses infected chickens. Infection of parental and revertant MDV-1 resulted in severe bursa atrophy, which can be fully eliminated by MDV-1 U_S3 deletion and HVT U_S3 replacement, but

not MDV-2 U_S3 replacement; and the parental and revertant MDV-1 viruses infection induced thymus atrophy can be partially restored by MDV-1 U_S3 deletion, and replacement with MDV-2 and HVT U_S3 (Figure 3-9B). The exact mechanisms behind this phenotype need further study. We speculate that MDV-2 U_S3 does not affect the replication of chimeric virus in B-cells leading to severe bursa atrophy, while HVT U_S3 largely decreased the replication of chimeric virus in B-cells that led to no bursa atrophy. However, both MDV-2 and HVT U_S3 partially decreased the replication of chimeric virus in T-cells that led to mild thymus atrophy. These results suggest that deletion of MDV-1 U_S3, and expression of MDV-2 and HVT U_S3 attenuated MDV-1 by different levels to cause less lymphoid organ atrophy. This conclusion was confirmed in chimeric viruses infected chickens in which deletion of U_S3, and expression of MDV-2 and HVT U_S3 delayed the MDV associated death of infected chickens and reduced MDV specific tumor incidence (Figure 3-9C and 9D). Next generation sequencing with splenocytes isolated from chimeric viruses infected chickens at different infection stages will help to investigate cellular genes and pathways that are differentially regulated by U_S3 from all three MDV serotypes.

In conclusion, our study identified chHDAC1 and 2 as novel substrates and interaction partners of MDV U_S3, and identified novel phosphorylation sites in chHDAC1 and 2. Our results demonstrate that U_S3 of all three MDV serotypes function differently in phosphorylating chHDAC1 and 2. Biochemical analysis further characterized the effect of MDV U_S3 induced phosphorylation in regulating functions of chHDAC1 and 2. In addition, using a natural MDV chicken model, our studies provide

the first *in vivo* evidence on the role of MDV-1 U_S3 in MDV-1 replication and pathogenesis, and demonstrate that U_S3 from MDV-2 and HVT can partially compensate the functions of MDV-1 U_S3 *in vitro* and *in vivo*. The interaction between herpesvirus U_S3 protein kinase and HDACs studied in a natural virus-host model presented here will have a broader impact on our understanding of herpesvirus biology.

3.4. Materials and methods

Cell culture. 10-11 day old chicken embryos were used to prepare chicken embryonic fibroblasts (CEF) (177). CEF were maintained in Leibowitz–McCoy (LM, 1:1) medium supplemented with 5% newborn calf serum. Chicken DF-1 cells and human embryonic kidney 293T cells were maintained in Dulbecco's modified Eagle medium (DMEM) supplemented with 10% fetal bovine serum. All cells were maintained at 37°C with the presence of 5% CO_2. CEF were used for recombinant virus production, virus titration and MDV *in vitro* growth kinetics assay. DF-1 and 293T cells were used for transient transfections.

Mutagenesis of MDV-1 bacterial artificial chromosome (BAC). Construction of MDV-1-ΔU_S3 virus was described previously (163). All primers used for mutagenesis of MDV-1 BAC are listed in APPENDIX B, Table S1. To generate a chimeric MDV-1 virus expressing MDV-2 U_S3 (MDV-1-MDV-2/U_S3) BAC, MDV-2 U_S3 ORF was amplified using MDV-2/U_S3_F and MDV-2/U_S3_R primers, and cloned into pUC19 plasmid to generate pUC19- MDV-2/U_S3. Then, *Kan*^{R} gene was amplified with primers MDV-2/U_S3Kan-F and MDV-2/U_S3Kan-R with pEPKan-S plasmid as the template. The

amplified product was digested and cloned into *EcoR*V site of pUC19-MDV-2/U_S3 to generate pUC19-MDV-2/U_S3-Kan. Next, the MDV-2 U_S3 with *Kan*^{R} insertion was amplified with primers MDV-2/U_S3-T-F and MDV-2/U_S3-T-R to generate MDV-2/Us3-Kan transfer cassette that was transformed by electroporation into competent cells carrying MDV-1-ΔU_S3 BAC DNA to generate MDV-1-MDV-2/U_S3 BAC. A chimeric MDV-1 virus expressing HVT U_S3 (MDV-1-HVT/U_S3) and revertant BAC clones containing MDV-1 U_S3 (MDV-1-ΔU_S3_Rev) were generated using the same method (primers 7 to 12 and 13 to 18, respectively; APPENDIX B, Table S1). All BAC DNAs were transfected into CEF to produce recombinant viruses.

Plasmid constructions. All MDV U_S3, Meq, chHDAC1 and 2 expression plasmids were constructed using pcDNA™3.1/Zeo (+) mammalian expression vector (Invitrogen). pGL3-pp14_promoter and pGL3-pp38_promoter plasmids were described previously (14). All primers used for PCR amplification and gene cloning are listed in Table S1. All cloned genes were confirmed by sequence analysis.

U_S3 plasmids. FLAG and HA tagged wild type MDV-1 U_S3 were amplified from the genome of 686 strain (178) using primers 19, 20, and 21 (APPENDIX B, Table S1). The amplified products were digested and cloned into pcDNA. To generate kinase dead MDV-1 U_S3 (MDV-1_U_S3-K220A), lysine (K) 220 of MDV-1 U_S3 was mutated to alanine (A) using primers 22 and 23. Similar overlapping PCR method (179) was used to generate FLAG and HA tagged wild type and kinase dead MDV-2 U_S3 (APPENDIX B, Table S1, primer number 24 to 28) amplified from the genome of SB1 strain (GenBank: HQ840738.1), as well as FLAG and HA tagged wild type and kinase dead HVT U_S3

(APPENDIX B, Table S1, primer number 29 to 33) amplified from the genome of FC-126 strain (GenBank: NC_002641.1).

Meq plasmids. HA tagged MDV-1 Meq was amplified from the genome of 686 strain (178) using primers 34 and 35 (APPENDIX B, Table S1), followed by digestion and cloning into pcDNA vector.

chHDAC1 plasmids. FLAG, HA, and T7 tagged wild type chHDAC1 were amplified from chicken cDNA using primer 36 to 39 (APPENDIX B, Table S1), followed by digestion and cloning into pcDNA vector. Single, double, and triple S to A or S to D mutations of chHDAC1 were generated by overlapping PCR using primers 40 to 69 (APPENDIX B, Table S1).

chHDAC2 plasmids. FLAG, HA, and T7 tagged wild type chHDAC2 were amplified from chicken cDNA using primers 70 to 73 (APPENDIX B, Table S1) followed by digestion and cloning into pcDNA vector. Single and double S to A or S to D mutations of chHDAC2 were generated as stated above using primers 74 to 91 (APPENDIX B, Table S1).

Chemicals. Sodium butyrate (NaB) (Millipore-Sigma) was reconstituted with water and used at 1 mM to inhibit enzymatic activities of chicken HDACs. Cycloheximide (CHX) (Millipore-Sigma) was reconstituted in DMSO and used at 1 mg/ml to examine the half-life of proteins.

Immunoprecipitation (IP) and Western blot (WB) analysis. To determine the interaction network of chHDAC1 and 2, as well as the interaction between MDV Us3 and chHDAC1 and 2, IP and WB were performed as described previously (163). Briefly,

cells were lysed 48 hours after transfection, followed by incubation with mouse anti-FLAG agarose beads overnight at 4°C with gentle rotation. Next day, beads were washed five times and boiled in 2x sodium dodecyl sulfate (SDS) buffer for 5 min. The eluted samples were subjected to SDS-polyacrylamide gel electrophoresis (PAGE) and transferred to polyvinylidene fluoride (PVDF) membrane. After blocking with 5% nonfat milk, PVDF membranes were incubated with primary antibody followed by horseradish peroxidase (HRP) conjugated secondary antibody, and visualized with a chemiluminescent substrate.

Dephosphorylation assay. To confirm MDV U_S3 mediates chHDAC1 and 2 phosphorylation, cell lysates were subjected to a dephosphorylation assay (162). Briefly, 30 μg of whole cell lysates were incubated with or without 20 units of Lambda Protein Phosphatase (Lambda PP, New England Biolabs) in the buffer provided by the manufacturer and supplemented with additional protease inhibitors at 30°C for 15 min. The reaction was stopped by adding 2x SDS buffer, followed by SDS-PAGE and WB as described above.

Immunofluorescence assay (IFA).

IFA was performed to determine the sub-cellular localization of MDV-1 U_S3, chHDAC1 and 2 in DF-1 cells, and to visualize viral plaques formed by MDV infection in CEF.

Transfected DF-1 cells. IFA of DF-1 cells was carried out as described previously (163). Briefly, pcDNA-FLAG-MDV-1 U_S3 plasmid was transfected into DF-1 cells seeded on coverslips using polyethylenimine (PEI, 1 mg/ml) reagent. After 48 hours, cells were fixed and permeabilized prior to blocking in 5% nonfat milk for 1 hour at room

temperature. After three washes with phosphate-buffered saline (PBS), cells were incubated with rabbit anti-FLAG antibody and mouse anti-HDAC1 antibody or mouse anti-HDAC2 antibody for 1 hour followed by another hour incubation with goat anti-rabbit-Alexa Fluor 488 antibody and goat anti-mouse-Texas Red antibody, at room temperature. 4',6-diamidino-2-phenylindole (DAPI) was used to stain cell nuclei. Coverslips were mounted on glass slides with ProLong™ Diamond Antifade Mountant (Thermo Fisher Scientific) and imaged with a Zeiss LSM 780 NLO Multiphoton Microscope.

Infected CEF. One day before infection, CEF were seeded in 35 mm cell culture plates. Next day, CEF were treated with NaB (1 mM) or mock treated for 6 hours prior to infection with different viruses. After infection, cell culture medium was changed every two days with or without the addition of fresh NaB. Seven days later, cells were fixed with ice-cold acetone-methanol (3:2) for 5 min, followed by blocking with 5% nonfat milk for 1 hour at room temperature. Cells were probed with mouse anti-pp38 monoclonal antibody followed by goat anti-mouse-Alexa Fluor 488 antibody for 1 hour at room temperature. After three washes, cells were viewed with a fluorescence microscope.

RNA isolation and quantitative reverse transcriptase real time polymerase chain reaction (qRT-PCR). To determine the role of MDV U_S3 in regulating the transcription of chHDAC1 and 2 target genes, DF-1 cells were transfected with wild type or kinase dead U_S3 from MDV-1, MDV-2 and HVT or Ev. Forty-eight hours later, total RNA was isolated using TRIzol reagent (Invitrogen) according to manufacturer's

protocol. 1-5 µg of total RNA was converted to cDNA, followed by qRT-PCR analysis using primers 92 to 101 (Table S1) and iTaq™ Universal SYBR® Green Supermix (Bio-Rad) in a CFX96™ Real time PCR Detection System (Bio-Rad). qRT-PCR results were analyzed using the $2^{-\Delta\Delta CT}$ method (157).

Dual luciferase assay. To study the role of chHDAC1 and 2 in regulating transcriptional activity of the pp14/pp38 by directional MDV promoters, 293T cells were cotransfected with plasmids expressing chHDAC1 or 2 or Ev and pGL3-pp14_promoter or pGL3-pp38_promoter. *Renilla* luciferase vector was included as normalization control. Forty-eight hours later, cells were lysed and *Firefly* and *Renilla* luciferase activities were measured according to the manufacturer's protocol (Promega).

***In vitro* growth kinetics and plaque area determination.** To evaluate the role of MDV U_S3 in regulating the growth properties and plaque size of MDV, the growth kinetics of parental, chimeric and revertant viruses (MDV-1, MDV-1-ΔU_S3, MDV-1-ΔU_S3_Rev, MDV-1- MDV-2/U_S3, and MDV-1-HVT/U_S3) were determined as previously described (11). Briefly, CEF seeded on 60 mm cell culture plates were infected with parental, chimeric or revertant viruses at 100 plaque-forming units (PFU). On 0, 1, 2, 3, 4, and 5 days post infection, infected CEF were trypsinized, serially diluted, and used to infect CEF seeded on 35 mm cell culture plates. Cells were fixed at 7 days post infection and subjected to IFA with mouse anti-pp38 antibody. Plaque numbers were counted for each virus and individual plaque areas measured by Image J software as described previously (65).

MDV genome copy number. To determine the MDV genome replication, qPCR assay was performed to measure MDV genome copy number. Briefly, CEF seeded on 35 mm cell culture plates were infected with 100 PFU of wild type, chimeric or revertant viruses. On 1, 2, 3, 4, and 5 days post infection, cells were harvested for genomic DNA isolation. MDV genome copy number of each virus was determined by qPCR assay with primers specific to MDV *ICP4,* and chicken *GAPDH* as internal control, (primers 102 to 105; Table S1) and calculated using a standard curve method, as previously described (159). The relative MDV genome copy number was presented as the ratio of ICP4 to GAPDH copy number.

Animal experiment 1. All animal experiments were conducted following protocols approved by the Texas A&M University Institutional Animal Care and Use Committee (IACUC). To study the role of MDV U_S3 in regulating MDV replication in chickens, *in vivo* replication properties of chimeric and revertant viruses were determined in spleens of infected chickens. One-day-old chickens were randomly sorted into 6 experimental groups of 15 chickens each. Five groups of chickens were inoculated subcutaneously with 2000 PFU of parental (MDV-1), U_S3 deletion mutant (MDV-1-ΔU_S3), U_S3 revertant (MDV-1-ΔU_S3_Rev), or U_S3 chimera (MDV-1- MDV-2/U_S3, and MDV-1-HVT/U_S3) viruses; a group remained as uninoculated control. Five chickens were randomly selected from each group at 6, 14, and 28 days post inoculation, and spleens collected for lymphocyte isolation using Histopaque® (Sigma) followed by genomic DNA isolation. The viral genome copy number was determined as stated above. At day

14 post inoculation, thymus, bursa, and body weight of 5 chickens per group were measured to evaluate lymphoid organ atrophy.

Animal experiment 2. To evaluate the role of MDV U_S3 on MD pathogenesis, survival rate and tumor development were determined in chickens inoculated with parental, chimeric and revertant viruses. One-day-old chickens were randomly sorted into 6 experimental groups of 12 chickens each. Five groups were inoculated subcutaneously with 2000 PFU of parental (MDV-1), U_S3 deletion mutant (MDV-1-ΔU_S3), U_S3 revertant (MDV-1-ΔU_S3_Rev), or U_S3 chimera (MDV-1- MDV-2/U_S3, and MDV-1-HVT/U_S3) viruses; a group remained as uninoculated control. Chickens were monitored daily for 10 weeks. All chickens were necropsied at the time of death or at the end of the experiment to evaluate MDV-specific lesions in visceral organs and nerves.

4. MAREK'S DISEASE VIRUS MEQ ONCOPROTEIN INTERACTS WITH CHICKEN HDAC 1 AND 2 AND MEDIATES THEIR DEGRADATION VIA PROTEASOME DEPENDENT PATHWAY [*]

4.1. Introduction

Marek's disease (MD) is a highly contagious lymphoproliferative disease of chicken caused by an avian alphaherpesvirus, Marek's disease virus (MDV). Infection with MDV results in paralysis, neurological disease, T-cell lymphomas, and immunosuppression in infected chickens (1). Due to occasional outbreaks and the use of more than five billion doses of MDV vaccine annually, MD is still an economically significant disease for the poultry industry (180). The genome of MDV consists of two unique regions flanked by inverted repeat regions; proteins and RNAs that are highly expressed in MDV latent infected cells are encoded by the repeat regions (11). Among those genes encoded in the repeat region, *meq* is the most characterized and is consistently expressed both during the lytic phase and in lymphoblastoid tumor cells (133). Meq has been shown to be essential for MDV induced transformation of T lymphocytes, but dispensable for lytic infection (11).

MDV Meq is a 339 amino acid long protein, encoded in the MDV EcoRI Q fragment of the MDV-1 genome (133). Meq is characterized by a N-terminal basic

---

[*]Reprinted with permission from "Marek's disease virus Meq oncoprotein interacts with chicken HDAC 1 and 2 and mediates their degradation via proteasome dependent pathway" by Yifei Liao, Blanca Lupiani, Yoshihiro Izumiya, Sanjay M. Reddy, 2021. Scientific Reports, Volume 11, Copyright [2021] by The Author(s).

region (BR) and leucine zipper (ZIP) domain, as well as a C-terminal transcriptional regulatory domain (111). The basic-leucine zipper (BZIP) domain of Meq shares significant homology with the Jun/Fos family of transcription factors and also forms heterodimer with Jun/Fos as well as homodimer with itself (135). Using antisense RNA that specifically targets the *meq* gene, Xie *et al*. demonstrated the importance of Meq in maintaining the transformed status of MSB-1, an MDV transformed lymphoblastoid cell line (181). Without an optimal *in vitro* chicken T cell transformation system, the direct transformation properties of Meq were first characterized in a rodent fibroblast (Rat-2) cell line (182). Ectopic expression of Meq resulted in transformation of Rat-2 cells characterized by anchorage- and serum- independent growth as well as morphological transformation, and resistance to apoptosis (182). Lupiani *et al*. showed that infection with a Meq null virus did not induce MD associated lymphomas in infected chickens, even though the virus replicated robustly during early cytolytic phase, providing the first conclusive evidence that Meq plays an essential role in transformation of lymphocytes (11). Later, Levy *et al.* revealed that Meq induced transformation of DF-1 cells, an immortalized chicken embryo fibroblast cell line, is through a v-Jun pathway (183). In addition to transformation, Meq has been shown to interact with multiple cellular proteins, regulate cellular signaling pathways, and bind to both viral and host genomes (136). The interaction of Meq and c-Jun has been well studied, and Meq-Jun heterodimers binds to AP-1 sequence to transactivate target gene expression (111). Some other AP-1 transcription factors, including Fos, CREB, and ATF family members, also interact with Meq (14). It has been shown that Meq interacts with p53 tumor suppressor

protein and suppresses p53 mediated apoptosis and transcriptional regulation (15). In addition, the interaction between Meq and C-terminal binding protein 1 (CtBP) has been demonstrated to be critical for Meq induced T cell lymphomas (12).

Recently, post-translational modifications of histones have been identified as a critical regulatory factors of viral gene expression during herpesvirus infection, which is one of the mechanisms that host cells utilize as anti-viral response towards incoming herpesvirus genomes (184). As a consequence, herpesvirus have developed mechanisms to manipulate and interfere with histone-modifying enzymes to benefit their replication and gene expression in host cells. Acetylation is one of the most well studied modifications of histone proteins, a reversible modification that occurs on lysine (K) residues. There are numerous histone acetyltransferases (HATs) and their activity can be reversed by the activity of histone deacetylases (HDACs). In mammals, eighteen HDACs have been identified and are classified into four different groups. Class I HDACs, including HDAC1, 2, 3 and 8, are the most studied. Especially, HDAC1 and HDAC2 (HDAC1 and 2) have been showed to be involved in the formation of at least three distinct repressor complexes, including Sin3, CoREST and NuRD (185). Post-translational modifications, including phosphorylation, ubiquitination, and SUMOylation, of HDAC1 and 2 have also been extensively studied (102). Phosphorylation of HDAC1 and 2 regulates their transcriptional regulation activity, enzymatic activity, and protein interactions (102). Casein kinase II (CKII) has been identified as the main cellular upstream protein kinase responsible for phosphorylation of HDAC1 and 2 *in vivo* (166). Early studies have shown that HDAC1 and 2 are also

phosphorylated by alphaherpesvirus encoded U_S3 serine/threonine protein kinase (58, 162). Ubiquitin and small ubiquitin-like modifier (SUMO) are small regulatory proteins which share a similar modification machinery, mediated by three enzymes: E1 activating enzyme, E2 conjugating enzyme and E3 ligase. Covalent attachment of ubiquitin targets proteins for degradation through the proteasome pathway, while modification by SUMO usually regulates the target protein activity and cellular localization (186, 187). Both HDAC1 and HDAC2 have been reported to be ubiquitinated and degraded by the proteasome dependent pathway (102). Ubiquitination and degradation of HDAC1 has been shown to correlate with the enhanced metastatic activity of prostate and breast cancer cell lines (188). However, even though both HDAC1 and HDAC2 have been shown to be SUMOylated, the biological significances of their SUMOylation are still under investigation (102).

The interaction between *alpha*, *beta*, and *gamma* herpesviruses with HDACs has been widely studied, and exhibits different effects. Treatment of herpesvirus latently infected cells with HDAC inhibitors (HDACi), reactivates virus and dramatically remodels viral genome architecture indicating HDACs play an important role in regulating herpesvirus latency (185, 189). Upon infection with herpes simplex virus 1 (HSV-1), viral protein ICP8 translocates HDAC1/CoREST/LSD1 to the cytoplasm, and ICP0 interacts with HDAC1 to disrupt the CoREST repressor complex and translocates HDAC1 to ND10 bodies (190). It has been shown that human cytomegalovirus (HCMV) pUL28/29 and pUL38 proteins cooperate with NuRD complex to promote the expression of immediate-early genes during infection (191). Epstein–Barr virus (EBV) nuclear

antigen 3C (EBNA3C) interacts with HDAC1 and 2 to repress viral gene expression and promote the association between HDAC1 and CBF1/RPB-Jk (192). In addition, like MDV, EBV and Kaposi's sarcoma-associated herpesvirus (KSHV) encode a BZIP protein, BZLF1 and K-bZIP, respectively, and it has been reported that the SUMOylated BZLF1 interacts with and recruits HDAC3 to BZLF1 responsive promoters to repress their transcriptional activity (119); on the other hand, K-bZIP interacts with HDAC2 via the leucine zipper domain and recruits it to the promoters of OriLyt and ORF50 (121). Even though HDACs play an important role in herpesvirus gene regulation, there are no studies on MDV-HDACs interaction. Here, we investigate the importance of Meq-HDAC interactions.

In this study, we show that Meq interacts with chicken HDAC1 and HDAC2 (chHDAC1 and 2) at the N-terminal dimerization domain of chHDAC1 and 2, and that Meq mediates the degradation of chHDAC1 and 2 via the proteasome dependent pathway. We also identified that the N-terminal, mainly the BZIP domain, of Meq is important for its association with chHDAC1 and 2. In addition, our results demonstrate that the N-terminal region of Meq is also important for Meq mediated degradation of global ubiquitinated proteins. In conclusion, our results illustrate that MDV Meq functionally interacts with chHDAC1 and 2, leading to their degradation through proteasome dependent pathway.

4.2. Results

MDV Meq co-localizes and interacts with chHDAC1 and 2. To explore the potential association between MDV Meq with chHDAC1 and 2, we first examined the subcellular localization of Meq and chHDAC1 and 2 in MDV lymphoblastoid tumor cells. We performed immunofluorescence assay (IFA) with two MDV lymphoblastoid tumor cell lines, MSB-1 and MCT-1, using antibodies against Meq and HDAC1 or HDAC2. As shown in Figure 4-1A, MDV Meq (green) co-localizes with chHDAC1 and 2 (red) in cell nuclei (blue) of MDV lymphoblastoid tumor cells. As stated in the introduction, HDAC1 and 2 are components of CoREST, NuRD and Sin3 protein complexes (102). We further studied the physical interaction between MDV Meq and HDAC1 and 2, as well as other protein components of these protein complexes. Immunoprecipitation (IP) assays with whole cell lysates of pcDNA-FLAG-Meq transfected 293T cells and MDV lymphoblastoid tumor cell line show that Meq could efficiently co-precipitate HDAC1 and 2, as well as protein components of the CoREST (CoREST and LSD-1), NuRD (MTA-1), and Sin3 (Sin3A) complexes in 293T cells (Figure 4-1B) and MDV lymphoblastoid tumor cells (MCT-1) (Figure 4-1C). The interactions between Meq and chHDAC1 and 2 were also observed in MDV infected chicken embryonic fibroblasts (data not shown).

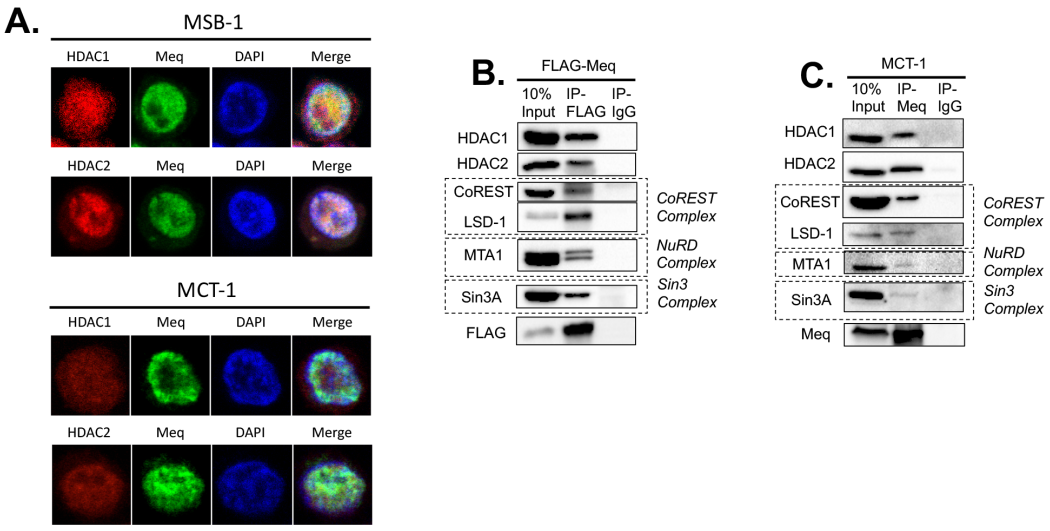

Figure 4-1 MDV Meq co-localizes and interacts with chHDAC1 and 2.
(A) MSB-1 and MCT-1 tumor cells were fixed and incubated with mouse anti-HDAC1 or mouse anti-HDAC2 and rabbit anti-Meq antibodies, followed by goat anti-mouse-Texas Red and goat anti-rabbit-Alex Flour 488. DAPI was used to stain cell nuclei. All images were taken by confocal microscopy. (B) 293T cells were transfected with pcDNA-FLAG-Meq. Forty-eight hours later, whole cell lysates were subjected to immunoprecipitation (IP) with FLAG antibody and normal mouse IgG. Western blot (WB) analysis was performed with the indicated antibodies target HDAC1, HDAC2 and other components in CoREST, NuRD, and Sin3 protein complexes. (C) MCT-1 tumor cells were lysed and subjected to IP with Meq polyclonal antibody and normal rabbit IgG, followed by WB with the indicated antibodies.

N-terminal dimerization domains of chHDAC1 and 2 mediate the interaction with Meq. After demonstrating the interaction between Meq and chHDAC1 and 2, we investigated the domains of chHDAC1 and 2 responsible for this interaction. We first generated several FLAG tagged N-terminal or C-terminal deletion mutants of chHDAC1 in pcDNA (Figure 4-2A). These mutants were cotransfected with pcDNA-HA-Meq into 293T cells, followed by IP. Our results show that both N-terminal, N-160 and N-320, of chHDAC1 interact with Meq at levels similar to wild type (WT) chHDAC1 (Figure 4-2B), while the C-terminal, 161-C and 321-C, constructs did not

interact with Meq (Figure 4-2C), indicating that N-terminal 160 amino acids of chHDAC1 are enough to mediate its association with Meq. We further shorten the essential interaction domain to the N-terminal 52 amino acids since constructs 53-C, 81-C, and 121-C of chHDAC1 failed to interact with Meq (Figure 4-2D). Similar results were observed for chHDAC2 with the N-terminal 53 amino acids being required for its interaction with Meq (Figure 4-3A to 3C).

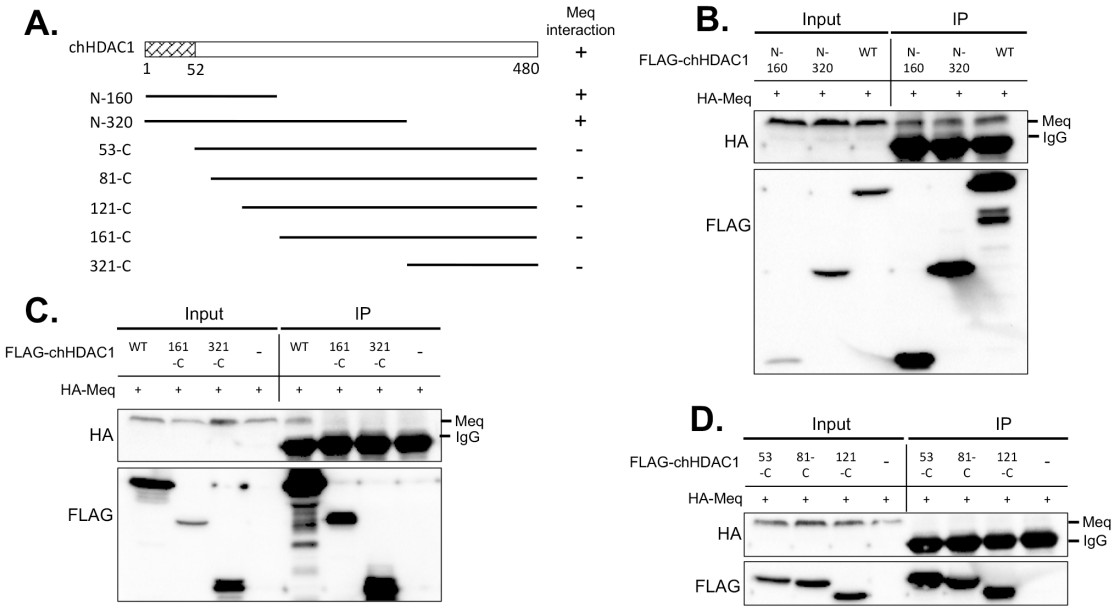

Figure 4-2 Mapping the domain in chHDAC1 that mediates its interaction with MDV Meq.
(A) Schematic representation of FLAG tagged pcDNA-chHDAC1 deletion mutants. The N-terminal 52 amino acids were marked as homodimerization domain and Meq interaction domain. The interaction of each chHDAC1 mutant with Meq is indicated on the right: "+" indicates interaction, "-" indicates no interaction. (B, C, D) The indicated FLAG tagged pcDNA-chHDAC1 deletion mutants were cotransfected with pcDNA-HA-Meq into 293T cells. Cells were lysed 48 hours post transfection and subjected to immunoprecipitation with mouse anti-FLAG agarose beads. Western blot was processed with HA and FLAG antibodies.

Since the N-terminal 52 and 53 amino acids of HDAC1 and HDAC2, respectively, were shown to be their homodimerization domains (165), we next examined whether the presence of Meq would affect their homodimerization. Plasmids expressing FLAG-chHDAC1 were cotransfected with HA-chHDAC1 in the presence of T7-Meq or empty vector (Ev) into 293T cells. Immunoprecipitation analysis shows that the interaction between FLAG-chHDAC1 and HA-chHDAC1 was not affected by the presence of Meq (Figure 4-3D). Interestingly, the levels of chHDAC1 were lower in the presence of Meq, in both input and IP results, due to Meq mediated degradation of chHDAC1 as shown in the following section. Similarly, Meq did not interfere with the homodimerization of chHDAC2 (Figure 4-3E).

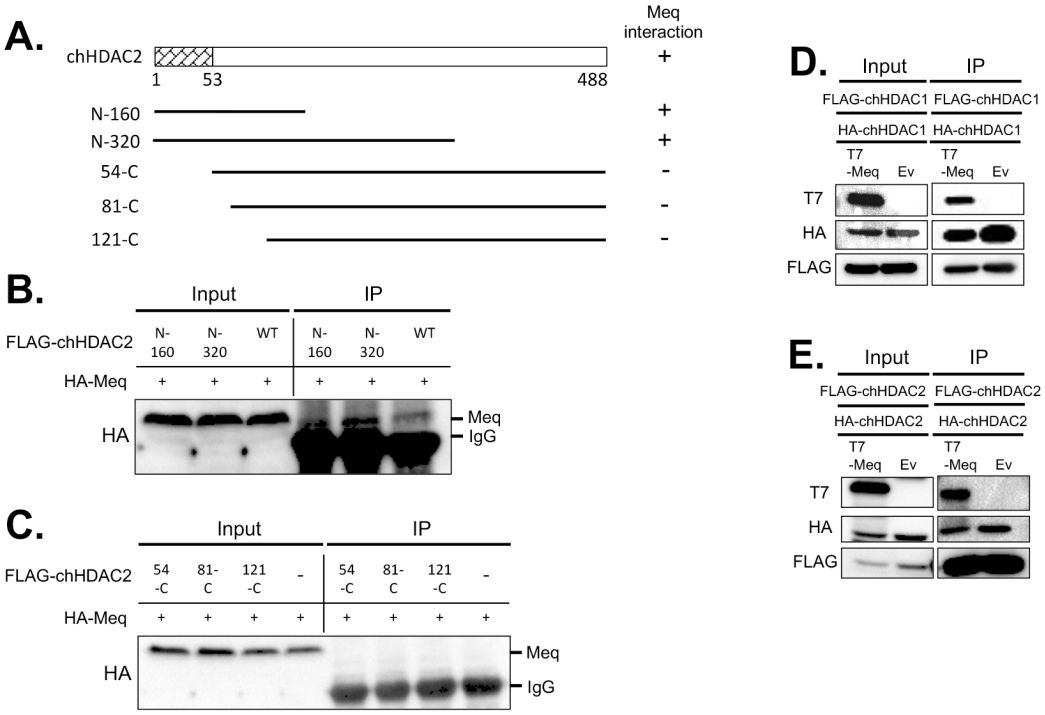

Figure 4-3 Mapping the domain in chHDAC2 that mediates its interaction with MDV Meq.

(A) Schematic representation of FLAG tagged pcDNA-chHDAC2 deletion mutants. The N terminal 53 amino acids were marked as homodimerization domain and Meq interaction domain. The interaction of each chHDAC2 mutant with Meq is indicated on the right: "+" indicates interaction, "-" indicates no interaction. (B, C) The indicated pcDNA-FLAG-chHDAC2 deletion mutants were cotransfected with pcDNA-HA-Meq into 293T cells for 48 hours. Immunoprecipitation (IP) was performed with mouse anti-FLAG agarose beads, followed by Western blot (WB) analysis with HA antibody. pcDNA-T7-Meq or pcDNA empty vector (Ev) were cotransfected with pcDNA-FLAG-chHDAC1 and pcDNA-HA-chHDAC1 (D) or pcDNA-FLAG-chHDAC2 and pcDNA-HA-chHDAC2 (E) into 293T cells. Forty-eight hours later, IP was processed with FLAG antibody and normal mouse IgG, followed by WB with T7, HA, and FLAG antibodies.

BZIP domain of Meq is important for its interaction with chHDAC1 and 2.

To identify the domain/s of Meq involved in its interaction with chHDAC1 and 2, we constructed a series of FLAG tagged pcDNA-Meq deletion mutants (Figure 4-4). First, FLAG tagged Meq basic region deletion (BR_del), leucine zipper deletion (ZIP_del), and double deletion (BZIP_del) mutants were cotransfected into 293T cells. Our IP results show that Meq-BR_del, Meq-ZIP_del, and Meq-BZIP_del mutants only weakly interact with chHDAC1 compared to wild type Meq (Figure 4-5A), indicating that the BZIP region of Meq is important for its association with chHDAC1. We also included c-Jun as a control, since it has been shown to interact with Meq at the ZIP region (193). Our IP results confirmed that Meq BR deletion mutant, but not Meq ZIP deletion and BZIP deletion mutants, could interact with c-Jun (Figure 4-5A).

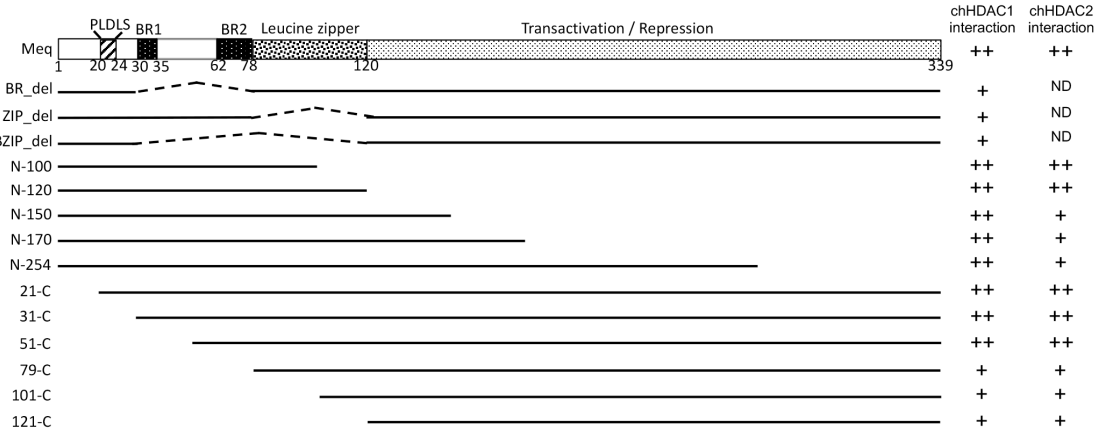

Figure 4-4 Schematic representation of Meq deletion mutants.
Schematic representation of Meq domains and FLAG tagged pcDNA-Meq deletion mutants. The interaction of each Meq mutant with chHDAC1 and 2 is indicated on the right: "++" indicates strong interaction, "+" indicates weak interaction, "ND" indicates not determined.

To further explore the interaction region, additional Meq deletion mutants were examined in transfected 293T cells (Figure 4-4). Our IP results show that N-100 of Meq is enough to interact with chHDAC1 at similar level to WT Meq (Figure 4-5B). Furthermore, 51-C of Meq strongly associates with chHDAC1, but 79-C, 101-C and 121-C of Meq only weakly interacts with chHDAC1 (Figure 4-5B), indicating that the N-terminal 50 amino acids of Meq are not important for its association with chHDAC1. Overall, Figure 4-5B suggests that the 51-100 amino acid region, which is within the BZIP region, of Meq is important for its interaction with chHDAC1. Similarly, the same region, 51-100 amino acids, of Meq is also important for its interaction with chHDAC2 (Figure 4-5C). However, we also observed that although both N-100 and N-120 of Meq strongly interact with chHDAC2, N-150, N-170 and N-254 of Meq only weakly interact

with chHDAC2 (Figure 4-5C), indicating that the 121-150 amino acid region of Meq may partially inhibit the interaction between Meq and chHDAC2.

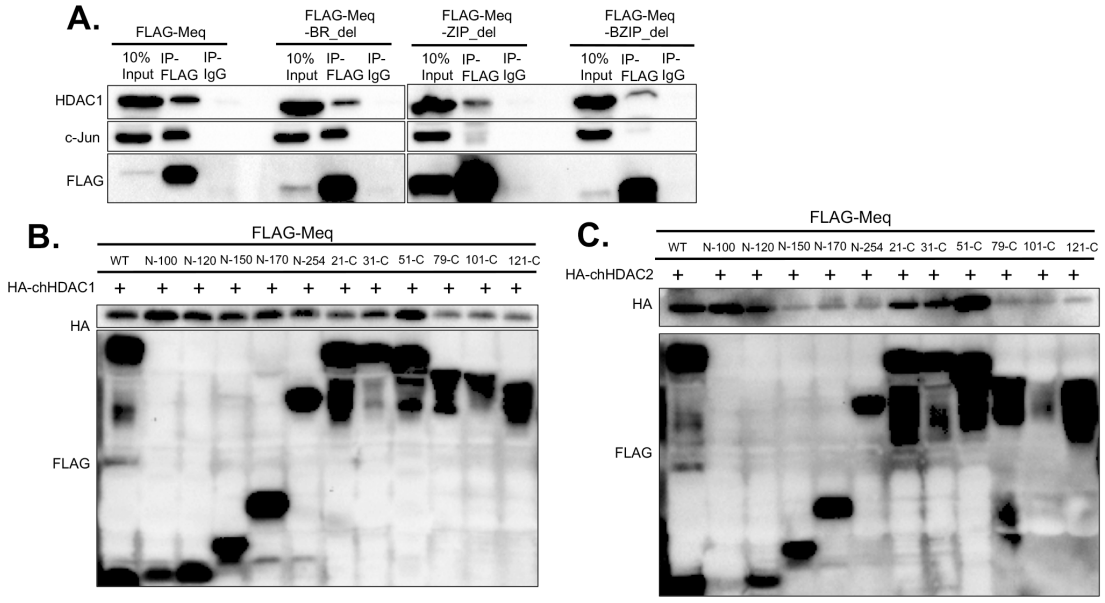

Figure 4-5 Mapping the domain in Meq that mediates its interaction with chHDAC1 and 2.
(A) pcDNA-FLAG-Meq deletion mutants were transfected into 293T cells for 48 hours. Whole cell lysates were subjected to immunoprecipitation (IP) with rabbit anti-FLAG antibody or normal rabbit IgG, followed by Western blot (WB) analysis with HDAC1, c-Jun, and FLAG antibodies. pcDNA-Meq deletion mutants were cotransfected with pcDNA-HA-chHDAC1 (B) or pcDNA-HA-chHDAC2 (C) into 293T cells. Whole cell lysates were harvested 48 hours post transfection and subjected to IP with mouse anti-FLAG agarose beads. WB was processed with HA and FLAG antibodies.

MDV Meq mediates the degradation of chHDAC1 and 2. During the course of our studies, apart from interaction, we observed that levels of chHDAC1 and 2 proteins were lower in the presence of Meq (Figure 4-3D and 3E) in transfected 293T cells. We further confirmed our results in DF-1 cells transfected with pcDNA-FLAG-Meq. As shown in Figure 4-6A left, levels of endogenous chHDAC1 and 2 were reduced in the presence of Meq and this reduced levels of chHDAC1 and 2 by Meq were not

regulated at the transcriptional level as only the protein levels (Figure 4-6A middle, Protein), but not mRNA levels (Figure 4-6A right, mRNA), of chHDAC1 and 2 were affected by the presence of Meq. Furthermore, our results show that chHDAC1 (Figure 4-6B) or chHDAC2 (Figure 4-6C) levels were reduced in a Meq dose dependent manner. Next, we examined the stability of chHDAC1 and 2 in cells cotransfected with pcDNA-FLAG-Meq or pcDNA empty vector (Ev), in the presence of cycloheximide (CHX), a protein synthesis inhibitor. Compared to Ev, levels of chHDAC1 were significantly lower in the presence of Meq at 4- and 6-hours post CHX treatment (Figure 4-6D). Similarly, levels of chHDAC2 were significantly lower in the presence of Meq at all time points post CHX treatment (Figure 4-6E). In addition, we examined the effect of Meq on levels of other interaction partners, including p53, CREB, and c-Jun (14, 15, 163). Our results show that the levels of chicken p53 (chp53), but not chCREB and chc-Jun, were reduced by increasing amounts of Meq protein (Figure 4-6F), indicating that Meq does not mediate the degradation of all interaction partners. Overall, these results suggest that MDV Meq could mediate the degradation of endogenous and exogenous chHDAC1 and 2.

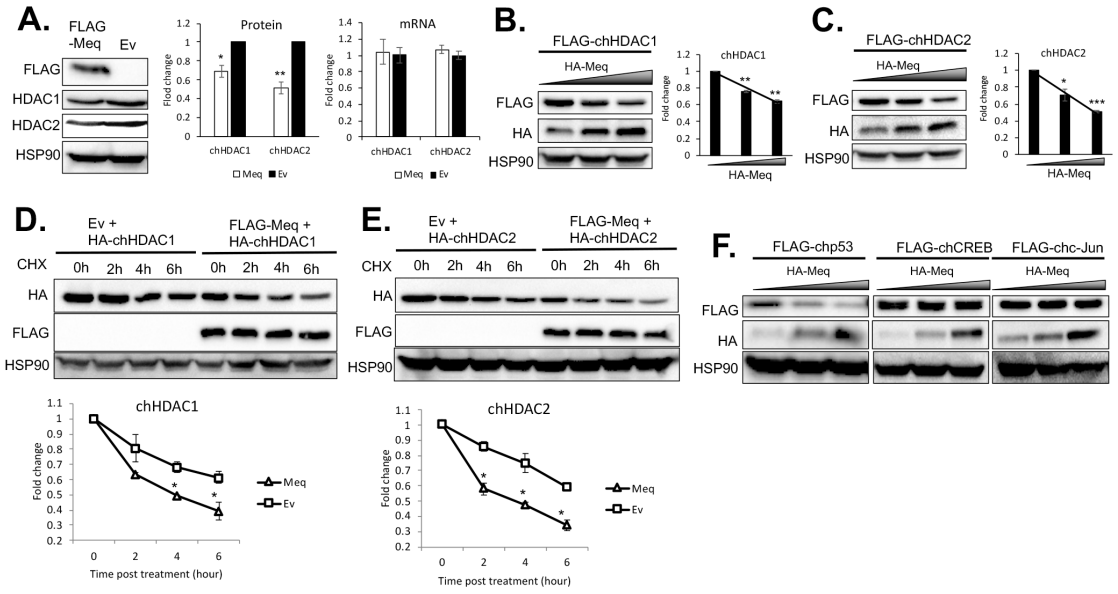

Figure 4-6 Meq mediates the degradation of chHDAC1 and 2.
(A) DF-1 cells were transfected with pcDNA-FLAG-Meq or pcDNA empty vector (Ev) and 48 hours later, cells were harvested for protein and RNA extraction. Western blot (WB) analysis was processed with the indicated antibodies (left) and quantified with Image J and presented as fold change compared to Ev (middle). qRT-PCR was processed with primers targeting chHDAC1 and chHDAC2 and presented as fold change compared to Ev (right). pcDNA-FLAG-chHDAC1 (B) or pcDNA-FLAG-chHDAC2 (C) were cotransfected with different amounts of pcDNA-HA-Meq into 293T cells for 48 hours. Whole cell lysates were subjected to WB with the indicated antibodies (left). WB results were quantified with Image J, normalized to HSP90, and presented as fold change compared to the least amount of Meq transfection (right). pcDNA-FLAG-Meq or pcDNA Ev were cotransfected with pcDNA-HA-chHDAC1 (D) or pcDNA-HA-chHDAC2 (E) into 293T cells and 24 hours later, cells were treated with cycloheximide (CHX, 1 mg/ml) for the indicated length of time. WB were performed with HA, FLAG, and HSP90 antibodies (upper). HA-chHDAC1 or HA-chHDAC2 protein levels were quantified with Image J, normalized to HSP90, and presented as fold change compared to non-treated cells (bottom). All experiments were repeated two times. Error bars indicate standard deviation (SD). (F) pcDNA-FLAG-chp53, pcDNA-FLAG-chCREB, or pcDNA-FLAG-chc-Jun were cotransfected with different amounts of pcDNA-HA-Meq into 293T cells and 48 hours later, cell lysates were subjected to WB with the indicated antibodies. *: $p<0.05$, **: $p<0.01$, ***: $p<0.001$.

MDV Meq mediates the degradation of chHDAC1 and 2 via the proteasome dependent pathway. To determine the mechanism responsible for Meq mediated

degradation of chHDAC1 and 2, we used a proteasome inhibitor, MG132, to treat Meq and chHDAC1 or chHDAC2 cotransfected 293T cells. As shown in Figure 4-7A, without MG132 treatment, levels of HA-chHDAC1 or HA-chHDAC2 are significant lower in FLAG-Meq compared to empty vector (Ev) transfected cells; with MG132 (10 μM) treatment, levels of HA-chHDAC1 or HA-chHDAC2 were no different between FLAG-Meq and empty vector (Ev) transfected cells. These results demonstrated that MG132 treatment could inhibit chHDAC1 and 2 degradation, indicating that Meq degrades chHDAC1 and 2 through a proteasome dependent pathway. We further confirmed our results by treating transfected cells with different concentration of MG132 and the results show that 5 μM MG132 treatment is sufficient to efficiently inhibit Meq mediated degradation of chHDAC1 and 2 (APPENDIX A, Figure S6A and S6B). In addition, MG132 (10 μM) treatment also rescued the degradation of chHDAC1 and 2 in the presence of Meq and CHX (1 mg/ml) (APPENDIX A, Figure S6C and S6D).

Since chHDAC1 and 2 appears to be degraded by a proteasome dependent pathway, a mechanism normally initialized by ubiquitination, we next investigated the ubiquitination of chHDAC1 and 2 in the presence or absence of Meq. 293T cells were cotransfected with pcDNA-FLAG-chHDAC1 or pcDNA-FLAG-chHDAC2 and pcDNA HA tagged ubiquitin (HA-Ub) in the presence or absence of pcDNA-HA-Meq. Twenty-four hours later, cells were treated overnight with DMSO or MG132 and subjected to IP using mouse anti-FLAG agarose beads to precipitate FLAG tagged chHDAC1 and chHDAC2, followed by Western blot analysis with ubiquitin antibody. Our results show that chHDAC1 and 2 were ubiquitinated resulting in higher molecular weight protein

species (Figure 4-7B and 7C). In addition, ubiquitinated chHDAC1 and 2 were degraded in the presence of Meq (Figure 4-7B and 7C, DMSO treatment), which can be inhibited by treatment of MG132 (Figure 4-7B and 7C, MG132 treatment). In conclusion, the above results suggest that Meq utilizes a proteasome dependent pathway to induce the degradation of chHDAC1 and 2.

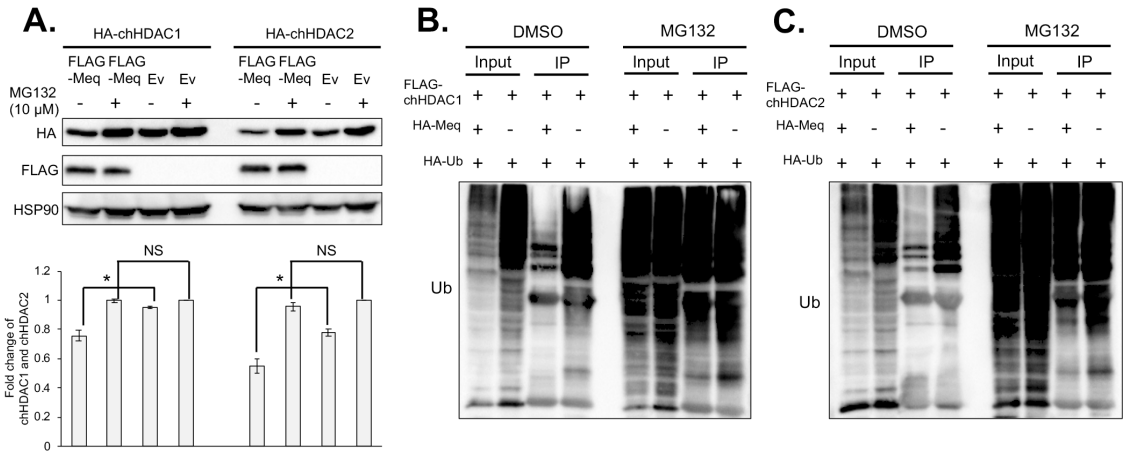

Figure 4-7 MDV Meq mediates the degradation of chHDAC1 and 2 via the proteasome dependent pathway.
(A) pcDNA-HA-chHDAC1 or pcDNA-HA-chHDAC2 were cotransfected with pcDNA-FLAG-Meq or pcDNA empty vector (Ev) into 293T cells and 24 hours later, cells were treated overnight with or without MG132 (10 μM). Western blot (WB) analysis was performed with whole cell lysates using the indicated antibodies. Representative WB images were shown (upper). Protein levels of HA-chHDAC1 or HA-chHDAC2 were quantified with Image J, normalized to HSP90, and presented as fold change compared to MG132 treated pcDNA-HA-chHDAC1 or pcDNA-HA-chHDAC2 and pcDNA Ev cotransfected cells (bottom). *: $p<0.05$, NS: not significant. pcDNA-FLAG-chHDAC1 (B) or pcDNA-FLAG-chHDAC2 (C) were cotransfected with pcDNA-HA-Meq or pcDNA Ev and pcDNA-HA-Ub into 293T cells. Twenty-four hours post transfection, cells were treated with MG132 (10 μM) or DMSO overnight. Immunoprecipitations were performed with mouse anti-FLAG agarose beads, followed by WB with ubiquitin antibody.

MDV Meq mediates the degradation of global ubiquitinated proteins via proteasome dependent pathway. Apart from chHDAC1 and 2, we found that MDV

Meq could degrade ubiquitinated protein globally in a proteasome dependent pathway as MG132 treatment restored high molecular weight ubiquitinated proteins in Meq overexpressed cells (Figure 4-8A). We further mapped the domain of Meq important for its ability to mediate the degradation of ubiquitinated proteins. We cotransfected the indicated pcDNA-FLAG-Meq deletion mutants and pcDNA-HA-Ub into 293T cells. Western blot results show that N-120 to N-254 of Meq, but not N-100 of Meq, reduce levels of global ubiquitinated proteins (Figure 4-8B). In addition, we observed that 21-C to 51-C of Meq, but not 79-C, BR_del, ZIP_del and BZIP_del of Meq, reduce levels of global ubiquitinated proteins (Figure 4-8B). Taken together, we concluded that amino acids 51-120, which are within the BZIP region, are important for Meq mediated degradation of global ubiquitinated proteins.

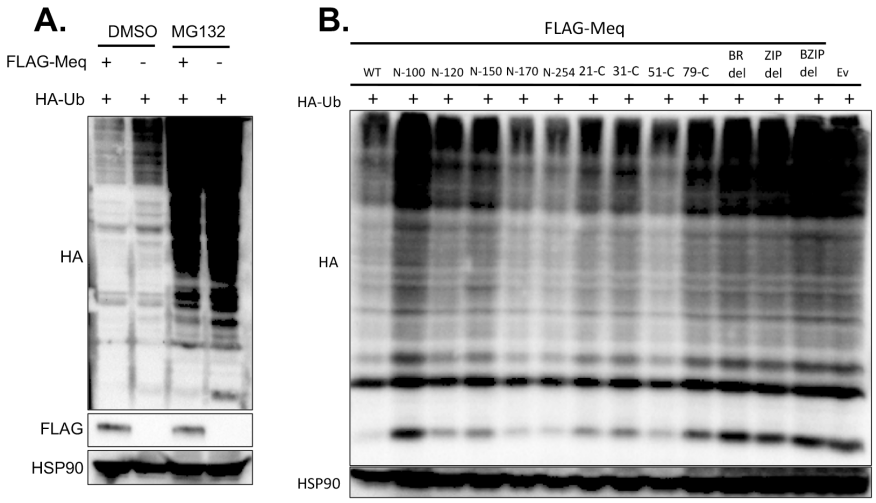

Figure 4-8 MDV Meq mediates the degradation of global ubiquitinated proteins via the proteasome dependent pathway.
(A) pcDNA-FLAG-Meq or pcDNA empty vector (Ev) were cotransfected with pcDNA-HA-Ub into 293T cells. Twenty-four hours later, cells were treated with DMSO or MG132 (10 μM) overnight. Cells were lysed and subjected to Western blot (WB) analysis with HA, FLAG, and HSP90 antibodies. (B) pcDNA-HA-Ub was cotransfected with the indicated pcDNA-FLAG-Meq deletion mutants or pcDNA Ev into 293T cells

and 48 hours later, cells were lysed and subjected to WB with HA and HSP90 antibodies.

4.3. Discussion

Meq is a oncoprotein encoded by MDV, which plays an essential role in MDV induced transformation of T lymphocytes in chickens (11). Apart from its transformation property, multiple functions have been attributed to Meq, including transcription regulation, apoptosis inhibition, protein interactions and DNA binding (12, 14, 15, 110, 183). However, the molecular mechanisms of Meq-host interactions are still not fully understood. It has been shown that the oncogenic property of Meq are related to its interaction with CtBP, which also interacts with adenovirus encoded E1A protein and EBV encoded EBNA3A and EBNA3C proteins (12).

HDACs are a class of modification enzymes that can remove acetyl molecules from lysine ε-NH_3 groups. In total, 18 HDACs have been identified so far in humans and have been classified into four classes. Numerous studies emphasize the critical role of histone and non-histone proteins acetylation in herpesviruses infection (184, 194). HDACs are prominent regulators of protein acetylation and play essential roles in gene expression regulation, thus herpesviruses have evolved a variety of mechanisms to modulate HDACs functions. It has been reported that varicella zoster virus (VZV) encoded ORF66 protein kinase (the U_S3 ortholog in VZV) phosphorylates HDAC1 at serine 406 (S406) and HDAC2 at S407 which are unique to cellular protein kinase target sites (162), however, the biological functions of this phosphorylation are still not clear. In addition, EBV encoded EBNA3C and KSHV encoded K-bZIP protein both have been

reported to interact with HDAC1 and HDAC2 to regulate viral gene expression (121, 195, 196). These observations prompted us to study the interaction between Meq and HDAC1 and 2.

To examine whether Meq associates with chHDAC1 and 2, we first visualized the subcellular localization of Meq and chHDAC1 and 2 in two MDV lymphoblastoid tumor cell lines. Co-localization of Meq and chHDAC1 and 2 was observed in the cell nuclei of MDV lymphoblastoid tumor cells (Figure 4-1A). Our IP results further demonstrate that Meq physically associates with chHDAC1 and 2 in transfected 293T cells (Figure 4-1B) and MDV lymphoblastoid tumor cells (Figure 4-1C). In addition, we observed that Meq directly or indirectly interacts with other components of the chHDAC1 and 2 associated CoREST, NuRD, and Sin3 protein complexes (Figure 4-1B and 1C). We next identified the N-terminal homodimerization domain of chHDAC1 and 2 as essential for their interaction with Meq (Figure 4-2 and 3). Our results also showed that FLAG-chHDAC1 and FLAG-chHDAC2 could still efficiently co-precipitate HA tagged chHDAC1 and chHDAC2 in the presence of Meq (Figure 4-3D and 3E), indicating Meq does not interfere the homodimerization of chHDAC1 and chHDAC2. In addition, we showed that the BZIP domain of Meq is important its interaction with chHDAC1 and 2 (Figure 4-5). Interestingly, we observed that N-120 of Meq strongly interacts with chHDAC2, but N-150 just slightly pull down chHDAC2, suggesting that that amino acids 121-150 of Meq may interfere its interaction with chHDAC2 (Figure 4-5C). These results suggest that Meq may associate with chHDAC1 and chHDAC2 via different mechanisms despite the high homology between chHDAC1 and chHDAC2.

Another interesting point we noticed throughout our study is that overexpression of Meq resulted in lower levels of chHDAC1 and 2 (Figure 4-3D and 3E). This observation was confirmed by results showing that Meq induces the degradation of endogenous and exogenous chHDAC1 and 2 protein but does not affect levels of mRNA (Figure 4-6A-E), and this process is specific to chHDAC1 and 2 as Meq did not degrade other interaction partners, including CREB and c-Jun (Figure 4-6F). Then, we investigated the potential mechanisms utilized by Meq to facilitate the degradation of chHDAC1 and 2. Proteasome dependent pathway and autophagy are the two major proteolytic pathways for protein degradation (197). The proteasome is a protein complex that is present in both nucleus and cytoplasm, and which can eliminate misfolded or unnecessary proteins. The main proteasome is 26S proteasome which consists of a 20S core particle and two 19S regulatory particles (198). Mostly, proteins targeted for degradation are dependent on ubiquitin conjugation, however there are exceptions of degradation via an ubiquitin independent proteasome degradation (UIPD) pathway (199). Ubiquitination is a sequential procedure mediated by three enzymes: E1 ubiquitin activating enzyme, E2 ubiquitin conjugating enzymes, and E3 ubiquitin ligase enzyme. Autophagy is another proteolysis mechanism used by the cell to degrade unnecessary proteins, and consists of three different type: macroautophagy, microautophagy, and chaperone-mediated autophagy (CMA) (198). Unlike ubiquitin dependent proteasome degradation, proteins eliminated by autophagy are indiscriminately degraded upon binding to lysosomes. A number of viral proteins have been showed to degrade cellular proteins via proteasome, and some viral proteins even contain E3 ubiquitin ligase

domains. It has been shown that HSV-1 ICP0 has two distinct E3 ligase domains that play an important role in mediating ubiquitination and degradation (73). KSHV encoded transcription activator (RTA) has been shown to act as an E3 ligase to ubiquitinate and degrade interferon regulatory factor 7 (IRF7) and KSHV-RTA binding protein (K-RBP) (80, 200). In addition, pp71, a transactivator encoded by HCMV, has been reported to degrade Rb and Daxx through UIPD (201). With the treatment of proteasome inhibitor MG132, we showed that Meq mediates the degradation of chHDAC1 and 2 through a proteasome dependent pathway (Figure 4-7 and APPENDIX A, Figure S6). Considering importance of chHDACs in gene expression regulation and MDV genome replication, we speculate that Meq is involved in transcriptional regulation and MDV replication through, at least partially, its role in manipulating chHDAC1 and 2. To further study the interplay between Meq and the cellular proteasome pathway, we found that ectopic expression of Meq reduces levels of global ubiquitinated proteins via the proteasome dependent pathway, for which amino acids 51-120 of Meq are important (Figure 4-8). The proteasome dependent degradation pathway is a complex sequential process, in which a large number of cellular components are involved. Further studies will be needed to reveal exact mechanisms behind the interplay between MDV Meq and the proteasome dependent degradation pathway.

4.4. Materials and methods

Cells. Human embryonic kidney 293T cells and chicken DF-1 cells were grown in Dulbecco's modified Eagle medium (DMEM) supplemented with 10% fetal bovine

serum (FBS). MDV lymphoblastoid tumor cell lines, MSB-1 (202) and MCT-1, were grown in RPMI 1640 medium supplemented with 15% FBS. MCT-1 cell line was established from a kidney lymphoma of chickens infected with a very virulent strain of MDV. All cells were grown at 37°C in the presence of 5% CO_2. 293T and DF-1 cells were used for transient transfections, and MDV tumor cell lines were used for immunofluorescence and immunoprecipitation assays.

Chemicals. Cycloheximide (CHX) and MG132 were purchased from Millipore-Sigma and reconstituted in dimethyl sulfoxide (DMSO) to prepare stock solution according to manufacturer's instruction. CHX was used to determine the protein half-life and MG132 was used to study the proteasome degradation pathway.

Plasmids construction. pcDNA™3.1/Zeo (+) mammalian expression vector (Invitrogen) was used for the generation of Meq and chHDAC1 and 2 constructs. All primers are listed in APPENDIX B, Table S2 and all cloned genes were validated by sequencing.

Meq plasmids. FLAG, HA, and T7 tagged full length Meq was amplified from MDV (686 strain) bacterial artificial chromosome (BAC) DNA (178) using primers 1 to 4 (APPENDIX B, Table S2). The PCR products were purified using QIAEX II Gel Extraction Kit (Qiagen) followed by digestion and cloning into pcDNA™3.1/Zeo (+) plasmid. Same processes were performed to generate FLAG tagged N- and C-terminal truncate plasmids using primers 1 and 5 to 16 (APPENDIX B, Table S2). Overlapping PCR (179) was performed to generate FLAG tagged BR, ZIP, and BZIP deletion Meq expression plasmids using primers 1, 4, and 17 to 22 (APPENDIX B, Table S2).

chHDAC1 plasmids. FLAG and HA tagged full length chHDAC1 was amplified from chicken cDNA using primers 23 to 25 (APPENDIX B, Table S2), followed by digestion and cloning into pcDNA™3.1/Zeo (+) plasmid. Same experiments were performed using primers 23 and 26 to 33 (APPENDIX B, Table S2) to generate FLAG tagged N- and C-terminal truncated chHDAC1 constructs.

chHDAC2 plasmids. FLAG and HA tagged full length chHDAC2 was amplified from chicken cDNA using primers 34 to 36 (APPENDIX B, Table S2), followed by digestion and cloning into pcDNA™3.1/Zeo (+) plasmid. FLAG tagged N- and C-terminal truncated chHDAC2 constructs were generated using primers 34 and 37 to 42 (APPENDIX B, Table S2).

Immunofluorescence assay (IFA). To examine the co-localization of Meq with chHDAC1 and 2, IFA was performed using MDV lymphoblastoid tumor cell lines. MSB-1 and MCT-1 tumor cells were pelleted by centrifuge at 500 x g for 5 min followed by three washes with phosphate buffered saline (PBS). Cell pellets were resuspended with 200 µl PBS and settled onto coverslips for 2 min at room temperature. Then, cells were fixed with 3.7% formaldehyde-PBS solution followed by quenching with 100 mM glycine-PBS solution for 5 min and permeabilized with acetone-methanol (1:1) solution for 15 min at room temperature. After three washes with PBS, cells were incubated with mouse anti-HDAC1 (Santa cruz biotechnology) or mouse anti-HDAC2 (Santa cruz biotechnology) and rabbit anti-Meq antibodies for 1 hour, followed by another hour incubation with goat anti-mouse-Texas Red antibody and goat anti-rabbit-Alex Flour 488 antibody at room temperature. After three washes with PBS, cells were

stained with 4',6-diamidino-2-phenylindole (DAPI) for 5 min at room temperature. Cells on coverslips were then mounted on glass slides with ProLong™ Diamond Antifade Mountant (Thermo Fisher Scientific) and imaged with Zeiss LSM 780 NLO Multiphoton Microscope.

Immunoprecipitation (IP) and Western blot (WB).

To study the interactions between Meq and chHDAC1 and 2, IP and WB were performed with MDV lymphoblastoid tumor cell lines and transfected 293T cells. *For MDV lymphoblastoid tumor cells.* MDV lymphoblastoid tumor cells were lysed in EBC lysis buffer (50 mM Tris-HCl, 120 mM NaCl, 0.5% NP-40, 50 mM NaF, 200 μM Na2VO4) with 1 mM phenylmethylsulfonyl fluoride (PMSF) and additional protease inhibitor cocktail (Thermo Fisher Scientific). For IP, 500 μg cell lysates were gently rotated overnight in the presence of 2 μg rabbit anti-Meq antibody or normal rabbit IgG (Cell Signaling Technology) at 4°C. Next day, the immune complexes were incubated with protein A and protein G Sepharose beads (Invitrogen) mixture for 2 hours at 4°C. After five washes with EBC lysis buffer, proteins were eluted by adding 2x sodium dodecyl sulfate (SDS) buffer and boiled for 5 min. Then, the immunoprecipitated samples and 10% input (50 μg cell lysates) were subjected to SDS-polyacrylamide gel electrophoresis (PAGE) followed by transferring to polyvinylidene fluoride (PVDF) membrane (Millipore-Sigma). PVDF membrane was incubated with 5% nonfat milk at room temperature for 1 hour, followed by WB with primary antibody incubation overnight at 4°C and horseradish peroxidase (HRP) conjugated secondary antibody incubation 1 hour at room temperature. After three washes with PBST (0.1% Tween 20),

PVDF membrane was visualized with Super Signal West Pico PLUS Chemiluminescent Substrate (Thermo Fisher Scientific).

For 293T cells. Transfected 293T cells were lysed in EBC lysis buffer for general IP or SDS lysis buffer (1% SDS, 50 mM Tris HCl, 10% glycerol) for detection of ubiquitinated proteins. 500 µg cell lysates were incubated overnight with mouse anti-FLAG agarose beads (Sigma) at 4°C with gentle rotation. The subsequent IP and WB processes are as described above.

Quantification of WB bands intensity was performed with Image J software.

RNA isolation and quantitative reverse transcriptase polymerase chain reaction (qRT-PCR). To determine the effect of Meq in the transcription of chHDAC1 and 2, DF-1 cells were transfected with pcDNA-FLAG-Meq or pcDNA empty vector (Ev). Forty-eight hours later, cells were harvested for RNA isolation using PureLink™ RNA Mini Kit (Invitrogen) as per manufacturer's instructions, followed by cDNA systhesis. qRT-PCR reactions, including melt cure analysis, were processed on a CFX96™ Real time PCR Detection System (Bio-Rad) using iTaq™ Universal SYBR® Green Supermix (Bio-Rad) with primers 43 to 48 (Table S1). Gene expression was normalized to signal of chicken *GAPDH*, and qRT-PCR results were analyzed using the $2^{-\Delta\Delta CT}$ method. Fold changes were calculated as to values derived from Ev transfected cells, and presented as average of three independent cell culture experiments with error bars representing standard deviation (SD).

5. SUMMARY AND FUTURE DIRECTIONS

5.1. Summary of research

MDV is the most potent avian oncogenic alphaherpesvirus that causes T-cell lymphoma in chickens as early as two weeks post infection. U_S3, a multifunctional protein kinase of alphaherpesviruses, is not essential for virus growth *in vitro*, but plays important roles in transcription regulation, cytoskeletal rearrangements, anti-apoptosis, and interferon (IFN) system interference (41). Although the functions of U_S3 have been extensively studied in HSV-1, the biological function of MDV U_S3 and its substrates has not been studied in detail. In addition, even Meq has been shown to be essential for MDV latency and/or transformation (11), the exact mechanisms associated with MDV tumorigenesis and virus replication/latency remain unknown. In Chapter 2 and Chapter 3, we identified novel substrates of MDV U_S3 and characterize the potential function of MDV U_S3 induced phosphorylation, as well as the role of U_S3 in MDV pathogenesis. In Chapter 4, we characterized the interaction between MDV Meq with chHDAC1 and 2, and demonstrated that Meq utilizes host proteasome dependent pathway to degrade chHDAC1 and 2 as well as global ubiquitinated proteins.

To study the biological functions of MDV-1 U_S3, using luciferase reporter systems, we first investigated potential cellular pathways that are regulated by MDV-1 U_S3 and identified chCREB as a substrate of MDV-1 U_S3. We showed that wild type MDV-1 U_S3, but not kinase dead U_S3 (U_S3-K220A), increases CREB phosphorylation, leading to recruitment of pCREB to the promoter of CREB responsive gene and

activation of CREB target gene expression. Interestingly, the ability to phosphorylate CREB is conserved among U_S3 from all three MDV serotypes. Apart from cellular genes, we also investigated the role of U_S3 in regulating viral gene expression. Using U_S3 deletion and U_S3 kinase dead recombinant MDV-1, we identified U_S3 responsive MDV-1 genes during infection, and found that the majority of U_S3 responsive genes were located in the MDV-1 repeat regions. ChIP-Seq studies determined that some U_S3 regulated genes co-localized with Meq recruitment sites. ChIP-PCR further confirmed Meq binding to the *ICP4/LAT* region, which are also regulated by U_S3. Furthermore, biochemical studies demonstrated that MDV-1 U_S3 interacts with Meq in transfected cells and MDV-1 infected chicken embryonic fibroblasts in a phosphorylation dependent manner. Finally, *in vitro* kinase studies revealed that Meq is a U_S3 substrate. MDV-1 U_S3 thus acts as an upstream kinase of the CREB signaling pathway to regulate the transcription function of CREB/Meq heterodimer, which regulates cellular and viral gene expression.

Then, we aimed to identify more substrates of MDV U_S3 and compared the function of U_S3 from three MDV serotypes. Our results showed that chHDAC1 is another conserved substrate of U_S3 from three MDV serotypes, while only MDV-1 and MDV-2 can phosphorylate chHDAC2. We further identified the modified residues in chHDAC1 and 2. We found that MDV-1 and HVT U_S3 phosphorylate chHDAC1 at S406, and MDV-2 U_S3 phosphorylates chHDAC1 at S406, S410, and S415; however, MDV-1 U_S3 and MDV-2 U_S3 phosphorylate chHDAC2 at S407, and S407 and S411, respectively. To our knowledge, this is the first comparatively study of the functions of

three serotypes MDV U_S3. Furthermore, biochemical studies showed that MDV U_S3 mediated phosphorylation of chHDAC1 and 2 affect their protein stability, transcriptional regulation activity, and protein interactions. In addition, we demonstrated that MDV U_S3 physically interacts with chHDAC1 and 2. We further generated chimeric viruses by replacing MDV-1 U_S3 with MDV-2 or HVT U_S3 respectively to study their role in MDV replication and oncogenicity. Our data showed that MDV-2 or HVT U_S3 partially rescued the growth deficiency of MDV-1 U_S3 null virus in cell culture and chickens. In addition, deletion of MDV-1 U_S3 attenuated the virus resulted in higher survival rate and lower MDV specific tumor incidence, which can also be partially compensated by MDV-2 and HVT U_S3. This finding provides the first evidence that alphaherpesvirus encoded U_S3 protein kinase is involved in the replication and oncogenicity of virus in the natural host. Overall, we identified novel substrates of U_S3 from three MDV serotypes and characterized their role in MDV pathogenesis, which is an important finding that towards the better understanding of the function of U_S3 protein kinase.

Based on our above results, we demonstrated chHDAC1 and 2 as well as Meq are the interaction partners of MDV U_S3. MDV Meq has been considered as the major MDV oncoprotein and plays important role in transcription regulation. It has been reported that Meq interacts with various cellular proteins and the oncogenicity of Meq is connected to its interaction with CtBP. These facts promote us to examine the interaction between Meq and chHDAC1 and 2. Our confocal microscopic analysis showed that Meq co-localizes with chHDAC1 and 2 in the nuclei of MDV transformed tumor cells. The

immunoprecipitation assay demonstrated that Meq physically interacts with chHDAC1 and 2 in transfected cells and MDV transformed tumor cells. In addition, we found Meq interacts the protein components in chHDAC1 and 2 associated CoREST, NuRD and Sin3 repressor protein complexes, indicating that Meq may exhibit transcriptional repressive function by associating with host repressors. Furthermore, the interaction domain has been mapped to N-terminal of chHDAC1 and chHDAC2, and BZIP domain of Meq. Next, we found that Meq mediates the degradation of chHDAC1 and chHDAC2 via proteasome dependent pathway, and our results showed that Meq also degrades global ubiquitinated proteins through proteasome dependent pathway. Overall, our results showed that Meq interacts with and degrades chHDAC1 and chHDAC2. These findings provide insights in understanding the interplay between viral oncoprotein and host transcription repressor, as well as host proteasome degradation pathway.

5.2. Future directions

Even though we identified novel viral and cellular substrates of MDV-1 U_S3, the mechanisms behind the different phenotypes exhibited by U_S3 from three MDV serotypes needed to be studied. We speculate that U_S3 from three MDV serotypes interact with different host factors to behavior differently. In addition, our luciferase reporter screening results showed that MDV-1 U_S3 regulates more cellular pathways other than CREB activation pathway. Next generation sequencing and mass spectrogram or proteomic methods would be great tools to globally analyze genes and pathways that are regulated by U_S3 from three MDV serotypes and identify their interaction partners,

which would help to reveal the functional differences between Us3 from three MDV serotypes.

The interaction between MDV infection and host ubiquitin-proteasome pathways is another interesting area needs further study. Our results showed that MDV Meq oncoprotein utilizes ubiquitin-proteasome pathways to degrade chHDAC1 and 2, as well as global ubiquitinated proteins. Given the dynamic properties of MDV Meq expression in different infection stage and the complexity of proteasome mediated protein degradation, researches for interplay between MDV Meq and host ubiquitin-proteasome pathways in different MDV infection stages would help to better understand MDV and host interaction. These data would also benefit the research of other herpesviruses, especially herpesviruses encoded oncoproteins and BZIP proteins. Ubiquitin pathway qPCR array or RNA sequencing and proteomic methods would help to investigate the role of MDV Meq in regulating host ubiquitin-proteasome pathways at transcriptome and proteome levels.

It has been widely studied that HDACs play an important role in maintaining herpesvirus latency. Our studies showed that HDACs activity is required for efficient MDV replication in cell culture. However, most of these researches were done using HDAC inhibitors that inhibit the activity of multiple HDACs (58, 162, 189), therefore the specific roles of individual HDAC remain unknown. Using the advanced CRISPR method, individual HDAC would be targeted for deletion or silencing; in combination with stable cell lines generation, we would reveal the specific functions of each chHDAC in regulating MDV replication, viral gene expression, and MDV latency and

reactivation. The knowledge we gained from MDV research would also be applied to human herpesvirus researches and the CRISPR-Cas9 system established will have broad application perspective to study mechanisms of herpesvirus and host interaction.

The single cell sequencing developed rapidly in the recent years and have been applied to virology research (203). Herpesvirus infection consists of distinct lytic and latent stage, and the dynamic switch between stages is a mysterious process. Most human herpesviruses researches using human cell lines or humanized animal models, which may not represent the real situation in human. With well-established Two-step Red-mediated recombination system and the recent developed CRISPR system to manipulate viral genomes, as well as a natural host animal model to evaluate the pathogenicity, MDV represents a unique and important model to study herpesvirus-host interaction and herpesvirus mediated transformation. Single cell sequencing of splenocytes isolated from infected chickens at different stages would provide comprehensive viral and cellular gene expression picture during MDV infection, which will greatly facilitate our understanding about MDV biology and MD progression.

REFERENCES

1. Calnek BW. 2001. Pathogenesis of Marek's disease virus infection. Curr Top Microbiol Immunol 255:25-55.
2. Davison A. 2002. Comments on the phylogenetics and evolution of herpesviruses and other large DNA viruses. Virus Res 82:127-32.
3. Denesvre C. 2013. Marek's disease virus morphogenesis. Avian Dis 57:340-50.
4. Tulman ER, Afonso CL, Lu Z, Zsak L, Rock DL, Kutish GF. 2000. The genome of a very virulent Marek's disease virus. J Virol 74:7980-8.
5. Bertzbach LD, Laparidou M, Hartle S, Etches RJ, Kaspers B, Schusser B, Kaufer BB. 2018. Unraveling the role of B cells in the pathogenesis of an oncogenic avian herpesvirus. Proc Natl Acad Sci U S A 115:11603-11607.
6. Osterrieder N, Kamil JP, Schumacher D, Tischer BK, Trapp S. 2006. Marek's disease virus: from miasma to model. Nat Rev Microbiol 4:283-94.
7. Reddy SM, Izumiya Y, Lupiani B. 2017. Marek's disease vaccines: Current status, and strategies for improvement and development of vector vaccines. Vet Microbiol 206:113-120.
8. Davison F, Nair V. 2005. Use of Marek's disease vaccines: could they be driving the virus to increasing virulence? Expert Rev Vaccines 4:77-88.
9. Gandon S, Mackinnon MJ, Nee S, Read AF. 2001. Imperfect vaccines and the evolution of pathogen virulence. Nature 414:751-6.
10. Gimeno IM. 2008. Marek's disease vaccines: a solution for today but a worry for tomorrow? Vaccine 26 Suppl 3:C31-41.
11. Lupiani B, Lee LF, Cui X, Gimeno I, Anderson A, Morgan RW, Silva RF, Witter RL, Kung HJ, Reddy SM. 2004. Marek's disease virus-encoded Meq gene is involved in transformation of lymphocytes but is dispensable for replication. Proc Natl Acad Sci U S A 101:11815-20.
12. Brown AC, Baigent SJ, Smith LP, Chattoo JP, Petherbridge LJ, Hawes P, Allday MJ, Nair V. 2006. Interaction of MEQ protein and C-terminal-binding protein is critical for induction of lymphomas by Marek's disease virus. Proc Natl Acad Sci U S A 103:1687-92.
13. Touitou R, Hickabottom M, Parker G, Crook T, Allday MJ. 2001. Physical and functional interactions between the corepressor CtBP and the Epstein-Barr virus nuclear antigen EBNA3C. J Virol 75:7749-55.
14. Levy AM, Izumiya Y, Brunovskis P, Xia L, Parcells MS, Reddy SM, Lee L, Chen HW, Kung HJ. 2003. Characterization of the chromosomal binding sites and dimerization partners of the viral oncoprotein Meq in Marek's disease virus-transformed T cells. J Virol 77:12841-51.
15. Deng X, Li X, Shen Y, Qiu Y, Shi Z, Shao D, Jin Y, Chen H, Ding C, Li L, Chen P, Ma Z. 2010. The Meq oncoprotein of Marek's disease virus interacts with p53 and inhibits its transcriptional and apoptotic activities. Virol J 7:348.
16. An J, Sun Y, Rettig MB. 2004. Transcriptional coactivation of c-Jun by the KSHV-encoded LANA. Blood 103:222-8.

17. Friborg J, Jr., Kong W, Hottiger MO, Nabel GJ. 1999. p53 inhibition by the LANA protein of KSHV protects against cell death. Nature 402:889-94.
18. Gershburg E, Pagano JS. 2008. Conserved herpesvirus protein kinases. Biochim Biophys Acta 1784:203-12.
19. Li R, Zhu J, Xie Z, Liao G, Liu J, Chen MR, Hu S, Woodard C, Lin J, Taverna SD, Desai P, Ambinder RF, Hayward GS, Qian J, Zhu H, Hayward SD. 2011. Conserved herpesvirus kinases target the DNA damage response pathway and TIP60 histone acetyltransferase to promote virus replication. Cell Host Microbe 10:390-400.
20. Morrison EE, Wang YF, Meredith DM. 1998. Phosphorylation of structural components promotes dissociation of the herpes simplex virus type 1 tegument. J Virol 72:7108-14.
21. Purves FC, Ogle WO, Roizman B. 1993. Processing of the herpes simplex virus regulatory protein alpha 22 mediated by the UL13 protein kinase determines the accumulation of a subset of alpha and gamma mRNAs and proteins in infected cells. Proc Natl Acad Sci U S A 90:6701-5.
22. Kato A, Yamamoto M, Ohno T, Tanaka M, Sata T, Nishiyama Y, Kawaguchi Y. 2006. Herpes simplex virus 1-encoded protein kinase UL13 phosphorylates viral Us3 protein kinase and regulates nuclear localization of viral envelopment factors UL34 and UL31. J Virol 80:1476-86.
23. Long MC, Leong V, Schaffer PA, Spencer CA, Rice SA. 1999. ICP22 and the UL13 protein kinase are both required for herpes simplex virus-induced modification of the large subunit of RNA polymerase II. J Virol 73:5593-604.
24. Jarosinski KW, Margulis NG, Kamil JP, Spatz SJ, Nair VK, Osterrieder N. 2007. Horizontal transmission of Marek's disease virus requires US2, the UL13 protein kinase, and gC. J Virol 81:10575-87.
25. Krieter A, Ponnuraj N, Jarosinski KW. 2020. Expression of the Conserved Herpesvirus Protein Kinase (CHPK) of Marek's Disease Alphaherpesvirus in the Skin Reveals a Mechanistic Importance for CHPK during Interindividual Spread in Chickens. J Virol 94.
26. Littler E, Stuart AD, Chee MS. 1992. Human cytomegalovirus UL97 open reading frame encodes a protein that phosphorylates the antiviral nucleoside analogue ganciclovir. Nature 358:160-2.
27. Sullivan V, Talarico CL, Stanat SC, Davis M, Coen DM, Biron KK. 1992. A protein kinase homologue controls phosphorylation of ganciclovir in human cytomegalovirus-infected cells. Nature 358:162-4.
28. Sharma M, Bender BJ, Kamil JP, Lye MF, Pesola JM, Reim NI, Hogle JM, Coen DM. 2015. Human cytomegalovirus UL97 phosphorylates the viral nuclear egress complex. J Virol 89:523-34.
29. Biron KK. 2006. Antiviral drugs for cytomegalovirus diseases. Antiviral Res 71:154-63.
30. Baek MC, Krosky PM, Pearson A, Coen DM. 2004. Phosphorylation of the RNA polymerase II carboxyl-terminal domain in human cytomegalovirus-infected cells and in vitro by the viral UL97 protein kinase. Virology 324:184-93.

31. Bigley TM, Reitsma JM, Mirza SP, Terhune SS. 2013. Human cytomegalovirus pUL97 regulates the viral major immediate early promoter by phosphorylation-mediated disruption of histone deacetylase 1 binding. J Virol 87:7393-408.
32. Reim NI, Kamil JP, Wang D, Lin A, Sharma M, Ericsson M, Pesola JM, Golan DE, Coen DM. 2013. Inactivation of retinoblastoma protein does not overcome the requirement for human cytomegalovirus UL97 in lamina disruption and nuclear egress. J Virol 87:5019-27.
33. Hwang S, Kim KS, Flano E, Wu TT, Tong LM, Park AN, Song MJ, Sanchez DJ, O'Connell RM, Cheng G, Sun R. 2009. Conserved herpesviral kinase promotes viral persistence by inhibiting the IRF-3-mediated type I interferon response. Cell Host Microbe 5:166-78.
34. Wang JT, Doong SL, Teng SC, Lee CP, Tsai CH, Chen MR. 2009. Epstein-Barr virus BGLF4 kinase suppresses the interferon regulatory factor 3 signaling pathway. J Virol 83:1856-69.
35. Izumiya Y, Izumiya C, Van Geelen A, Wang DH, Lam KS, Luciw PA, Kung HJ. 2007. Kaposi's sarcoma-associated herpesvirus-encoded protein kinase and its interaction with K-bZIP. J Virol 81:1072-82.
36. Asai R, Kato A, Kawaguchi Y. 2009. Epstein-Barr virus protein kinase BGLF4 interacts with viral transactivator BZLF1 and regulates its transactivation activity. J Gen Virol 90:1575-1581.
37. Polson AG, Huang L, Lukac DM, Blethrow JD, Morgan DO, Burlingame AL, Ganem D. 2001. Kaposi's sarcoma-associated herpesvirus K-bZIP protein is phosphorylated by cyclin-dependent kinases. J Virol 75:3175-84.
38. Hamza MS, Reyes RA, Izumiya Y, Wisdom R, Kung HJ, Luciw PA. 2004. ORF36 protein kinase of Kaposi's sarcoma herpesvirus activates the c-Jun N-terminal kinase signaling pathway. J Biol Chem 279:38325-30.
39. Bhatt AP, Wong JP, Weinberg MS, Host KM, Giffin LC, Buijnink J, van Dijk E, Izumiya Y, Kung HJ, Temple BR, Damania B. 2016. A viral kinase mimics S6 kinase to enhance cell proliferation. Proc Natl Acad Sci U S A 113:7876-81.
40. Chang LS, Wang JT, Doong SL, Lee CP, Chang CW, Tsai CH, Yeh SW, Hsieh CY, Chen MR. 2012. Epstein-Barr virus BGLF4 kinase downregulates NF-kappaB transactivation through phosphorylation of coactivator UXT. J Virol 86:12176-86.
41. Deruelle MJ, Favoreel HW. 2011. Keep it in the subfamily: the conserved alphaherpesvirus US3 protein kinase. J Gen Virol 92:18-30.
42. Poon AP, Benetti L, Roizman B. 2006. U(S)3 and U(S)3.5 protein kinases of herpes simplex virus 1 differ with respect to their functions in blocking apoptosis and in virion maturation and egress. J Virol 80:3752-64.
43. Poon AP, Roizman B. 2005. Herpes simplex virus 1 ICP22 regulates the accumulation of a shorter mRNA and of a truncated US3 protein kinase that exhibits altered functions. J Virol 79:8470-9.
44. van Zijl M, van der Gulden H, de Wind N, Gielkens A, Berns A. 1990. Identification of two genes in the unique short region of pseudorabies virus;

comparison with herpes simplex virus and varicella-zoster virus. J Gen Virol 71 (Pt 8):1747-55.
45. Wang X, Patenode C, Roizman B. 2011. US3 protein kinase of HSV-1 cycles between the cytoplasm and nucleus and interacts with programmed cell death protein 4 (PDCD4) to block apoptosis. Proc Natl Acad Sci U S A 108:14632-6.
46. Munger J, Roizman B. 2001. The US3 protein kinase of herpes simplex virus 1 mediates the posttranslational modification of BAD and prevents BAD-induced programmed cell death in the absence of other viral proteins. Proc Natl Acad Sci U S A 98:10410-5.
47. Leopardi R, Van Sant C, Roizman B. 1997. The herpes simplex virus 1 protein kinase US3 is required for protection from apoptosis induced by the virus. Proc Natl Acad Sci U S A 94:7891-6.
48. Rao P, Pham HT, Kulkarni A, Yang Y, Liu X, Knipe DM, Cresswell P, Yuan W. 2011. Herpes simplex virus 1 glycoprotein B and US3 collaborate to inhibit CD1d antigen presentation and NKT cell function. J Virol 85:8093-104.
49. Wang S, Wang K, Lin R, Zheng C. 2013. Herpes simplex virus 1 serine/threonine kinase US3 hyperphosphorylates IRF3 and inhibits beta interferon production. J Virol 87:12814-27.
50. Norman KL, Sarnow P. 2010. Herpes Simplex Virus is Akt-ing in translational control. Genes Dev 24:2583-6.
51. Kato A, Arii J, Shiratori I, Akashi H, Arase H, Kawaguchi Y. 2009. Herpes simplex virus 1 protein kinase Us3 phosphorylates viral envelope glycoprotein B and regulates its expression on the cell surface. J Virol 83:250-61.
52. Ryckman BJ, Roller RJ. 2004. Herpes simplex virus type 1 primary envelopment: UL34 protein modification and the US3-UL34 catalytic relationship. J Virol 78:399-412.
53. Sagou K, Imai T, Sagara H, Uema M, Kawaguchi Y. 2009. Regulation of the catalytic activity of herpes simplex virus 1 protein kinase Us3 by autophosphorylation and its role in pathogenesis. J Virol 83:5773-83.
54. Imai T, Sagou K, Arii J, Kawaguchi Y. 2010. Effects of phosphorylation of herpes simplex virus 1 envelope glycoprotein B by Us3 kinase in vivo and in vitro. J Virol 84:153-62.
55. Eaton HE, Saffran HA, Wu FW, Quach K, Smiley JR. 2014. Herpes simplex virus protein kinases US3 and UL13 modulate VP11/12 phosphorylation, virion packaging, and phosphatidylinositol 3-kinase/Akt signaling activity. J Virol 88:7379-88.
56. Mou F, Wills EG, Park R, Baines JD. 2008. Effects of lamin A/C, lamin B1, and viral US3 kinase activity on viral infectivity, virion egress, and the targeting of herpes simplex virus U(L)34-encoded protein to the inner nuclear membrane. J Virol 82:8094-104.
57. Mou F, Wills E, Baines JD. 2009. Phosphorylation of the U(L)31 protein of herpes simplex virus 1 by the U(S)3-encoded kinase regulates localization of the nuclear envelopment complex and egress of nucleocapsids. J Virol 83:5181-91.

58. Walters MS, Kinchington PR, Banfield BW, Silverstein S. 2010. Hyperphosphorylation of histone deacetylase 2 by alphaherpesvirus US3 kinases. J Virol 84:9666-76.
59. Wang K, Ni L, Wang S, Zheng C. 2014. Herpes simplex virus 1 protein kinase US3 hyperphosphorylates p65/RelA and dampens NF-kappaB activation. J Virol 88:7941-51.
60. Xiong R, Rao P, Kim S, Li M, Wen X, Yuan W. 2015. Herpes Simplex Virus 1 US3 Phosphorylates Cellular KIF3A To Downregulate CD1d Expression. J Virol 89:6646-55.
61. Mou F, Forest T, Baines JD. 2007. US3 of herpes simplex virus type 1 encodes a promiscuous protein kinase that phosphorylates and alters localization of lamin A/C in infected cells. J Virol 81:6459-70.
62. Jung M, Finnen RL, Neron CE, Banfield BW. 2011. The alphaherpesvirus serine/threonine kinase us3 disrupts promyelocytic leukemia protein nuclear bodies. J Virol 85:5301-11.
63. Geoffroy MC, Chelbi-Alix MK. 2011. Role of promyelocytic leukemia protein in host antiviral defense. J Interferon Cytokine Res 31:145-58.
64. Schumacher D, McKinney C, Kaufer BB, Osterrieder N. 2008. Enzymatically inactive U(S)3 protein kinase of Marek's disease virus (MDV) is capable of depolymerizing F-actin but results in accumulation of virions in perinuclear invaginations and reduced virus growth. Virology 375:37-47.
65. Schumacher D, Tischer BK, Trapp S, Osterrieder N. 2005. The protein encoded by the US3 orthologue of Marek's disease virus is required for efficient de-envelopment of perinuclear virions and involved in actin stress fiber breakdown. J Virol 79:3987-97.
66. Nakamura N. 2018. Ubiquitin System. Int J Mol Sci 19.
67. Komander D, Rape M. 2012. The ubiquitin code. Annu Rev Biochem 81:203-29.
68. Glickman MH, Ciechanover A. 2002. The ubiquitin-proteasome proteolytic pathway: destruction for the sake of construction. Physiol Rev 82:373-428.
69. Mukhopadhyay D, Riezman H. 2007. Proteasome-independent functions of ubiquitin in endocytosis and signaling. Science 315:201-5.
70. Schnell JD, Hicke L. 2003. Non-traditional functions of ubiquitin and ubiquitin-binding proteins. J Biol Chem 278:35857-60.
71. Swatek KN, Komander D. 2016. Ubiquitin modifications. Cell Res 26:399-422.
72. Lecker SH, Goldberg AL, Mitch WE. 2006. Protein degradation by the ubiquitin-proteasome pathway in normal and disease states. J Am Soc Nephrol 17:1807-19.
73. Hagglund R, Van Sant C, Lopez P, Roizman B. 2002. Herpes simplex virus 1-infected cell protein 0 contains two E3 ubiquitin ligase sites specific for different E2 ubiquitin-conjugating enzymes. Proc Natl Acad Sci U S A 99:631-6.
74. Stow ND, Stow EC. 1986. Isolation and characterization of a herpes simplex virus type 1 mutant containing a deletion within the gene encoding the immediate early polypeptide Vmw110. J Gen Virol 67 (Pt 12):2571-85.
75. Everett RD. 2000. ICP0 induces the accumulation of colocalizing conjugated ubiquitin. J Virol 74:9994-10005.

76. Chelbi-Alix MK, de The H. 1999. Herpes virus induced proteasome-dependent degradation of the nuclear bodies-associated PML and Sp100 proteins. Oncogene 18:935-41.
77. Lilley CE, Chaurushiya MS, Boutell C, Landry S, Suh J, Panier S, Everett RD, Stewart GS, Durocher D, Weitzman MD. 2010. A viral E3 ligase targets RNF8 and RNF168 to control histone ubiquitination and DNA damage responses. EMBO J 29:943-55.
78. Boutell C, Canning M, Orr A, Everett RD. 2005. Reciprocal activities between herpes simplex virus type 1 regulatory protein ICP0, a ubiquitin E3 ligase, and ubiquitin-specific protease USP7. J Virol 79:12342-54.
79. Campbell M, Izumiya Y. 2012. Post-Translational Modifications of Kaposi's Sarcoma-Associated Herpesvirus Regulatory Proteins - SUMO and KSHV. Front Microbiol 3:31.
80. Yu Y, Wang SE, Hayward GS. 2005. The KSHV immediate-early transcription factor RTA encodes ubiquitin E3 ligase activity that targets IRF7 for proteosome-mediated degradation. Immunity 22:59-70.
81. Gould F, Harrison SM, Hewitt EW, Whitehouse A. 2009. Kaposi's sarcoma-associated herpesvirus RTA promotes degradation of the Hey1 repressor protein through the ubiquitin proteasome pathway. J Virol 83:6727-38.
82. Yang Z, Wood C. 2007. The transcriptional repressor K-RBP modulates RTA-mediated transactivation and lytic replication of Kaposi's sarcoma-associated herpesvirus. J Virol 81:6294-306.
83. Kattenhorn LM, Korbel GA, Kessler BM, Spooner E, Ploegh HL. 2005. A deubiquitinating enzyme encoded by HSV-1 belongs to a family of cysteine proteases that is conserved across the family Herpesviridae. Mol Cell 19:547-57.
84. Schlieker C, Korbel GA, Kattenhorn LM, Ploegh HL. 2005. A deubiquitinating activity is conserved in the large tegument protein of the herpesviridae. J Virol 79:15582-5.
85. Kim ET, Oh SE, Lee YO, Gibson W, Ahn JH. 2009. Cleavage specificity of the UL48 deubiquitinating protease activity of human cytomegalovirus and the growth of an active-site mutant virus in cultured cells. J Virol 83:12046-56.
86. Wang S, Wang K, Li J, Zheng C. 2013. Herpes simplex virus 1 ubiquitin-specific protease UL36 inhibits beta interferon production by deubiquitinating TRAF3. J Virol 87:11851-60.
87. Ye R, Su C, Xu H, Zheng C. 2017. Herpes Simplex Virus 1 Ubiquitin-Specific Protease UL36 Abrogates NF-kappaB Activation in DNA Sensing Signal Pathway. J Virol 91.
88. Kumari P, Saha I, Narayanan A, Narayanan S, Takaoka A, Kumar NS, Tailor P, Kumar H. 2017. Essential role of HCMV deubiquitinase in promoting oncogenesis by targeting anti-viral innate immune signaling pathways. Cell Death Dis 8:e3078.
89. Jarosinski K, Kattenhorn L, Kaufer B, Ploegh H, Osterrieder N. 2007. A herpesvirus ubiquitin-specific protease is critical for efficient T cell lymphoma formation. Proc Natl Acad Sci U S A 104:20025-30.

90. Gonzalez CM, Wang L, Damania B. 2009. Kaposi's sarcoma-associated herpesvirus encodes a viral deubiquitinase. J Virol 83:10224-33.
91. Mahajan R, Delphin C, Guan T, Gerace L, Melchior F. 1997. A small ubiquitin-related polypeptide involved in targeting RanGAP1 to nuclear pore complex protein RanBP2. Cell 88:97-107.
92. Lowrey AJ, Cramblet W, Bentz GL. 2017. Viral manipulation of the cellular sumoylation machinery. Cell Commun Signal 15:27.
93. Boutell C, Sadis S, Everett RD. 2002. Herpes simplex virus type 1 immediate-early protein ICP0 and is isolated RING finger domain act as ubiquitin E3 ligases in vitro. J Virol 76:841-50.
94. Li R, Wang L, Liao G, Guzzo CM, Matunis MJ, Zhu H, Hayward SD. 2012. SUMO binding by the Epstein-Barr virus protein kinase BGLF4 is crucial for BGLF4 function. J Virol 86:5412-21.
95. Bentz GL, Whitehurst CB, Pagano JS. 2011. Epstein-Barr virus latent membrane protein 1 (LMP1) C-terminal-activating region 3 contributes to LMP1-mediated cellular migration via its interaction with Ubc9. J Virol 85:10144-53.
96. Izumiya Y, Kobayashi K, Kim KY, Pochampalli M, Izumiya C, Shevchenko B, Wang DH, Huerta SB, Martinez A, Campbell M, Kung HJ. 2013. Kaposi's sarcoma-associated herpesvirus K-Rta exhibits SUMO-targeting ubiquitin ligase (STUbL) like activity and is essential for viral reactivation. PLoS Pathog 9:e1003506.
97. Izumiya Y, Ellison TJ, Yeh ET, Jung JU, Luciw PA, Kung HJ. 2005. Kaposi's sarcoma-associated herpesvirus K-bZIP represses gene transcription via SUMO modification. J Virol 79:9912-25.
98. Chang PC, Izumiya Y, Wu CY, Fitzgerald LD, Campbell M, Ellison TJ, Lam KS, Luciw PA, Kung HJ. 2010. Kaposi's sarcoma-associated herpesvirus (KSHV) encodes a SUMO E3 ligase that is SIM-dependent and SUMO-2/3-specific. J Biol Chem 285:5266-73.
99. Woodsmith J, Kamburov A, Stelzl U. 2013. Dual coordination of post translational modifications in human protein networks. PLoS Comput Biol 9:e1002933.
100. Sakaguchi K, Herrera JE, Saito S, Miki T, Bustin M, Vassilev A, Anderson CW, Appella E. 1998. DNA damage activates p53 through a phosphorylation-acetylation cascade. Genes Dev 12:2831-41.
101. Hofmann TG, Moller A, Sirma H, Zentgraf H, Taya Y, Droge W, Will H, Schmitz ML. 2002. Regulation of p53 activity by its interaction with homeodomain-interacting protein kinase-2. Nat Cell Biol 4:1-10.
102. Segre CV, Chiocca S. 2011. Regulating the regulators: the post-translational code of class I HDAC1 and HDAC2. J Biomed Biotechnol 2011:690848.
103. Pflum MK, Tong JK, Lane WS, Schreiber SL. 2001. Histone deacetylase 1 phosphorylation promotes enzymatic activity and complex formation. J Biol Chem 276:47733-41.
104. Tsai SC, Seto E. 2002. Regulation of histone deacetylase 2 by protein kinase CK2. J Biol Chem 277:31826-33.

105. Sun JM, Chen HY, Davie JR. 2007. Differential distribution of unmodified and phosphorylated histone deacetylase 2 in chromatin. J Biol Chem 282:33227-36.
106. Landschulz WH, Johnson PF, McKnight SL. 1988. The leucine zipper: a hypothetical structure common to a new class of DNA binding proteins. Science 240:1759-64.
107. Vlahopoulos SA, Logotheti S, Mikas D, Giarika A, Gorgoulis V, Zoumpourlis V. 2008. The role of ATF-2 in oncogenesis. Bioessays 30:314-27.
108. Vogt PK. 2001. Jun, the oncoprotein. Oncogene 20:2365-77.
109. Vinson C, Myakishev M, Acharya A, Mir AA, Moll JR, Bonovich M. 2002. Classification of human B-ZIP proteins based on dimerization properties. Mol Cell Biol 22:6321-35.
110. Liu JL, Ye Y, Qian Z, Qian Y, Templeton DJ, Lee LF, Kung HJ. 1999. Functional interactions between herpesvirus oncoprotein MEQ and cell cycle regulator CDK2. J Virol 73:4208-19.
111. Suchodolski PF, Izumiya Y, Lupiani B, Ajithdoss DK, Lee LF, Kung HJ, Reddy SM. 2010. Both homo and heterodimers of Marek's disease virus encoded Meq protein contribute to transformation of lymphocytes in chickens. Virology 399:312-21.
112. Zhao Y, Kurian D, Xu H, Petherbridge L, Smith LP, Hunt L, Nair V. 2009. Interaction of Marek's disease virus oncoprotein Meq with heat-shock protein 70 in lymphoid tumour cells. J Gen Virol 90:2201-8.
113. Li H, Zhu J, He M, Luo Q, Liu F, Chen R. 2018. Marek's Disease Virus Activates the PI3K/Akt Pathway Through Interaction of Its Protein Meq With the P85 Subunit of PI3K to Promote Viral Replication. Front Microbiol 9:2547.
114. Wen W, Iwakiri D, Yamamoto K, Maruo S, Kanda T, Takada K. 2007. Epstein-Barr virus BZLF1 gene, a switch from latency to lytic infection, is expressed as an immediate-early gene after primary infection of B lymphocytes. J Virol 81:1037-42.
115. Schaeffner M, Mrozek-Gorska P, Buschle A, Woellmer A, Tagawa T, Cernilogar FM, Schotta G, Krietenstein N, Lieleg C, Korber P, Hammerschmidt W. 2019. BZLF1 interacts with chromatin remodelers promoting escape from latent infections with EBV. Life Sci Alliance 2.
116. Zhang Q, Hong Y, Dorsky D, Holley-Guthrie E, Zalani S, Elshiekh NA, Kiehl A, Le T, Kenney S. 1996. Functional and physical interactions between the Epstein-Barr virus (EBV) proteins BZLF1 and BMRF1: Effects on EBV transcription and lytic replication. J Virol 70:5131-42.
117. Adamson AL, Kenney S. 1999. The Epstein-Barr virus BZLF1 protein interacts physically and functionally with the histone acetylase CREB-binding protein. J Virol 73:6551-8.
118. Kusano S, Ikeda M. 2019. Interaction of phospholipid scramblase 1 with the Epstein-Barr virus protein BZLF1 represses BZLF1-mediated lytic gene transcription. J Biol Chem 294:15104-15116.
119. Murata T, Hotta N, Toyama S, Nakayama S, Chiba S, Isomura H, Ohshima T, Kanda T, Tsurumi T. 2010. Transcriptional repression by sumoylation of

Epstein-Barr virus BZLF1 protein correlates with association of histone deacetylase. J Biol Chem 285:23925-35.
120. Park J, Seo T, Hwang S, Lee D, Gwack Y, Choe J. 2000. The K-bZIP protein from Kaposi's sarcoma-associated herpesvirus interacts with p53 and represses its transcriptional activity. J Virol 74:11977-82.
121. Martinez FP, Tang Q. 2012. Leucine zipper domain is required for Kaposi sarcoma-associated herpesvirus (KSHV) K-bZIP protein to interact with histone deacetylase and is important for KSHV replication. J Biol Chem 287:15622-34.
122. Hwang S, Gwack Y, Byun H, Lim C, Choe J. 2001. The Kaposi's sarcoma-associated herpesvirus K8 protein interacts with CREB-binding protein (CBP) and represses CBP-mediated transcription. J Virol 75:9509-16.
123. Wu FY, Ahn JH, Alcendor DJ, Jang WJ, Xiao J, Hayward SD, Hayward GS. 2001. Origin-independent assembly of Kaposi's sarcoma-associated herpesvirus DNA replication compartments in transient cotransfection assays and association with the ORF-K8 protein and cellular PML. J Virol 75:1487-506.
124. Izumiya Y, Lin SF, Ellison TJ, Levy AM, Mayeur GL, Izumiya C, Kung HJ. 2003. Cell cycle regulation by Kaposi's sarcoma-associated herpesvirus K-bZIP: direct interaction with cyclin-CDK2 and induction of G1 growth arrest. J Virol 77:9652-61.
125. Tomita M, Choe J, Tsukazaki T, Mori N. 2004. The Kaposi's sarcoma-associated herpesvirus K-bZIP protein represses transforming growth factor beta signaling through interaction with CREB-binding protein. Oncogene 23:8272-81.
126. Lefort S, Soucy-Faulkner A, Grandvaux N, Flamand L. 2007. Binding of Kaposi's sarcoma-associated herpesvirus K-bZIP to interferon-responsive factor 3 elements modulates antiviral gene expression. J Virol 81:10950-60.
127. Cebrian J, Kaschka-Dierich C, Berthelot N, Sheldrick P. 1982. Inverted repeat nucleotide sequences in the genomes of Marek disease virus and the herpesvirus of the turkey. Proc Natl Acad Sci U S A 79:555-8.
128. Fukuchi K, Sudo M, Lee YS, Tanaka A, Nonoyama M. 1984. Structure of Marek's disease virus DNA: detailed restriction enzyme map. J Virol 51:102-9.
129. Lee LF, Wu P, Sui D, Ren D, Kamil J, Kung HJ, Witter RL. 2000. The complete unique long sequence and the overall genomic organization of the GA strain of Marek's disease virus. Proc Natl Acad Sci U S A 97:6091-6.
130. Trapp S, Parcells MS, Kamil JP, Schumacher D, Tischer BK, Kumar PM, Nair VK, Osterrieder N. 2006. A virus-encoded telomerase RNA promotes malignant T cell lymphomagenesis. J Exp Med 203:1307-17.
131. Wu H, Li T, Zeng M, Peng T. 2012. Herpes simplex virus type 1 infection activates the Epstein-Barr virus replicative cycle via a CREB-dependent mechanism. Cell Microbiol 14:546-59.
132. Benetti L, Roizman B. 2004. Herpes simplex virus protein kinase US3 activates and functionally overlaps protein kinase A to block apoptosis. Proc Natl Acad Sci U S A 101:9411-6.
133. Jones D, Lee L, Liu JL, Kung HJ, Tillotson JK. 1992. Marek disease virus encodes a basic-leucine zipper gene resembling the fos/jun oncogenes that is

highly expressed in lymphoblastoid tumors. Proc Natl Acad Sci U S A 89:4042-6.
134. Suchodolski PF, Izumiya Y, Lupiani B, Ajithdoss DK, Gilad O, Lee LF, Kung HJ, Reddy SM. 2009. Homodimerization of Marek's disease virus-encoded Meq protein is not sufficient for transformation of lymphocytes in chickens. J Virol 83:859-69.
135. Brown AC, Smith LP, Kgosana L, Baigent SJ, Nair V, Allday MJ. 2009. Homodimerization of the Meq viral oncoprotein is necessary for induction of T-cell lymphoma by Marek's disease virus. J Virol 83:11142-51.
136. Subramaniam S, Johnston J, Preeyanon L, Brown CT, Kung HJ, Cheng HH. 2013. Integrated analyses of genome-wide DNA occupancy and expression profiling identify key genes and pathways involved in cellular transformation by a Marek's disease virus oncoprotein, Meq. J Virol 87:9016-29.
137. Carlezon WA, Jr., Duman RS, Nestler EJ. 2005. The many faces of CREB. Trends Neurosci 28:436-45.
138. Wu X, Spiro C, Owen WG, McMurray CT. 1998. cAMP response element-binding protein monomers cooperatively assemble to form dimers on DNA. J Biol Chem 273:20820-7.
139. Mayr B, Montminy M. 2001. Transcriptional regulation by the phosphorylation-dependent factor CREB. Nat Rev Mol Cell Biol 2:599-609.
140. Sharma-Walia N, George Paul A, Patel K, Chandran K, Ahmad W, Chandran B. 2010. NFAT and CREB regulate Kaposi's sarcoma-associated herpesvirus-induced cyclooxygenase 2 (COX-2). J Virol 84:12733-53.
141. Francois S, Sen N, Mitton B, Xiao X, Sakamoto KM, Arvin A. 2016. Varicella-Zoster Virus Activates CREB, and Inhibition of the pCREB-p300/CBP Interaction Inhibits Viral Replication In Vitro and Skin Pathogenesis In Vivo. J Virol 90:8686-97.
142. Lu F, Zhou J, Wiedmer A, Madden K, Yuan Y, Lieberman PM. 2003. Chromatin remodeling of the Kaposi's sarcoma-associated herpesvirus ORF50 promoter correlates with reactivation from latency. J Virol 77:11425-35.
143. Du T, Zhou G, Roizman B. 2013. Modulation of reactivation of latent herpes simplex virus 1 in ganglionic organ cultures by p300/CBP and STAT3. Proc Natl Acad Sci U S A 110:E2621-8.
144. de Oliveira PS, Ferraz FA, Pena DA, Pramio DT, Morais FA, Schechtman D. 2016. Revisiting protein kinase-substrate interactions: Toward therapeutic development. Sci Signal 9:re3.
145. Kim J, Li G, Walters MA, Taylor SS, Veglia G. 2016. Uncoupling Catalytic and Binding Functions in the Cyclic AMP-Dependent Protein Kinase A. Structure 24:353-63.
146. Chan JY, Chen WC, Lee HY, Chang TJ, Chan SH. 1999. Phosphorylation of transcription factor cyclic-AMP response element binding protein mediates c-fos induction elicited by sustained hypertension in rat nucleus tractus solitarii. Neuroscience 88:1199-212.

147. Haque R, Chong NW, Ali F, Chaurasia SS, Sengupta T, Chun E, Howell JC, Klein DC, Iuvone PM. 2011. Melatonin synthesis in retina: cAMP-dependent transcriptional regulation of chicken arylalkylamine N-acetyltransferase by a CRE-like sequence and a TTATT repeat motif in the proximal promoter. J Neurochem 119:6-17.
148. Cha-Molstad H, Keller DM, Yochum GS, Impey S, Goodman RH. 2004. Cell-type-specific binding of the transcription factor CREB to the cAMP-response element. Proc Natl Acad Sci U S A 101:13572-7.
149. Kato A, Yamamoto M, Ohno T, Kodaira H, Nishiyama Y, Kawaguchi Y. 2005. Identification of proteins phosphorylated directly by the Us3 protein kinase encoded by herpes simplex virus 1. J Virol 79:9325-31.
150. Erazo A, Kinchington PR. 2010. Varicella-zoster virus open reading frame 66 protein kinase and its relationship to alphaherpesvirus US3 kinases. Curr Top Microbiol Immunol 342:79-98.
151. Singh V, Ram M, Kumar R, Prasad R, Roy BK, Singh KK. 2017. Phosphorylation: Implications in Cancer. Protein J 36:1-6.
152. Kato A, Tsuda S, Liu Z, Kozuka-Hata H, Oyama M, Kawaguchi Y. 2014. Herpes simplex virus 1 protein kinase Us3 phosphorylates viral dUTPase and regulates its catalytic activity in infected cells. J Virol 88:655-66.
153. Delghandi MP, Johannessen M, Moens U. 2005. The cAMP signalling pathway activates CREB through PKA, p38 and MSK1 in NIH 3T3 cells. Cell Signal 17:1343-51.
154. Everett LJ, Le Lay J, Lukovac S, Bernstein D, Steger DJ, Lazar MA, Kaestner KH. 2013. Integrative genomic analysis of CREB defines a critical role for transcription factor networks in mediating the fed/fasted switch in liver. BMC Genomics 14:337.
155. Marechal A, Zou L. 2013. DNA damage sensing by the ATM and ATR kinases. Cold Spring Harb Perspect Biol 5.
156. Tischer BK, von Einem J, Kaufer B, Osterrieder N. 2006. Two-step red-mediated recombination for versatile high-efficiency markerless DNA manipulation in Escherichia coli. Biotechniques 40:191-7.
157. Nakayama K. 2013. cAMP-response element-binding protein (CREB) and NF-kappaB transcription factors are activated during prolonged hypoxia and cooperatively regulate the induction of matrix metalloproteinase MMP1. J Biol Chem 288:22584-95.
158. Silva RF, Reddy SM, Lupiani B. 2004. Expansion of a unique region in the Marek's disease virus genome occurs concomitantly with attenuation but is not sufficient to cause attenuation. J Virol 78:733-40.
159. Heidari M, Delekta PC. 2017. Transcriptomic Analysis of Host Immune Response in the Skin of Chickens Infected with Marek's Disease Virus. Viral Immunol 30:377-387.
160. Lyu Y, Nakano K, Davis RR, Tepper CG, Campbell M, Izumiya Y. 2017. ZIC2 Is Essential for Maintenance of Latency and Is a Target of an Immediate Early

Protein during Kaposi's Sarcoma-Associated Herpesvirus Lytic Reactivation. J Virol 91.
161. Kato A, Kawaguchi Y. 2018. Us3 Protein Kinase Encoded by HSV: The Precise Function and Mechanism on Viral Life Cycle. Adv Exp Med Biol 1045:45-62.
162. Walters MS, Erazo A, Kinchington PR, Silverstein S. 2009. Histone deacetylases 1 and 2 are phosphorylated at novel sites during varicella-zoster virus infection. J Virol 83:11502-13.
163. Liao Y, Lupiani B, Bajwa K, Khan OA, Izumiya Y, Reddy SM. 2020. Role of Marek's disease virus encoded US3 serine/threonine protein kinase in regulating MDV Meq and cellular CREB phosphorylation. J Virol doi:10.1128/JVI.00892-20.
164. Guise AJ, Budayeva HG, Diner BA, Cristea IM. 2013. Histone deacetylases in herpesvirus replication and virus-stimulated host defense. Viruses 5:1607-32.
165. Brunmeir R, Lagger S, Seiser C. 2009. Histone deacetylase HDAC1/HDAC2-controlled embryonic development and cell differentiation. Int J Dev Biol 53:275-89.
166. Khan DH, He S, Yu J, Winter S, Cao W, Seiser C, Davie JR. 2013. Protein kinase CK2 regulates the dimerization of histone deacetylase 1 (HDAC1) and HDAC2 during mitosis. J Biol Chem 288:16518-28.
167. Poon AP, Gu H, Roizman B. 2006. ICP0 and the US3 protein kinase of herpes simplex virus 1 independently block histone deacetylation to enable gene expression. Proc Natl Acad Sci U S A 103:9993-8.
168. Huang Y, Chen J, Lu C, Han J, Wang G, Song C, Zhu S, Wang C, Li G, Kang J, Wang J. 2014. HDAC1 and Klf4 interplay critically regulates human myeloid leukemia cell proliferation. Cell Death Dis 5:e1491.
169. Yamaguchi T, Cubizolles F, Zhang Y, Reichert N, Kohler H, Seiser C, Matthias P. 2010. Histone deacetylases 1 and 2 act in concert to promote the G1-to-S progression. Genes Dev 24:455-69.
170. Shindo K, Kato A, Koyanagi N, Sagara H, Arii J, Kawaguchi Y. 2016. Characterization of a Herpes Simplex Virus 1 (HSV-1) Chimera in Which the Us3 Protein Kinase Gene Is Replaced with the HSV-2 Us3 Gene. J Virol 90:457-73.
171. McPherson MC, Delany ME. 2016. Virus and host genomic, molecular, and cellular interactions during Marek's disease pathogenesis and oncogenesis. Poult Sci 95:412-29.
172. Karimian A, Ahmadi Y, Yousefi B. 2016. Multiple functions of p21 in cell cycle, apoptosis and transcriptional regulation after DNA damage. DNA Repair (Amst) 42:63-71.
173. Hiromura K, Pippin JW, Fero ML, Roberts JM, Shankland SJ. 1999. Modulation of apoptosis by the cyclin-dependent kinase inhibitor p27(Kip1). J Clin Invest 103:597-604.
174. Jerome KR, Fox R, Chen Z, Sears AE, Lee H, Corey L. 1999. Herpes simplex virus inhibits apoptosis through the action of two genes, Us5 and Us3. J Virol 73:8950-7.

175. Mounce BC, Mboko WP, Bigley TM, Terhune SS, Tarakanova VL. 2013. A conserved gammaherpesvirus protein kinase targets histone deacetylases 1 and 2 to facilitate viral replication in primary macrophages. J Virol 87:7314-25.
176. Wang ZY, Qin W, Yi F. 2015. Targeting histone deacetylases: perspectives for epigenetic-based therapy in cardio-cerebrovascular disease. J Geriatr Cardiol 12:153-64.
177. Hernandez R, Brown DT. 2010. Growth and maintenance of chick embryo fibroblasts (CEF). Curr Protoc Microbiol Appendix 4:4I.
178. Reddy SM, Sun A, Khan OA, Lee LF, Lupiani B. 2013. Cloning of a very virulent plus, 686 strain of Marek's disease virus as a bacterial artificial chromosome. Avian Dis 57:469-73.
179. Ho SN, Hunt HD, Horton RM, Pullen JK, Pease LR. 1989. Site-directed mutagenesis by overlap extension using the polymerase chain reaction. Gene 77:51-9.
180. Nair V. 2004. Successful control of Marek's disease by vaccination. Dev Biol (Basel) 119:147-54.
181. Xie Q, Anderson AS, Morgan RW. 1996. Marek's disease virus (MDV) ICP4, pp38, and meq genes are involved in the maintenance of transformation of MDCC-MSB1 MDV-transformed lymphoblastoid cells. J Virol 70:1125-31.
182. Liu JL, Ye Y, Lee LF, Kung HJ. 1998. Transforming potential of the herpesvirus oncoprotein MEQ: morphological transformation, serum-independent growth, and inhibition of apoptosis. J Virol 72:388-95.
183. Levy AM, Gilad O, Xia L, Izumiya Y, Choi J, Tsalenko A, Yakhini Z, Witter R, Lee L, Cardona CJ, Kung HJ. 2005. Marek's disease virus Meq transforms chicken cells via the v-Jun transcriptional cascade: a converging transforming pathway for avian oncoviruses. Proc Natl Acad Sci U S A 102:14831-6.
184. Van Opdenbosch N, Favoreel H, Van de Walle GR. 2012. Histone modifications in herpesvirus infections. Biol Cell 104:139-64.
185. Shin HJ, DeCotiis J, Giron M, Palmeri D, Lukac DM. 2014. Histone deacetylase classes I and II regulate Kaposi's sarcoma-associated herpesvirus reactivation. J Virol 88:1281-92.
186. Gill G. 2004. SUMO and ubiquitin in the nucleus: different functions, similar mechanisms? Genes Dev 18:2046-59.
187. Chang PC, Campbell M, Robertson ES. 2016. Human Oncogenic Herpesvirus and Post-translational Modifications - Phosphorylation and SUMOylation. Front Microbiol 7:962.
188. Oh YM, Kwon YE, Kim JM, Bae SJ, Lee BK, Yoo SJ, Chung CH, Deshaies RJ, Seol JH. 2009. Chfr is linked to tumour metastasis through the downregulation of HDAC1. Nat Cell Biol 11:295-302.
189. Brown AC, Nair V, Allday MJ. 2012. Epigenetic regulation of the latency-associated region of Marek's disease virus in tumor-derived T-cell lines and primary lymphoma. J Virol 86:1683-95.

190. Gu H, Liang Y, Mandel G, Roizman B. 2005. Components of the REST/CoREST/histone deacetylase repressor complex are disrupted, modified, and translocated in HSV-1-infected cells. Proc Natl Acad Sci U S A 102:7571-6.
191. Terhune SS, Moorman NJ, Cristea IM, Savaryn JP, Cuevas-Bennett C, Rout MP, Chait BT, Shenk T. 2010. Human cytomegalovirus UL29/28 protein interacts with components of the NuRD complex which promote accumulation of immediate-early RNA. PLoS Pathog 6:e1000965.
192. Kalchschmidt JS, Gillman AC, Paschos K, Bazot Q, Kempkes B, Allday MJ. 2016. EBNA3C Directs Recruitment of RBPJ (CBF1) to Chromatin during the Process of Gene Repression in EBV Infected B Cells. PLoS Pathog 12:e1005383.
193. Qian Z, Brunovskis P, Rauscher F, 3rd, Lee L, Kung HJ. 1995. Transactivation activity of Meq, a Marek's disease herpesvirus bZIP protein persistently expressed in latently infected transformed T cells. J Virol 69:4037-44.
194. Kutluay SB, Triezenberg SJ. 2009. Role of chromatin during herpesvirus infections. Biochim Biophys Acta 1790:456-66.
195. Radkov SA, Touitou R, Brehm A, Rowe M, West M, Kouzarides T, Allday MJ. 1999. Epstein-Barr virus nuclear antigen 3C interacts with histone deacetylase to repress transcription. J Virol 73:5688-97.
196. Knight JS, Lan K, Subramanian C, Robertson ES. 2003. Epstein-Barr virus nuclear antigen 3C recruits histone deacetylase activity and associates with the corepressors mSin3A and NCoR in human B-cell lines. J Virol 77:4261-72.
197. Liebl MP, Hoppe T. 2016. It's all about talking: two-way communication between proteasomal and lysosomal degradation pathways via ubiquitin. Am J Physiol Cell Physiol 311:C166-78.
198. Jang HH. 2018. Regulation of Protein Degradation by Proteasomes in Cancer. J Cancer Prev 23:153-161.
199. Erales J, Coffino P. 2014. Ubiquitin-independent proteasomal degradation. Biochim Biophys Acta 1843:216-21.
200. Yang Z, Yan Z, Wood C. 2008. Kaposi's sarcoma-associated herpesvirus transactivator RTA promotes degradation of the repressors to regulate viral lytic replication. J Virol 82:3590-603.
201. Winkler LL, Hwang J, Kalejta RF. 2013. Ubiquitin-independent proteasomal degradation of tumor suppressors by human cytomegalovirus pp71 requires the 19S regulatory particle. J Virol 87:4665-71.
202. Akiyama Y, Kato S. 1974. Two cell lines from lymphomas of Marek's disease. Biken J 17:105-16.
203. Cristinelli S, Ciuffi A. 2018. The use of single-cell RNA-Seq to understand virus-host interactions. Curr Opin Virol 29:39-50.

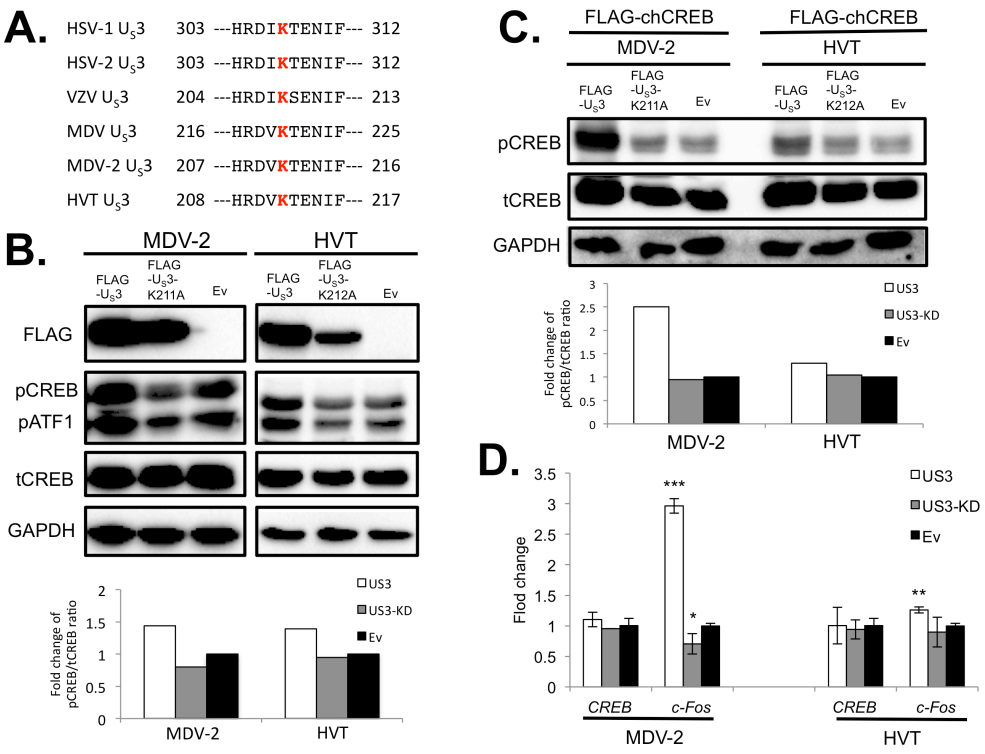

Figure S1. MDV-2 and HVT U_S3 enhance CREB phosphorylation and up-regulate the expression of CREB target gene. (A) Multiple amino acid sequence alignment of the catalytic active site of alphaherpesvirus encoded U_S3 protein. The lysine (K) residue that was mutated to alanine (A) is shown in bold red, numbers indicate amino acid location. MDV-2 and HVT wild type U_S3 (pcDNA-FLAG-U_S3-MDV2, pcDNA-FLAG-U_S3-HVT), kinase dead mutant U_S3 (U_S3-KD, pcDNA-FLAG-U_S3-K211A for MDV-2 or pcDNA-FLAG-U_S3-K212A for HVT) or pcDNA empty vector (Ev) were transfected alone (B) or co-transfected with pcDNA-FLAG-chCREB (C) into 293T cells. Forty-eight hours after transfection, total cell lysates were subjected to SDS-PAGE and WB with the indicated antibodies. Upper panels show WB results, bottom panels show fold changes of pCREB/tCREB ratio. (D) 293T cells were transfected with MDV-2 and HVT wild type U_S3 (pcDNA-U_S3-MDV2, pcDNA-U_S3-HVT), kinase dead mutant U_S3 (pcDNA-U_S3-K211A for MDV-2 or pcDNA-U_S3-K212A for HVT) or pcDNA-empty vector (Ev). Forty-eight hours after transfection, cells were harvested for RNA isolation followed by cDNA synthesis and qRT-PCR analysis with primers for the indicated genes. qRT-PCR data were analyzed using the $2^{-\Delta\Delta CT}$ method. Human GAPDH was used as an internal control. Data represent average ± SD of three independent experiments. Values are presented as fold change relative to Ev. *: $p<0.05$, **: $p<0.01$, ***: $p<0.001$.

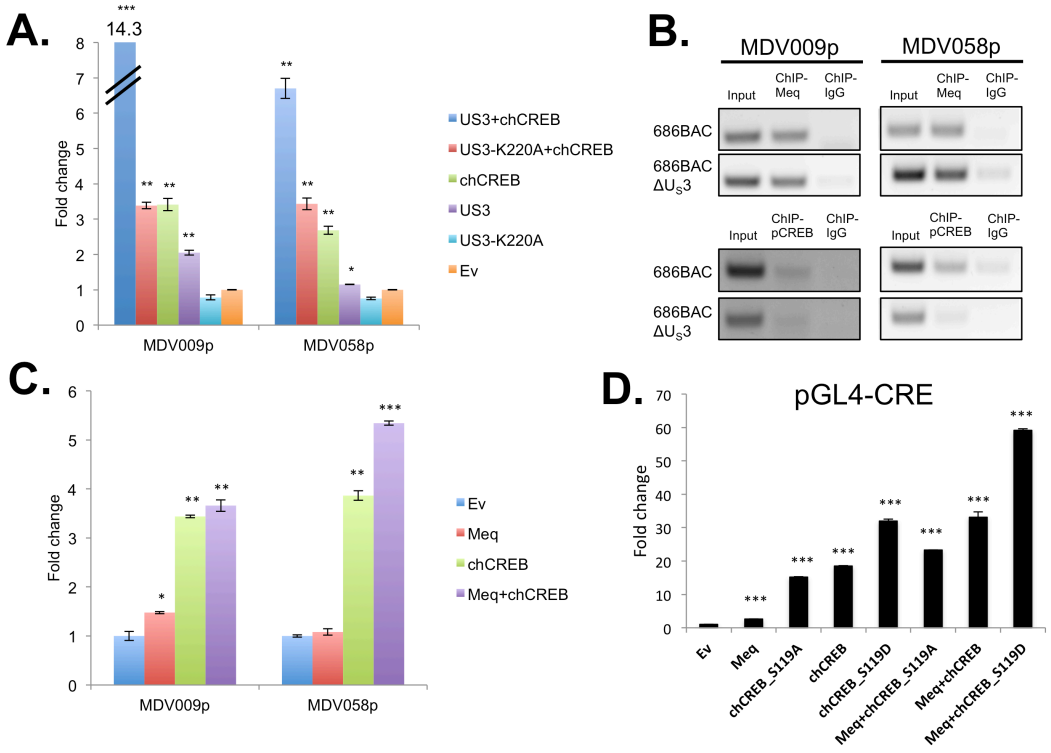

Figure S2. Role of MDV U_S3, Meq and chCREB in regulating transcription of viral promoters. (A, C, D) Indicated plasmids were co-transfected with reporter and *Renilla* luciferase vectors into 293T cells. Forty-eight hours after transfection, *firefly* luciferase and *Renillla* luciferase activity were measured using the Dual-Glo® Luciferase Assay System. Numbers above the column indicate fold change relative to empty vector (Ev). Data represent average ± standard error of the mean (SEM) of three independent experiments. Fold changes are shown relative to Ev. *: $p<0.05$, **: $p<0.01$, ***: $p<0.001$. (B) Seven days after infection with 686-BAC or 686-BACΔU_S3 viruses, CEF were fixed and subjected to ChIP with rabbit anti-Meq, rabbit anti-pCREB or normal rabbit IgG antibodies. ChIP-PCR was performed with the indicated primers.

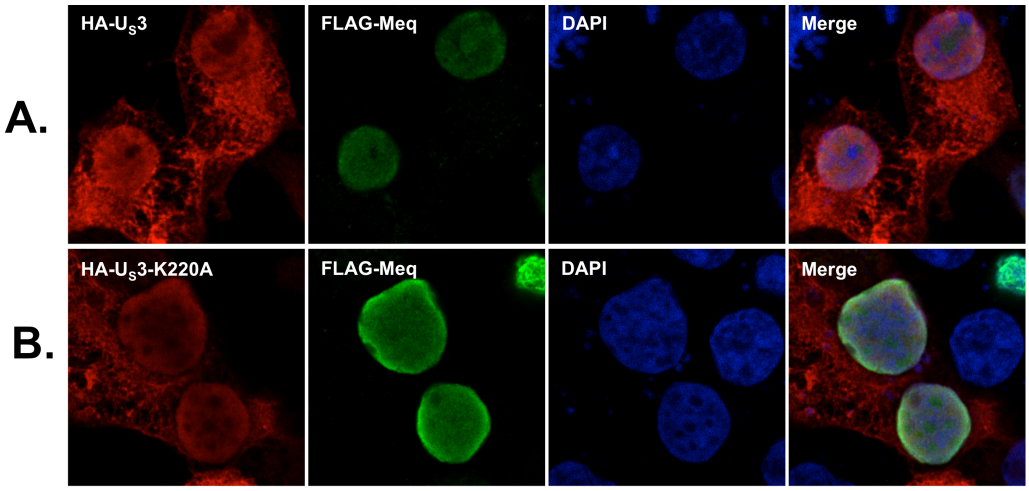

Figure S3. Co-localization of MDV U_S3 and U_S3-K220A with Meq oncoprotein. pcDNA-HA-U_S3 (A) or pcDNA-HA-U_S3-K220A (B) were co-transfected with pcDNA-FLAG-Meq into 293T cells. Forty-eight hours post transfection, cells were fixed and subjected to immunofluorescence assays (IFA) with primary mouse anti-HA and rabbit anti-FLAG antibodies, and secondary goat anti-mouse-Texas Red and goat anti-rabbit-Alex Flour 488 antibodies. Cell nuclei were stained with DAPI. Images were recorded using a Zeiss LSM 780 NLO Multiphoton Microscope.

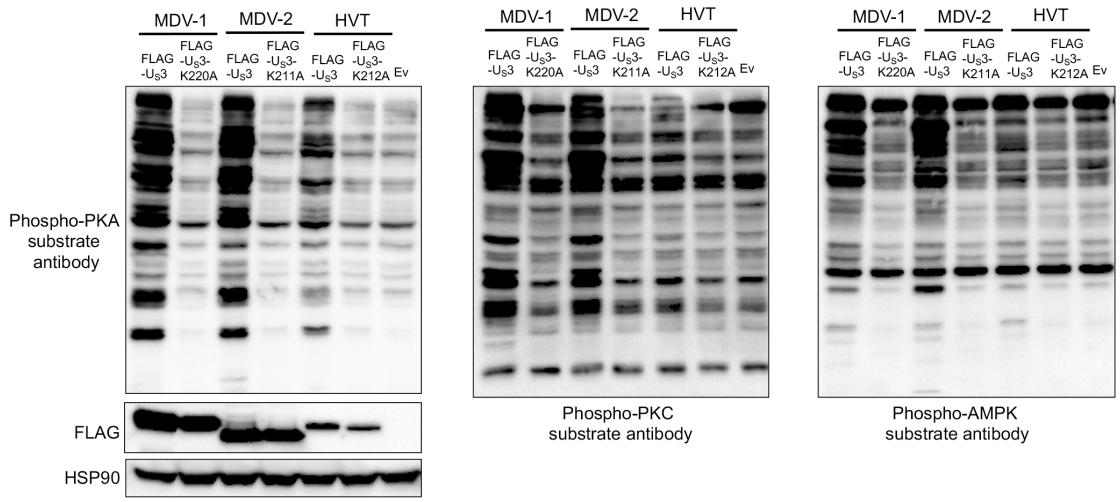

Figure S4. MDV U_S3 induces phosphorylation of cellular protein kinase substrates. pcDNA FLAG tagged wild type MDV-1, MDV-2, or HVT U_S3, pcDNA kinase dead U_S3 (pcDNA-FLAG-U_S3-K220A for MDV-1, pcDNA-FLAG-U_S3-K211A for MDV-2, and pcDNA-FLAG-U_S3-K212A for HVT), or pcDNA empty vector (Ev) were cotransfected into 293T cells. After 48 hours, whole cell lysates were subjected to Western blot with anti-phospho-PKA substrate antibody (left), anti-phospho-PKC substrate antibody (middle), and anti-phospho-AMPK substrate antibody (right). Staining for FLAG and HSP90 was performed to show U_S3 expression and protein loading control, respectively.

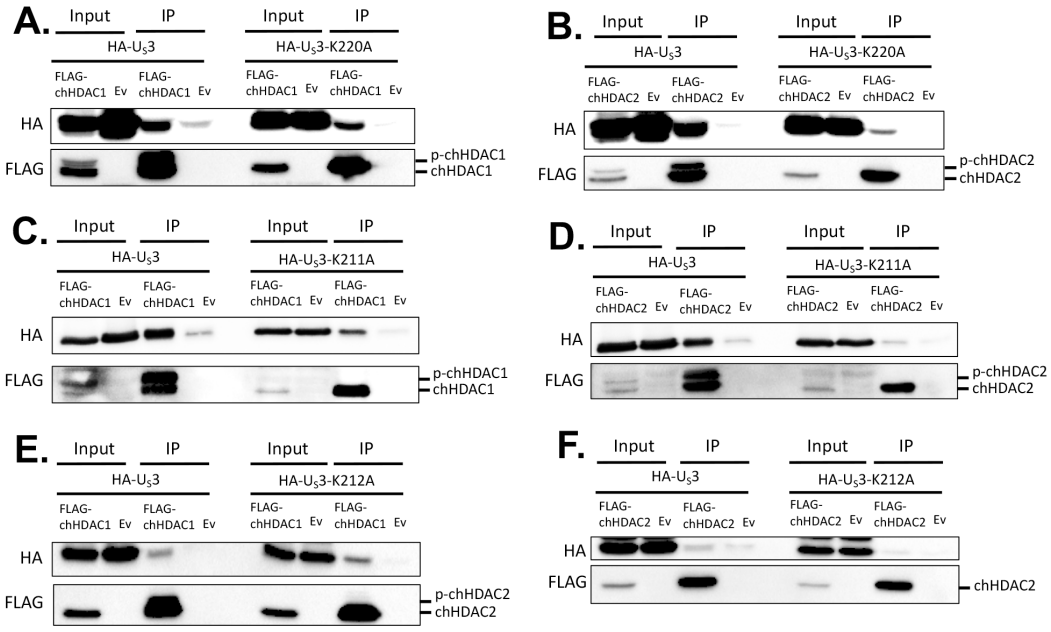

Figure S5. MDV U_S3 physically associates with chHDAC1 and 2. pcDNA-FLAG-chHDAC1 and pcDNA empty vector (Ev) (A, C, E), or pcDNA-FLAG-chHDAC2 and pcDNA Ev (B, D, F) were cotransfected with pcDNA HA tagged MDV-1 U_S3 or MDV-1 U_S3-K220A (A, B), MDV-2 U_S3 or MDV-2 U_S3-K211A (C, D), or HVT U_S3 or HVT U_S3-K212A (E, F). Forty-eight hours later, cells were lysed and subjected to immunoprecipitation with mouse anti-FLAG agarose beads, followed by Western blot with HA and FLAG antibodies.

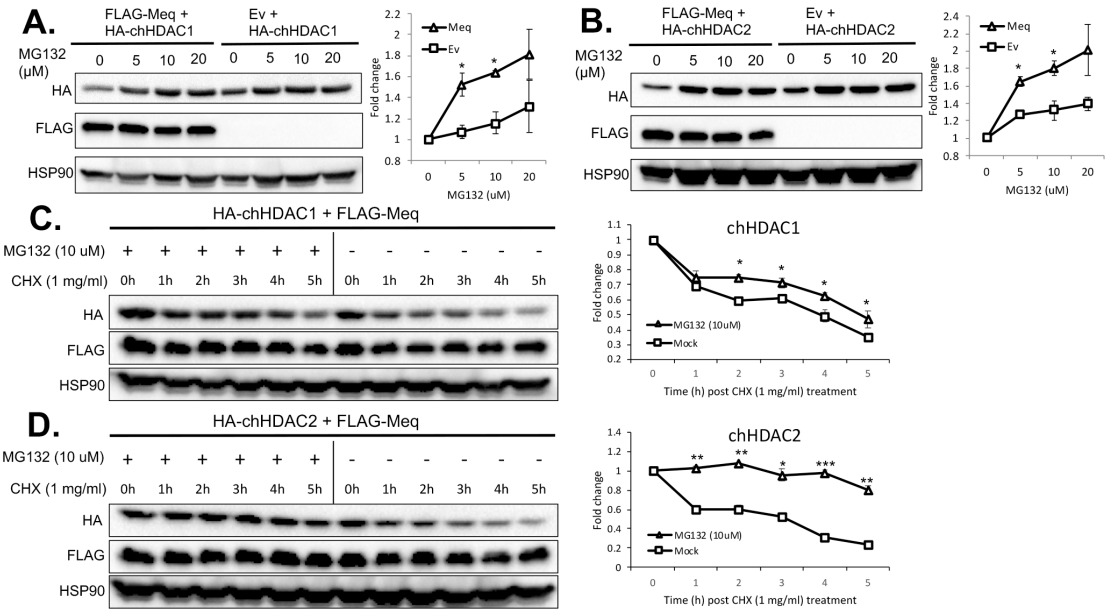

Figure S6. MG132 treatment inhibits the degradation of chHDAC1 and 2 induced by Meq. pcDNA-FLAG-Meq or pcDNA empty vector (Ev) were cotransfected with pcDNA-HA-chHDAC1 (A) or pcDNA-HA-chHDAC2 (B) into 293T cells and 24 hours post transfection, cells were treated with different concentration of MG132 overnight. Western blot (WB) analysis was performed with HA, FLAG, and HSP90 antibodies (left) and quantified by Image J. Level HA-chHDAC1 or HA-chHDAC2 were normalized to HPS90 and presented as fold change compared to non-treated cells (right). pcDNA-FLAG-Meq was cotransfected with pcDNA-HA-chHDAC1 (C) or pcDNA-HA-chHDAC2 (D) into 293T cells and 24 hours post transfection, cells were treated with MG132 (10 μM) overnight. Next day, cells were treated with cycloheximide (CHX, 1 mg/ml) for the indicated length of time, in the presence of MG132 (10 μM). WB analysis was performed with HA, FLAG, and HSP90 antibodies (left). Levels of HA-chHDAC1 or HA-chHDAC2 were quantified and normalized to HPS90, and presented as fold change compared to no CHX treated cells (right). Error bars indicate standard deviation (SD). All experiments were repeated at least two times. *: $p<0.05$, *: $p<0.01$, *: $p<0.001$.

APPENDIX B

Table S1. List of primers used in MDV-1 BAC mutagenesis and pcDNA plasmid constructions.

Primer number	Primer name	Sequence (5′ to 3′)	Purpose
1	MDV-2/U_S3_F	GATC**GAATTC**ATGGAAACTAACGAGCTTTC	Generation of MDV-1-MDV-2/US3 BAC
2	MDV-2/U_S3_R	GATC**GGATCC**TTAGGGAACAAATAGGGCCTGGA	
3	MDV-2/U_S3Kan-F	GATC**GATATC**TGGAGTGCCGGGCTTGTGTTATTCGAGATGTCTGCCAAAAAAAGGAC ACTAGGATGACGACGATAAGTAGGG	
4	MDV-2/U_S3Kan-R	GATC**GATATC**CAACCAATTAACCAATTCTGATTAG	
5	MDV-2/U_S3-T-F	TTATACTCTGGTAGAATATGAAACAGGGTTAAAACTAGGTAATAGACTGGATGGAAACT AACGAGCTTTC	
6	MDV-2/U_S3-T-R	GCGTAGTATATATTATAAAATGAATCATTGAAGTTATTTTTGACGGGTGTTTAGGGAACA AATAGGGCCTGGA	
7	HVT/U_S3_F	GATC**GAATTC**ATGGAAGTAGATGTTGAGTC	Generation of MDV-1-HVT/US3 BAC
8	HVT/U_S3_R	GATC**GGATCC**TTAGACACTGTCAGAGGGTGTGATA	
9	HVT/U_S3Kan-F	GATC**GATATC**AGGGAAGTGGATATTTTAAAAACCATCTCACATAAATCAATTATAAAAT TAGGATGACGACGATAAGTAGGG	
10	HVT/U_S3Kan-R	GATC**GATATC**CAACCAATTAACCAATTCTGATTAG	
11	HVT/U_S3-T-F	TTATACTCTGGTAGAATATGAAACAGGGTTAAAACTAGGTAATAGACTGGATGGAAGTA GATGTTGAGTC	
12	HVT/U_S3-T-R	GCGTAGTATATATTATAAAATGAATCATTGAAGTTATTTTTGACGGGTGTTTAGACACTG TCAGAGGGTGTGATA	
13	MDV-1/U_S3_F	GATC**GAATTC**ATGTCTTCGAGTCCGGAGGC	Generation of MDV-1-ΔUS3_Rev BAC
14	MDV-1/U_S3_R	GATC**GGATCC**TTACATATGAGCGGCAGTTA	
15	MDV-1/U_S3Kan-F	GATC**GATATC**ATGGGACCATTGCCACTAAATCAAATAATTACGATAGAACGGGGTTTG CTAGGATGACGACGATAAGTAGGG	
16	MDV-1/U_S3Kan-R	GATC**GATATC**CAACCAATTAACCAATTCTGATTAG	
17	MDV-1/U_S3-T-F	TTATACTCTGGTAGAATATGAAACAGGGTTAAAACTAGGTAATAGACTGGATGTCTTCG AGTCCGGAGGC	
18	MDV-1/U_S3-T-R	GCGTAGTATATATTATAAAATGAATCATTGAAGTTATTTTTGACGGGTGTTTACATATGA GCGGCAGTTATCG	
19	MDV-1_U_S3-FLAG-F	TC**GGATCC**ATG***GACTACAAAGACGATGACGACAAG***TCTTCGAGTCCGGAGGCA	FLAG and HA tagged wild type and kinase dead MDV-1 US3 plasmids
20	MDV-1_U_S3-HA-F	TC**GGATCC**ATG***TACCCATACGATGTTCCAGATTACGCT***TCTTCGAGTCCGGAGGCA	
21	MDV-1_U_S3-R	TC**GAATTC**TTACATATGAGCGGCAGTTA	
22	MDV-1_U_S3-K220A-F	TGATGTAGCAACTGAAAATA	
23	MDV-1_U_S3-K220A-R	TATTTTCAGTTGCTACATCA	
24	MDV-2_U_S3-FLAG-F	GATC**GGATCC**ATG***GACTACAAAGACGATGACGACAAG***gaaactaacgagctttct	FLAG and HA tagged wild type and kinase dead MDV-2 US3 plasmids
25	MDV-2_U_S3-HA-F	GATC**GGATCC**ATG***TACCCATACGATGTTCCAGATTACGCT***gaaactaacgagctttct	
26	MDV-2_U_S3-R	GATC**GAATTC**tcagggaacaaatagggcctggagatt	
27	MDV-2_U_S3-K211A-F	cgcgatgtaGCgacagaaaac	
28	MDV-2_U_S3-K211A-R	gttttctgtcGCtacatcgcg	
29	HVT_U_S3-FLAG-F	GATC**GGATCC**ATG***GACTACAAAGACGATGACGACAAG***gaagtagatgttgagtct	FLAG and HA tagged wild type and kinase dead HVT US3 plasmids
30	HVT_U_S3-HA-F	GATC**GGATCC**ATG***TACCCATACGATGTTCCAGATTACGCT***gaagtagatgttgagtct	
31	HVT_U_S3-R	GATC**GAATTC**ttagacactgtcagagggtgt	
32	HVT_U_S3-K212A-F	cgagacgtaGCgacggagaat	
33	HVT_U_S3-K212A-R	attctccgtcGCtacgtctcg	
34	MDV-1_Meq-HA-F	TC**GCTAGC**ATG***TACCCATACGATGTTCCAGATTACGCT***TCTCAGGAGCCAGAGCCG	HA tagged MDV-1 Meq plasmid
35	MDV-1_Meq-R	GATC**GCGGCCGC**TCAGGGTCTCCCGTCACCTG	
36	chHDAC1_FLAG-F	gatc**GCTAGC**atg***GACTACAAAGACGATGACGACAAG***gcgctgacgcaggggac	FLAG, HA, and T7 tagged wild type chHDAC1 plasmids
37	chHDAC1_HA-F	gatc**GCTAGC**atg***TACCCATACGATGTTCCAGATTACGCT***gcgctgacgcaggggac	
38	chHDAC1_T7-F	tc**GCTAGC**atg***ATGGCTAGCATGACTGGTGGACAGCAAATGGGT***gcgctgacgcaggggа	
39	chHDAC1-R	gatc**GCGGCCGC**ttaggtggatttttgtctctt	
40	chHDAC1-S393A-F	gaagacGCGggagatgaaga	Single, double, and triple mutations of chHDAC1 plasmids
41	chHDAC1-S393A-R	tcttcatctccCGCgtcttc	
42	chHDAC1-S406A-F	gcattGCGatccgcaattct	
43	chHDAC1-S406A-R	agaattgcggatCGCaatgc	
44	chHDAC1-S410A-F	ccgcaatGCGgataagagaat	
45	chHDAC1-S410A-R	attctcttatcCGCattgcgg	
46	chHDAC1-S415A-F	gagaataGCGtgtgatgaag	
47	chHDAC1-S415A-R	cttcatcacaCGCtattctc	
48	chHDAC1-S421A-F	tgaagaattcGCGgactctg	
49	chHDAC1-S421A-R	cagagtcCGCgaattcttca	
50	chHDAC1-S423A-F	tctgacGCGgaagatgaagg	
51	chHDAC1-S423A-R	ccttcatcttcCGCgtcaga	
52	chHDAC1-T445A-R	gatc**GCGGCCGC**ttaggtggattttgtctcttccttcacccccttgggttcggctttctcctcttttgcttttcctctttcctttctcatccttcttctcctcctcctcttttcctcctcCGCtttcacacgcttggccttc	
53	chHDAC1-T477A-R	gatc**GCGGCCGC**ttaGGTGGAtttCGCctcttccttca	
54	chHDAC1-S479A-R	gatc**GCGGCCGC**ttaGGTCGCtttTGTctcttccttca	
55	chHDAC1-T480A-R	gatc**GCGGCCGC**ttaCGCGGAtttTGTctcttccttca	
56	chHDAC1-S406/410A-F	cctgagaagcgcattGCGatccgcaatGCGgataagagaatatcctgtgatgaagaattc	
57	chHDAC1-S406/410A-R	gaattcttcatcacaggatattcttatcCGCattgcggatCGCaatgcgcttctcagg	
58	chHDAC1-S406/410/415A-F	cctgagaagcgcattGCGatccgcaatGCGgataagagaataGCGtgtgatgaagaattc	
59	chHDAC1-S406/410/415A-R	gaattcttcatcacaCGCtattctcttatcCGCattgcggatCGCaatgcgcttctcagg	
60	chHDAC1-S406D-F	cctgagaagcgcattGACatccgcaattct	
61	chHDAC1-S406D-R	agaattgcggatGTCaatgcgcttctcagg	
62	chHDAC1-S410D-F	catttcaatccgcaatGACgataagagaat	
63	chHDAC1-S410D-R	attctcttatcGTCattgcggattgaaatg	
64	chHDAC1-S415D-F	gagaataGACtgtgatgaag	
65	chHDAC1-S415D-R	cttcatcacaGTCtattctc	
66	chHDAC1-S406/410D-F	cctgagaagcgcattGACatccgcaatGACgataagagaatatcctgtgatgaagaattc	

	A	B	C	D
70	67	chHDAC1-S406/410D-R	gaattcttcatcacaggatattctcttatcGTCattgcggatGTCaatgcgcttctcagg	
71	68	chHDAC1-S406/410/415D-F	cctgagaagcgcattGACatccgcaatGACgataagagaataGACtgtgatgaagaattc	
72	69	chHDAC1-S406/410/415D-R	gaattcttcatcacaGTCtattctcttatcGTCattgcggatGTCaatgcgcttctcagg	
73	70	chHDAC2_FLAG-F	gatc**GCTAGC**atg***GACTACAAAGACGATGACGACAAG***gcgtacagtcagggcgg	FLAG, HA, and T7 tagged wild type chHDAC2 plasmids
74	71	chHDAC2_HA-F	gatc**GCTAGC**atg***TACCCATACGATGTTCCAGATTACGCT***gcgtacagtcagggcgg	
75	72	chHDAC2_T7-F	tc**GCTAGC**atg***ATGGCTAGCATGACTGGTGGACAGCAAATGGGT***gcgtacagtcagggcg	
76	73	chHDAC2-R	gatc**GCGGCCGC**tcaaggattgctgagctgtt	
77	74	chHDAC2-S394A-F	catgaagatGCGggagatga	Single and double mutations of chHDAC2 plasmids
78	75	chHDAC2-S394A-R	tcatctccCGCatcttcatg	
79	76	chHDAC2-S407A-F	aacgcattGCGattcgagca	
80	77	chHDAC2-S407A-R	tgctcgaatCGCaatgcgtt	
81	78	chHDAC2-S411A-F	tattcgagcaGCGgataagc	
82	79	chHDAC2-S411A-R	gcttatcCGCtgctcgaata	
83	80	chHDAC2-S422A-F	tgatgaggagtttGCGgact	
84	81	chHDAC2-S422A-R	agtcCGCaaactcctcatca	
85	82	chHDAC2-S424A-F	ttttcagacGCGgaagatga	
86	83	chHDAC2-S424A-R	tcatcttcCGCgtctgaaaa	
87	84	chHDAC2-S407/411A-F	gatccagacaaacgcattGCGattcgagcaGCGgataagcgcattgcctg	
88	85	chHDAC2-S407/411A-R	caggcaatgcgcttatcCGCtgctcgaatCGCaatgcgtttgtctggatc	
89	86	chHDAC2-S407D-F	aacgcattGACattcgagca	
90	87	chHDAC2-S407D-R	tgctcgaatGTCaatgcgtt	
91	88	chHDAC2-S411D-F	tattcgagcaGACgataagc	
92	89	chHDAC2-S411D-R	gcttatcGTCtgctcgaata	
93	90	chHDAC2-S407/411D-F	gatccagacaaacgcattGACattcgagcaGACgataagcgcattgcctg	
94	91	chHDAC2-S407/411D-R	caggcaatgcgcttatcGTCtgctcgaatGTCaatgcgtttgtctggatc	
95	92	chHDAC1_qPCR_F	GGATGAAGAAGAAGAAGATCC	Gene expression analysis
96	93	chHDAC1_qPCR_R	GATAACTATGCACTGACAGG	
97	94	chHDAC2_qPCR_F	AAGGTGGACGGCGAAATG	
98	95	chHDAC2_qPCR_R	GATACGGTCCATGCCAAATAG	
99	96	chp21_qPCR_F	CGTAGACCACGAGCAGATCC	
100	97	chp21_qPCR_R	AGGACCCTCTCCCACTTGAA	
101	98	chp27_qPCR_F	AAACGGGAATTGCCAAACCG	
102	99	chp27_qPCR_R	TGACTGCCAGCAACATCAGT	
103	100	chGAPDH_qPCR_F	GTCAACGGATTTGGCCGTAT	
104	101	chGAPDH_qPCR_R	CCACTTGGACTTTGCCAGAGA	
105	102	ICP4_F	CGCCACACGAGAACACAATG	MDV genome copy number
106	103	ICP4_R	GGTTGGAGTAGAGCTGCAACTGT	
107	104	chGAPDH_F	GTCAACGGATTTGGCCGTAT	
108	105	chGAPDH_R	CCACTTGGACTTTGCCAGAGA	
109				
110	* The sequences that highlighted in bold are restriction enzyme sites.			
111	** The sequences that underlined were used to amplify the *Kan* gene cassette from pEPKan-S plasmid.			
112	*** The sequences that highlighted in bold italics are the tag sequences.			

Table S2. List of primers used in pcDNA plasmid constructions.

Primer number	Primer name	Sequence (5' to 3')
1	Meq-FLAG-F	TC**GCTAGC**ATG***GACTACAAAGACGATGACGACAAG***TCTCAGGAGCCAGAGCCG
2	Meq-HA-F	TC**GCTAGC**ATG***TACCCATACGATGTTCCAGATTACGCT***TCTCAGGAGCCAGAGCCG
3	Meq-T7-F	TC**GCTAGC**ATG***ATGGCTAGCATGACTGGTGGACAGCAAATGGGT***TCTCAGGAGCCAGAGCCG
4	Meq-R	GATC**GCGGCCGC**TCAGGGTCTCCCGTCACCTG
5	Meq-N-100-R	gatc**GCGGCCGC**tcaACGTAGGTGTTCATTGGCCCT
6	Meq-N-120-R	gatc**GCGGCCGC**tcaATGACGAGCCAACTGTACACG
7	Meq-N-150-R	gatc**GCGGCCGC**tcaGCAAATGGGAGGTTCAGGAAC
8	Meq-N-170-R	gatc**GCGGCCGC**tcaAGGTTGGGAACCGGAGCAATG
9	Meq-N-254-R	gatc**GCGGCCGC**tcaGATGCCCTCCGGAGATGGAGG
10	Meq-21-C-F	gatc**GCTAGC**atgCCCCTCGATCTTTCTCTCGGG
11	Meq-31-C-F	gatc**GCTAGC**atgAGACGGAAAAAAAGGAAAAGT
12	Meq-51-C-F	gatc**GCTAGC**atgGACGGCCTATCTGAGGAGGAG
13	Meq-79-C-F	gatc**GCTAGC**atgCAGACGGACTATGTAGACAAA
14	Meq-101-C-F	gatc**GCTAGC**atgAAGGAAATTCGAGATCTAAGG
15	Meq-121-C-F	gatc**GCTAGC**atgGAGCCAGTTTGCCCTATGGCG
16	Meq-FLAG-R	TC**GCGGCCGC**TCA***CTTGTCGTCATCGTCTTTGTAGTC***GGGTCTCCCGTCACCTG
17	Meq-BR_del-F	TTTCTCTCGGGTCGACTTCGCTCCATGAAGCATGTGAAGA
18	Meq-BR_del-R	TCTTCACATGCTTCATGGAGCGAAGTCGACCCGAGAGAAA
19	Meq-ZIP_del-F	AGACGGACTATGTAGACAAAGAGCCAGTTTGCCCTATGGC
20	Meq-ZIP_del-R	GCCATAGGGCAAACTGGCTCTTTGTCTACATAGTCCGTCT
21	Meq-BZIP_del-F	TTTCTCTCGGGTCGACTTCGGAGCCAGTTTGCCCTATGGC
22	Meq-BZIP_del-R	GCCATAGGGCAAACTGGCTCCGAAGTCGACCCGAGAGAAA
23	chHDAC1-FLAG-F	gatc**GCTAGC**atg***GACTACAAAGACGATGACGACAAG***gcgctgacgcaggggac
24	chHDAC1-HA-F	gatc**GCTAGC**atg***TACCCATACGATGTTCCAGATTACGCT***gcgctgacgcaggggac
25	chHDAC1-R	gatc**GCGGCCGC**ttaggtggattttgtctctt
26	chHDAC1-N-160-R	gatc**GCGGCCGC**ttagatagccaggacaatatcgt
27	chHDAC1-N-320-R	gatc**GCGGCCGC**ttacaaagccacagcagtctcat
28	chHDAC1-53-C-F	gatc**GCTAGC**atgatatatcgccctcacaaggcg
29	chHDAC1-81-C-F	gatc**GCTAGC**atgccagacaacatgtctgagta
30	chHDAC1-121-C-F	gatc**GCTAGC**atggctgtgaagctgaacaagca
31	chHDAC1-161-C-F	gatc**GCTAGC**atgttggagctcttaaagtatca
32	chHDAC1-321-C-F	gatc**GCTAGC**atggacactgagatcccaaatga
33	chHDAC1-FLAG-R	gatc**GCGGCCGC**tta***CTTGTCGTCATCGTCTTTGTAGTC***ggtggattttgtctcttcct
34	chHDAC2-FLAG-F	gatc**GCTAGC**atg***GACTACAAAGACGATGACGACAAG***gcgtacagtcagggcgg
35	chHDAC2-HA-F	gatc**GCTAGC**atg***TACCCATACGATGTTCCAGATTACGCT***gcgtacagtcagggcgg
36	chHDAC2-R	gatc**GCGGCCGC**tcaaggattgctgagctgtt
37	chHDAC2-N-160-R	gatc**GCGGCCGC**tcaggcaagcacaatatcattga
38	chHDAC2-N-320-R	gatc**GCGGCCGC**tcaggcaacagcagtttcatatg
39	chHDAC2-54-C-F	gatc**GCTAGC**atgatttaccgaccccacaaagct
40	chHDAC2-81-C-F	gatc**GCTAGC**atgaggcctgacaatatgtctga
41	chHDAC2-121-C-F	gatc**GCTAGC**atgggggcggtaaaattgaacag
42	chHDAC2-FLAG-R	gatc**GCGGCCGC**tca***CTTGTCGTCATCGTCTTTGTAGTC***aggattgctgagctgttc
43	chHDAC1_qPCR_F	GGATGAAGAAGAAGAAGATCC
44	chHDAC1_qPCR_R	GATAACTATGCACTGACAGG
45	chHDAC2_qPCR_F	AAGGTGGACGGCGAAATG
46	chHDAC2_qPCR_R	GATACGGTCCATGCCAAATAG
47	chGAPDH_qPCR_F	GTCAACGGATTTGGCCGTAT
48	chGAPDH_qPCR_R	CCACTTGGACTTTGCCAGAGA

* The sequences that highlighted in bold are restriction enzyme sites.

** The sequences that highlighted in bold italics are the tag sequences.